University of São Paulo–USP
São Carlos School of Engineering
Department of Electrical and Computing Engineering
Electrical Engineering Graduate School

Luan Filipe dos Santos Colombari

An Approach to Handle Sudden Load Changes on Static Voltage Stability Analysis

São Carlos
2017

Luan Filipe dos Santos Colombari

An Approach to Handle Sudden Load Changes on Static Voltage Stability Analysis

Master Thesis presented to the Electrical Engineering Graduate School of the São Carlos School of Engineering to achieve the requirements to obtain the title of Master of Science.

Field of Research: Electric Power Systems

Advisor: Rodrigo Andrade Ramos

São Carlos

2017

Colombari, Luan Filipe dos Santos
C718a An approach to handle sudden load changes on static voltage stability analysis / Luan Filipe dos Santos Colombari; orientador Rodrigo Andrade Ramos. São Carlos, 2017.

Dissertação (Mestrado) - Programa de Pós-Graduação em Engenharia Elétrica e Área de Concentração em Sistemas Elétricos de Potência -- Escola de Engenharia de São Carlos da Universidade de São Paulo, 2017.

1. Electric Power Systems. 2. Voltage Stability. 3. Continuation Power Flow. 4. Distributed Generation. 5. Undervoltage Load Shedding. I. Título.

FOLHA DE JULGAMENTO

Candidato: Engenheiro **LUAN FILIPE DOS SANTOS COLOMBARI.**

Título da dissertação: "Abordagem para considerar variações súbitas de carga na análise estática de estabilidade de tensão".

Data da defesa: 03.03.2017.

Comissão Julgadora: **Resultado:**

Prof. Associado **Rodrigo Andrade Ramos (Orientador)** (Escola de Engenharia de São Carlos/EESC) — APROVADO

Profa. Dra. **Claudia Rahmann** (Universidad de Chile) — APROVADO

Prof. Dr. **Roman Kuiava** (Universidade Federal do Paraná/UFPR) — APROVADO

Coordenador do Programa de Pós-Graduação em Engenharia Elétrica:
Prof. Associado **Luís Fernando Costa Alberto**

Presidente da Comissão de Pós-Graduação:
Prof. Associado **Luís Fernando Costa Alberto**

To my father, Carlos Colombari, who sadly had to pass away to be awarded with this modest recognition. He was one of the smartest men I have ever met and didn't even know what a master thesis is.

Acknowledgments

In special, I thank Prof. Rodrigo Andrade Ramos, for advising this dissertation and contributing to my development as a researcher, a professional and a future professor.

Acknowledgments to CNPq (National Counsel of Technological and Scientific Development) for awarding me the grant 130750/2015-8.

Also, I thank my mother, Maria Clélia dos Santos, for supporting me emotionally and financially during my master studies.

I'm greatly thankful for my soon to be wife, Camila Silva Vieira, for her kindness, patience and understating, specially regarding the hours and weekends required to finish this research.

I am in huge debt to my friend Fabrício Mourinho for all the professional and personal help provided all over the years. Particularly, to get in this graduate program and to lend me his house in the beginning of my master studies. For this last support, I thank Rodolpho Neves, Breno Carvalho and Renzo Bastos as well.

Thanks to Prof. Roberto Lotero for his several contributions in my academic career and personal life.

I also thank my friend and roommate Mohamad Ismail for all the help and companionship. Furthermore, thanks to Marina Carvalho for her patience and understanding with my constant intrusion in her apartment.

Finally, thanks to my laboratory colleagues, William Pereira, Marcelo Santana, Edson Geraldi, Thales Almeida, Tatiane Fernandes, Jhonatan Andrade, Allan Gregori, Anna Moraco, Marley Tavares, Carlos de Oliveira, Artur Piardi, Geyverson de Paula, Rafael Borges, Murilo Bento and Paulo Ubaldo. Without them this work would probably have been accomplished faster, however it would also have been tedious and wearisome.

"Don't Panic"
(Douglas Adams)

Abstract

Colombari, Luan Filipe dos Santos **An Approach to Handle Sudden Load Changes on Static Voltage Stability Analysis**. 134 p. Master Thesis – São Carlos School of Engineering, University of São Paulo, 2017.

In the context of static Voltage Stability Assessment (VSA), as the power system load grows, bus voltages tend to drop. This reduction may lead to generator or load disconnections caused by undervoltage protection schemes. These events comprise sudden parametric variations that affect the equilibrium diagram and the Voltage Stability Margin (VSM) of power systems. Practical examples of such sudden load changes are caused by the mandatory disconnection of Distributed Generation (DG) units and Undervoltage Load Shedding (ULS). There are no thorough studies in the literature concerning these load parametric variations and the discontinuities that they cause in power system equilibria. This dissertation describes a predictor/corrector scheme specifically designed to handle these discontinuities, so it is possible to evaluate their effect on the VSM of power systems. This method successively calculates the load discontinuities that exist in the equilibrium locus of the system under analysis. It results in the sequence of sudden load variations that happens and their overall impact on the system. When applied to quantify the effect of DG mandatory disconnections and ULS, the proposed predictor/corrector scheme yielded better results than the traditional Continuation Power Flow (CPFLOW), which experienced convergence problems caused by the discontinuities under analysis. However, due to its design, the applicability of the proposed method should be restricted to power systems that go through several successive sudden load changes. In this sense, it should not be regarded as a replacement for the CPFLOW, but rather as a technique that could award this traditional VSA tool with new features to enhance its performance.

Keywords: Electric Power Systems; Voltage Stability; Continuation Power Flow; Distributed Generation; Undervoltage Load Shedding.

Resumo

Colombari, Luan Filipe dos Santos **Abordagem para Considerar Variações Súbitas de Carga na Análise Estática de Estabilidade de Tensão.**. 134 p. Dissertação de mestrado – Escola de Engenharia de São Carlos, Universidade de São Paulo, 2017.

No contexto de análise estática de estabilidade de tensão, conforme a carga de um sistema de potência cresce, as tensões nas suas barras tendem a cair. Essa redução pode causar a desconexão de geradores e cargas devido a atuação de proteções de subtensão. Esses eventos representam variações abruptas de demanda que alteram o diagrama de equilíbrio de um sistema e sua Margem de Estabilidade de Tensão (MET). Exemplos práticos dessas variações são causados pelo desligamento mandatório de unidades de Geração Distribuída (GD) e pelo Corte de Carga por Subtensão (CCS). Não há estudos detalhados na literatura que trabalham especificamente com essas variações nos parâmetros da carga, nem com as descontinuidades que elas causam no diagrama de equilíbrio de sistemas de potência. Essa dissertação descreve um procedimento especificamente projetado para lidar com essas descontinuidades, de modo que seja possível avaliar seu efeito na MET de sistemas elétricos. Esse método calcula sucessivamente as descontinuidades de carga que existem no diagrama de equilíbrio do sistema em análise. Ele resulta na sequência de variações súbitas de carga que ocorre e no seu impacto no sistema. Quando o método foi aplicado para quantificar o efeito do desligamento mandatório de GD e do CCS, ele apresentou resultados melhores do que o tradicional Fluxo de Carga Continuado (CPFLOW), o qual sofreu problemas de convergência causados pelas descontinuidades em questão. Entretanto, devido ao seu projeto, o método proposto só deve ser utilizado para sistemas de potência que estão sujeitos a várias sucessivas variações abruptas de carga. Por essa razão, esse método não pode ser considerado um substituto do CPFLOW, mas sim como uma técnica capaz de agregar novas funcionalidades a essa ferramenta tradicional, amentando assim seu horizonte de aplicações.

Palavras-chave: Sistemas Elétricos de Potência; Estabilidade de Tensão; Fluxo de Carga Continuado; Geração Distribuída; Corte de Carga por Subtensão.

Acronyms

CAISO California Independent System Operator
CPFLOW Continuation Power Flow
DG Distributed Generation
EPS Electric Power System
LIB Limit Induced Bifurcation
MLP Maximum Loadability Point
OLTC On-load Tap Changer
PCC Point of Common Coupling
SIB Structure Induced Bifurcation
SNB Saddle-Node Bifurcation
ULS Undervoltage Load Shedding
VSA Voltage Stability Assessment
VSM Voltage Stability Margin

Contents

Chapter 1

Introduction

For several years, investments in Electric Power Systems (EPSs) were made based on a economy of scale paradigm, where the increasing load demand was met by the construction of big generating facilities and long transmission lines. This scenario resulted in the interconnected bulk power systems of nowadays. In the last few decades, environmental and economical constraints obstructed this policy reducing drastically the investments in sizeable Electric Power System (EPS) expansion projects. As a consequence of that, power systems began to operate close to their operational limits (KUNDUR, 1994; CUTSEM; VOURNAS, 2003; GAO; KUNDUR; MORISON, 1996).

This scenario resulted in conditions that may lead to voltage instability in EPSs. This phenomenon is characterized by appreciable rise or drop in bus voltages magnitudes. In critical situations, these events may cause trip of several power system equipment and even originate blackouts (CUTSEM; VOURNAS, 2003; GAO; KUNDUR; MORISON, 1996; KUNDUR et al., 2004). An example of voltage instability was seen in Brazil in 2009, when the three transmission lines that connect Itaipu power plant to the southeast region of the country were disconnected. This disturbance caused voltage sags in the state of São Paulo, which was responsible for the trip of the direct current transmission link between Brazil and Paraguay. As a result of this succession of events, the interconnected Brazilian network became unable to supply 40% of its total load in 18 different federation states (ONS, 2009).

To avoid possible load shedding caused by voltage instability, power system utilities are interested in such phenomena during the planning and operation of their network (MANSOUR; ALBERTO; RAMOS, 2015; LI et al., 2014; CHIANG; WANG; FLUECK, 1997).

When time domain simulations are employed to assess the voltage stability of EPSs, they require high computational effort. This may interfere with their utilization in real time applications or situations that require the analysis of a multitude of scenarios (GAO; KUNDUR; MORISON, 1996; BIJWE; KOTHARI; KELAPURE, 2000). Time domain simulations examine the dynamic behaviour of the system based on detailed models of generators, compensators and loads, as well as their associated control loops and protection schemes (VAN CUTSEM et al., 2015).

A practical alternative to dynamic analysis comprises static techniques employing the power flow problem formulation. The goal of these methods is to identify the maximum capability of the EPS to supply the power demand. This corresponds to the Maximum Loadability Point (MLP) of the system, which is the highest load level where the power flow equations can be solved. Beyond this point there is no available stable equilibrium for the power system to operate (CANIZARES; ALVARADO, 1993; CHIANG et al., 1995; CAO; CHEN, 2010). Static techniques do not depict the behavior of the EPS as accurately as the dynamic ones, however they are computationally faster, which promotes their utilization in real time applications and situations that require the analysis several EPS configurations (GAO; KUNDUR; MORISON, 1996; BALU et al., 1992; ZHAO et al., 2015).

The goal of static analysis is to assess whether there is an adequate stable equilibrium point for the EPS to operate with a given topology. Generally, this is assessed augmenting the load until there is no available power flow solution. What results from this procedure is the bus voltage profiles as the load increases, which consist in the equilibrium diagrams known as PV curves. The nose of the PV curve corresponds to the MLP of the system under analysis (CHIANG et al., 1995; NETO; ALVES, 2010; MANSOUR; ALBERTO; RAMOS, 2015; LI et al., 2014).

A reliable and standard technique to trace EPS equilibrium diagrams and to estimate their MLP is the Continuation Power Flow (CPFLOW). In essence, this method solves the power flow equations several times as the load grows, tracing the PV curves of the system for a given load growth direction (CHIANG et al., 1995; AJJARAPU, 2007; CANIZARES; ALVARADO, 1993; ALVES et al., 2000; MOLZAHN; LESIEUTRE; CHEN, 2013; SUNDHARARAJAN et al., 2003).

During the CPFLOW execution, as the load increases, some EPS devices may suddenly change their parameters according to the system states. Examples of such equipment are On-load Tap Changer Transformers (OLTCs), switchable shunt capacitors, excitation limiters of generators and Undervoltage Load Shedding (ULS) protection schemes (XU; WANG; AJJARAPU, 2012). These devices are responsible for sudden parametric changes in power systems that, in turn, cause discontinuities in its equilibrium diagram. As a result of them, the PV curves are not smooth nor continuous anymore, as intuitively expected.

Out of the possible parametric discontinuities that may happen in EPSs, this dissertation will focus on sudden load variations caused by undervoltage protection schemes. These are of particular interest because they can cause very severe discontinuities in PV curves, impacting significantly the voltage profile and the MLP of power systems.

Practical examples of sudden load variations that will be dealt is this dissertation comprise Undervoltage Load Shedding (ULS) and the mandatory disconnection of Distributed Generation (DG) units.

The mandatory disconnection of DG comprises the trip of these units caused by protection schemes designed by distribution utilities to mitigate possible adverse effects

that they may have in the network. When assessing the static voltage stability of EPSs, as the load grows, the bus voltages are expected to fall. The voltage drop may reach levels that could cause pick-up of DG undervoltage protections and consequently lead to their trip. This is equivalent to suddenly stepping load up, which may reduce the MLP and even cause instability (WALLING; MILLER, 2002; CHEN; MALBASA; KEZUNOVIC, 2013).

Opposed to the disconnection of DG units, the ULS is responsible to increase the power system MLP. It sheds specific power loads, so the network is capable to supply critical consumers and expensive manufacturing processes. It is a last resource but an effective method to assure that voltage collapse does not happen (AMRAEE et al., 2007; LEFEBVRE; MOORS; CUTSEM, 2003; AFFONSO et al., 2004).

The numerical results of this dissertation will focus on these two types of sudden load variations. Nevertheless, the discussions presented here should not be restricted to them, being general to load parametric discontinuities.

In this context, this dissertation will address two main topics: (i) the effect of sudden load changes in the MLP of power systems and (ii) the impact of the equilibrium discontinuities caused by them in the performance of the CPFLOW.

Remarkable works dealing directly with possible discontinuities in EPS equilibrium diagrams were done by Xu, Wang and Ajjarapu (2012), Yorino, Li and Sasaki (2005). However, their analysis were restricted to reactive power limits of generators and switchable shunt capacitors. These papers and further bibliography regarding this field of research will be presented throughout the dissertation alongside with important theoretical concepts that will assist the understanding of the reader.

At this point, it is essential to point out that, to the extent of the author's knowledge, there is no thorough work in the literature dealing with the effects of load discontinuities on EPS equilibrium diagrams nor their influence on the performance of the continuation power flow.

1.1 Objectives

In face of this gap, the research objectives of this dissertation are:

1. Investigate the nature of the EPS equilibrium diagram discontinuities caused by sudden parametric variations in the load.
2. Evaluate the adequacy of the CPFLOW to account for sudden parametric variations in the load during its execution.
3. Quantify the impact of sudden parametric variations in the load on the MLP of electric power systems.
4. Propose a method specifically designed to account for sudden parametric variations in the load during the MLP estimation under a static voltage stability framework.

1.2 Dissertation Structure

In order to demonstrate the fulfillment of these objectives, this dissertation is divided into 5 other chapters:

Chapter 2: It presents basic concepts regarding static voltage stability assessment, alongside with the Continuation Power Flow (CPFLOW), which is the standard method in this field of research. Afterwards, it describes a variation of the CPFLOW to find discontinuities in PV curves.

Chapter 3: It qualitatively depicts the effect of sudden load variations in the equilibrium diagram of electric power systems. This leads to the description of a method designed to handle such parametric changes during voltage stability assessment.

Chapter 4: Numerical results are given to illustrate the effect of DG mandatory disconnections on the MLP of electric power systems.

Chapter 5: This time, the numerical results comprise the effect of Undervoltage Load Shedding (ULS) on the MLP of electric power systems.

Chapter 6: It presents the final conclusions of this work and possible future research that it could lead to.

Chapter 2

Static Voltage Stability Analysis

Both Kundur et al. (2004) and Anderson and Fouad (2002) define voltage stability as the EPS ability to sustain steady bus voltages before and after the system is subject to perturbations. Under this definition, voltage instability can be characterized by an unbounded voltage increase or reduction throughout the power system, that can lead to shut down of generators, transmission line disconnections and load shedding. In extreme cases, the power system may suffer with severe small bus voltages, cascading equipment outages and even blackouts. Phenomenon that is known as voltage collapse (KUNDUR et al., 2004).

In a EPS, instability phenomena may happen in a multitude of scenarios with different devices involved. As a consequence of that, it is useful to classify voltage stability according to the size of the disturbance under analysis and the time scale involved. Such classification is indicated in Figure 2.1.

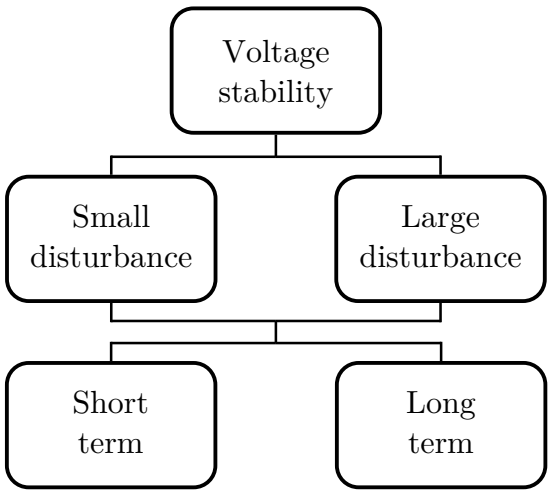

Figure 2.1: Classification of voltage instability phenomena.

Both classifications regarding disturbance size can be analysed in the two time frames mentioned. For example, it is possible to assess short and long term voltage stability after a small disturbance. Each voltage stability category is described briefly below:

Large disturbance voltage stability: It is the EPS ability to keep steady bus voltages after large disturbances such as severe faults, generator trips or critical transmission line disconnections. It depends strongly on the non-linear behavior of power systems and it should include dynamic models of loads and generators as well as protection settings and feedback control loops (KUNDUR et al., 2004).

Small disturbance voltage stability: It is related to the EPS ability to maintain steady voltages after small power injection variations or following a unimportant equipment disconnection. In most cases it allows the linearisation of the power system dynamic model (KUNDUR et al., 2004).

Short term voltage stability: It can be associated with the dynamic response of the EPS a few seconds after a disturbance. It depends on fast acting devices such as induction motors, electronically controlled loads and HVDC converters (CUTSEM; VOURNAS, 2003; KUNDUR et al., 2004).

Long term voltage stability: It is related to slow power system elements like On-load Tap Changer (OLTC), thermostatically controlled loads and generator current limiters. In this case, the goal is to assess the system behavior several minutes following a perturbation to identify situations where instability is a consequence of equipment outages and not the disturbance itself (KUNDUR et al., 2004).

Keeping in mind this classification, voltage stability can be assessed with different techniques. Static voltage stability analysis is characterized by the existence of stable power system equilibrium points after one of its parameters change. Commonly, increase of load is the parametric variation selected for such purpose. In this scenario, the total system power demand may reach values to which there is no stable equilibrium point available. The maximum total power that still have such point is called Maximum Loadability Point (MLP) (CUTSEM; VOURNAS, 2003; AJJARAPU, 2007; CANIZARES; ALVARADO, 1993). In this situation, static voltage stability analysis is related to the existence of stable equilibrium points for the power system to operate when it is subject to successive, small and slow load increments. In this analysis, instability is determined by the unavailability of a stable operating point (KUNDUR et al., 2004). Regarding the classification described above, static stability analysis assess the small disturbance voltage stability of a EPS in the long term.

Static voltage stability assessment is unfit to account for several dynamic aspects of power systems that could cause instability. Those scenarios would require time domain simulations of detailed dynamic models of power system equipment. When opposed to static techniques, dynamic tools are capable to examine the transition path between different equilibria and not simple appraise their stability feature. They can depict more accurately EPSs behavior, including their limiters, protections and controls (GAO; KUNDUR; MORISON, 1996). For this reason, dynamic stability analysis can identify instability situations that could be overlooked by static techniques. Therefore, the MLP estimated with static

applications should be regarded as an optimistic result (BIJWE; KOTHARI; KELAPURE, 2000; SAUER; PAI, 1990).

Despite being more accurate, dynamic analysis require high computational effort and simulation time. This makes it inadequate for applications that require stability assessment of several EPS configurations, which is the case of contingency screening and ranking (MANSOUR, 2013; BALU et al., 1992; GAO; KUNDUR; MORISON, 1996). In this circumstance, static tools are employed to identify critical configurations that would require further dynamic stability assessment. This means that this two techniques do not compete with each other and their utilization should be complementary and not exclusive (BIJWE; KOTHARI; KELAPURE, 2000).

Two engineering practice examples are given to demonstrate the relevance of static voltage stability analysis in electric power systems. Both the California Independent System Operator (CAISO) and the Brazilian System National Operator (ONS - *Operador Nacional do Sistema*) employ static simulations to assure safe operation of their respective system (LI et al., 2014; ONS, 2011).

This chapter will discuss basic concepts regarding static voltage stability analysis of bulk power systems in Section 2.1. Next, in Section 2.2, a load growth parametrization technique is described. Such formulation is indispensable to use the standard voltage stability assessment tool known as CPFLOW that is presented in Section 2.3. In Section 2.4, a method proposed by Yorino, Li and Sasaki (2005) to find equilibrium discontinuities caused by reactive limits of generators is described. This method is included here because it is a key reference dealing directly with PV curve discontinuities and it will be the basis of the study done in this dissertation regarding sudden load changes. Finally, the final remarks of the chapter are presented in section 2.5.

2.1 Static Voltage Stability Fundamentals

For stability analysis, power systems are generally modeled as a non-linear dynamic system described with a set of dynamic and algebraic equations (CUTSEM; VOURNAS, 2003; SAUER; PAI, 1990).

$$\begin{aligned} \dot{\hat{x}} &= \mathbf{h}(\hat{x}, \hat{y}) \\ 0 &= \mathbf{g}(\hat{x}, \hat{y}) \end{aligned} \tag{2.1}$$

where $\hat{x}$ and $\hat{y}$ are the vectors containing, respectively, the states and algebraic variables of the power system.

During static analysis the goal is to calculate equilibrium points of this dynamic model, which means solving (2.1) for the power system states when $\dot{\hat{x}}$ is equal to zero. After calculating an equilibrium, it is still indispensable to determine whether or not such point is stable. For this purpose it is possible to employ the Hartman–Grobman theorem, which guarantees that the stability characteristic of one equilibrium point can be determined from

the eigenvalues of the linearised dynamic system at this point. If none of its eigenvalues have positive or zero real part, then the this solution is said to be stable (CHICONE, 1999). As a consequence of the linearisation procedure, that is to say that the Jacobian of (2.1) evaluated at the given equilibrium define the power system stability around such point.

A simplification of this process commonly used in voltage stability assessment is to neglect the dynamic equations of the EPS and to consider that the traditional power flow formulation is enough to represent power system equilibrium points (CAO; CHEN, 2010; SAUER; PAI, 1990; KUNDUR et al., 2004; ZHAO et al., 2015; MANSOUR, 2013). From this approximation power flow solutions represent the bulk system steady state points and the Jacobian of such equations establish their stability.

Even though the power flow equations are contained in the algebraic set $\mathbf{g}(\hat{x}, \hat{y})$, they alone are not enough to represent the non-linear dynamic system that model EPS (SAUER; PAI, 1990). Still, power flow techniques are well established in the power system industry as a dependable tool to evaluate steady state characteristics and they will be used in this dissertation to define power system equilibrium points.

The power flow problem can be written in the following compact form:

$$0 = \mathbf{f}(\hat{V}, \hat{\theta}) + \lambda \hat{b} \tag{2.2}$$

where $\hat{V}$ and $\hat{\theta}$ are the vectors of bus voltages magnitudes and angles. The dimension of both these vectors is equal to the number of buses (nb) of the power system under analysis. Besides that, λ is a scalar that represents the loading level, as it increases so does the system total demand. Vector $\hat{b}$ defines the load growth direction. This means that it indicates at which buses this increase takes place and at which rate it happens. Its dimension is equal to twice the number of buses ($2 \cdot nb$), since there it has one component for the active and reactive power injection in each bus.

Varying the load parameter λ and solving the power flow equations, it is possible to draw the EPS equilibrium diagram when the load grows in direction $\hat{b}$. This results in the diagram known as PV curve or nose curve that depicts the system bus voltage variation as the load increases. A qualitative example of a PV curve is shown in Figure 2.2.

Investigating the power flow Jacobian eigenvalues, it is possible to conclude that the upper portion of the PV curve comprises stable equilibrium points, while the lower portion contains unstable ones. The latter can be associated with a single eigenvalue with positive real component. The PV curve nose represent the power system Maximum Loadability Point (MLP). If the system actual load is bigger than this value, then there is no equilibrium point for the system to operate resulting in instability.

The MLP is directly related to the capability of the transmission lines to deliver power and with the ability of the generators to supply the reactive power demanded by the network and the loads (LI et al., 2014; KUNDUR et al., 2004).

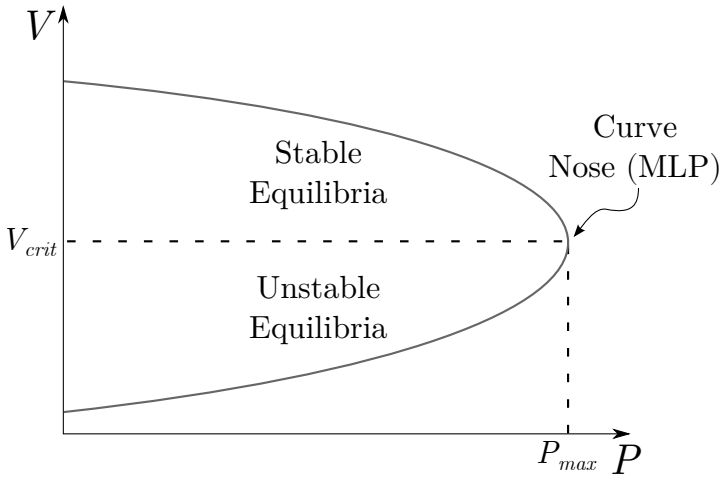

Figure 2.2: Qualitative example of PV curve. The abscissa is the power system total active load and the ordinate is the voltage magnitude at a selected bus.

Both the voltage profile and the MLP depend on the load growth direction, i.e. vector $\hat{b}$. That is to say, the location where the load increase takes place affects the EPS maximum capability to deliver power.

The distance from the current load demand to the maximum loadability point represents the operator's room for maneuver to deal with generation rejection, demand variations and line contingencies. The closer system operates to the MLP, more likely it is to be subject to voltage instability. In this context, it makes sense to define the Voltage Stability Margin (VSM) as the distance from the power system current loading to its maximum value (GAO; KUNDUR; MORISON, 1996; MANSOUR, 2013). Figure 2.3 displays the graphical interpretation of the VSM.

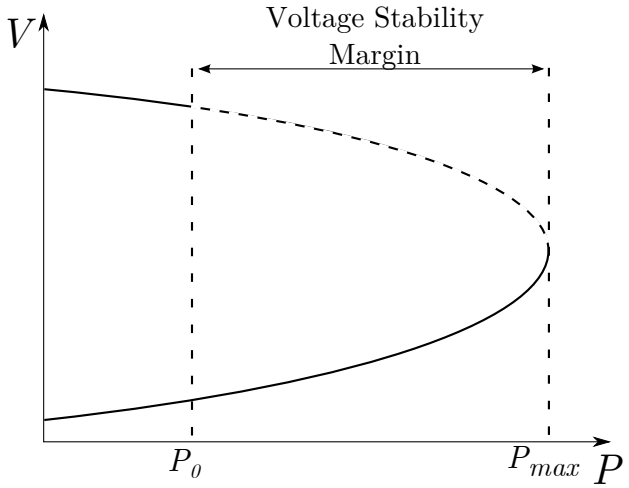

Figure 2.3: Graphical representation of the Voltage Stability Margin, where P_0 represents the current operation point and P_{max} is the system maximum loadability.

When the power flow problem is employed to obtain PV curves, an implicit assumption made is that such equations model the equilibrium points of the EPS. In such approach,

bifurcation theory can be used to investigate the system voltage stability.

A bifurcation is defined as any point in the parametric space of a dynamic system for which there is a qualitative structural change in the system after a small variation of the parameter vector. In other words, a bifurcation takes place in a point where a continuous and smooth parametric change is responsible to drive a sudden change in the system characteristic (CUTSEM; VOURNAS, 2003). The PV curve nose point is an example of a bifurcation, where a small increase of λ alter the number of equilibrium points of the power system, going from two to zero (CUTSEM; VOURNAS, 2003; AJJARAPU, 2007). At the MLP, a branch of stable equilibria meets with the unstable one and booth cease to exist for higher loading levels. This characterizes what is known as Saddle-Node Bifurcation (SNB) (CUTSEM; VOURNAS, 2003).

Moving on the PV curve going from the upper and stable equilibria branch to the unstable one, a eigenvalue of the power flow Jacobian changes its sign at the MLP, going from a negative value to a positive one. As a consequence of that, at the SNB, its value is necessarily equal to zero. Because of this null eigenvalue, the determinant of the power flow Jacobian is also equal to zero. This makes the Newton-Raphson numerical procedure (that is usually employed to solve the power flow equations) diverge when trying to find the MLP. Actually, for solutions close to the PV curve nose point, the Jacobian determinant is small enough to make such matrix poorly conditioned, which results in convergence problems for the numerical techniques employed to find the power flow solutions. In practice, this implies that it is not possible to trace the stable equilibrium branch all the way to the MLP simply increasing the system loading and solving the power flow equations with Newton-Raphson method. As a matter of fact, specific techniques are required to draw equilibrium diagrams near Saddle-Node bifurcations (CHIANG et al., 1995; AJJARAPU, 2007; CANIZARES; ALVARADO, 1993).

A second type of bifurcation that power flow equilibria may be subject to is called Limit Induced Bifurcation (LIB) or Structure Induced Bifurcation (SIB). As the load grows, generators reach their operational limits that, in turn, prevent them to contribute further with the EPS. During static voltage stability analysis, interest lies in constraints that limit the reactive power supplied by generating units, since they are capable to reduce significantly the MLP and even drive instability (YORINO; LI; SASAKI, 2005; CAO; CHEN, 2010; CHIANG et al., 1995; AJJARAPU, 2007; HISKENS; CHAKRABARTI, 1996).

Physically, these constraints can be associated with the thermal capability of the field and armature windings (DOBSON; LU, 1992). In power flow studies the effect of such limits are modeled considering that each generator has a constant maximum and minimum reactive power capability (Q-limit). When such upper/lower boundary is met the generator losses its ability to control its bus voltage, going from a PV bus type to a PQ one whose reactive power injection is equal to its limit (CANIZARES; ALVARADO, 1993; HISKENS; CHAKRABARTI, 1996; YANG et al., 2013; DOBSON; LU, 1992).

When such bus type modification takes place, the power flow equations also change and so does the power flow Jacobian. In nature, this represents a structural alteration in the Jacobian that is perceive as a discontinuity in the PV curve derivative. Such effect can be observed in Figure 2.4, where the solid curve represents the actual equilibrium diagram when a maximum Q-limit is met by a generator. In the same figure, the red curve portrays the PV curve when the generator is considered a PQ bus while in the blue curve it is a PV bus. In this graphical example, the generator limit reduced the maximum loadability of the system from P_{max2} to P_{max1}.

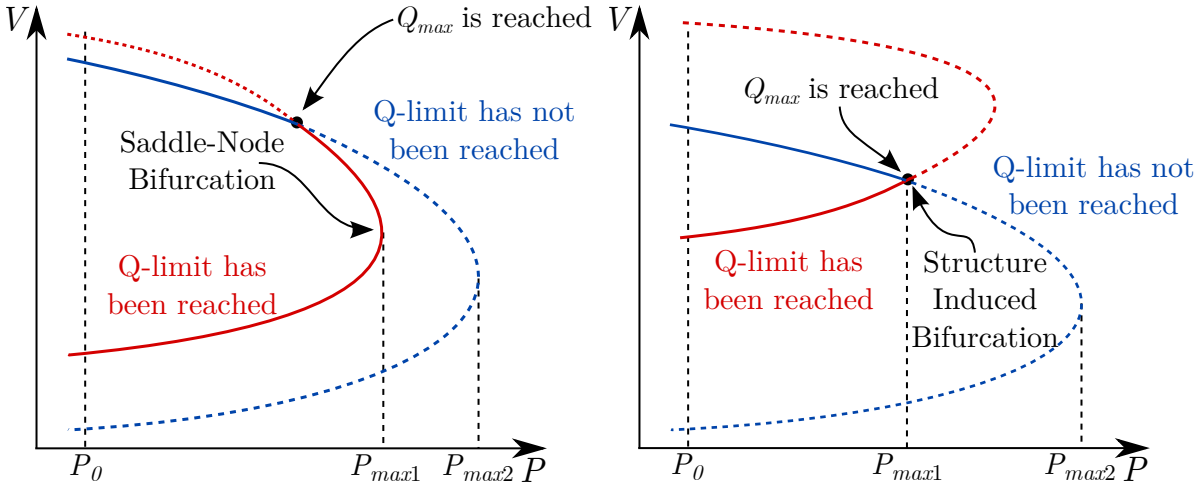

(a) Generator Q-limit does not cause instability. (b) Generator Q-limit causes instability.

Figure 2.4: Qualitative effect of a generator Q-limit on PV curves is depicted in the solid line. In the blue and red lines the generator is modeled as a PV and PQ bus respectively.

In addition to reducing the MLP, the Q-limits may also cause instability. Mathematically, this happens when the bus type alteration modify the power flow Jacobian in such way that the real component of one of its eigenvalues becomes positive. This point is called limit or structure induced bifurcation (CANIZARES; ALVARADO, 1993; HISKENS; CHAKRABARTI, 1996; YORINO; LI; SASAKI, 2005; DOBSON; LU, 1992). Such bifurcation can be seen in Figure 2.4(b) and compared with the SNB that is indicated in Figure 2.4(a), where the Q-limit does not cause instability but diminishes the MLP.

To obtain PV curves and identify the type and location of bifurcations, it is necessary to solve the power flow equations as the loading parameter λ increases. The estimated MLP depends on how this scalar is related with the actual power system loading, which is the active and reactive load in each bus. The relationship between λ and the real power consumed in the EPS is determined by the load growth direction $\hat{b}$ of (2.2).

2.2 Loading Parameter λ and the Load Growth Direction

Continuation methods are design to calculate the solutions of a set of non-linear equations while one parameter changes continuously. When such techniques are applied to analyse electric power systems, the parameter that is selected to vary is commonly the system loading level, indicated by the Greek letter λ.

This section describes the relationship between the scalar λ and the active and reactive loads in each bus of the power system. In this description and throughout the entire dissertation, all loads are considered to be of constant power. In general this is not true, but it constitutes a very severe situation and results in a pessimistic estimative of the VSM, which is desirable for security purposes (MANSOUR, 2013; LONDERO; AFFONSO; NUNES, 2009).

The load parametrization employed here is based on two premisses:

1. As the load parameter λ increases so does the active and reactive load in each bus.
2. When $\lambda = 1$ both the system loading level and the power generation corresponds to the base case of the EPS. This point should be interpreted as the current operating point of the system.

As a result of that it is possible to write the load growth parametrization with (2.3) and (2.4).

$$P_{Li} = P_{L0i} + (\lambda - 1)K_{Pi}P_{L0i} \tag{2.3}$$

$$Q_{Li} = Q_{L0i} + (\lambda - 1)K_{Qi}Q_{L0i} \tag{2.4}$$

where P_{Li} and Q_{Li} are the active and reactive loads in bus i respectively, P_{L0i} and Q_{L0i} are the same parameters, but now associated with the base case of the power system ($\lambda = 1$). K_{Pi} and K_{Qi} determine at which proportion the load in each bus grows, for example, if at a given bus $K_{Pi} = 2$, than its active load increases twice as much as the load associated with $K_{Pi} = 1$. The ratio between K_{Pi} and K_{Qi} at a given bus arbitrate how the power factor of this load varies as λ changes. If $K_{Qi} = K_{Pi}$ then the load increases with constant power factor.

As the load grows, generators need to be dispatched to meed such consumption increase. This is done with equation (2.5).

$$P_{Gi} = P_{G0i} + K_{Gi}\left[\sum_{i=1}^{nb} P_{Li} - \sum_{i=1}^{nb} P_{L0i}\right] \tag{2.5}$$

here, P_{Gi} and P_{G0i} are, respectively, the active power that is injected by the generator in bus i and how much it supplies in the base case. The parameter K_{Gi} is responsible to dispatch generators as the load grows. The bigger its value, more load the associated generator would take on.

To assure that the total load increase is met by the generators, the summation of all K_{Gi} needs to be equal to one. In this formulation, the generator associated with the slack bus is responsible to supply the increase in transmission system losses as the load grows with parameter λ.

$$\sum_{i=1}^{nb} K_{Gi} = 1 \tag{2.6}$$

To sum up, equations (2.3), (2.4) and (2.5) determine the load growth that occurs in the power system as a function of the loading parameter λ. This increase happens in a direction that is specified by parameters K_{Gi}, K_{Pi}, K_{Qi}, P_{L0i} and Q_{L0i}. In the power flow problem presented in (2.2), these parameters define the load growth direction vector ($\hat{b}$).

To give a physical meaning to λ it is possible to affirm that, as long as the base case loading (P_{L0i} and Q_{L0i}) does not change, the parameter λ is monotonically related with the total load in the EPS and it is possible to write:

$$\sum_{i=1}^{nb} P_{Li} = \lambda \sum_{i=1}^{nb} P_{L0i} \tag{2.7}$$

This means that, if $\lambda = 1.5$, then the total active power consumption in the system is 50% higher than the base case loading.

2.3 Continuation Power Flow (CPFLOW)

Due to the fact that the Jacobian matrix of the power flow equations is ill conditioned near the MLP, simply increasing the EPS load until divergence of the numerical method employed to solve such equations is not an adequate way to estimate the maximum loadability of the system (CANIZARES; ALVARADO, 1993). To solve this problem continuation methods are employed. They correspond to the mathematical techniques that trace solutions of a set of non-linear equations when one of its parameters changes. The application of such methods to trace PV curves characterizes what is known as Continuation Power Flow (CPFLOW) (CHIANG et al., 1995).

The CPFLOW is regarded as an efficient and precise method to estimate the MLP and obtain PV curves. It became a standard approach to perform Voltage Stability Assessment (VSA) under a static framework for a known load growth direction and it is also utilized as a comparison benchmark for other techniques being developed (CAO; CHEN, 2010; LI; CHIANG, 2008b).

In general, continuation techniques are divided into four parts, which are described in the following subsections. They are:

- ❏ Parametrization;
- ❏ Prediction;
- ❏ Correction;
- ❏ Step length control.

2.3.1 Parametrization

The power flow equations are indicated in (2.2). To simplify the notation, from now on the state vector that contain bus voltages magnitudes and angles $(\hat{V}, \hat{\theta})$ will be referred as $\hat{x}$, resulting in the compact power flow formulation (2.8).

$$0 = \mathbf{f}(\hat{x}) + \lambda \hat{b} \tag{2.8}$$

Remember that, λ and $\hat{b}$ are the loading parameter and the load growth direction respectively. If $\hat{b}$ is known, then for a given value of λ it is possible to solve the power flow equations to calculate the voltages and angles of the EPS. This is equivalent to the traditional load flow problem.

When executing the CPFLOW, the scalar λ is also regarded as an unknown variable. In such case, there are $2nb + 1$ variables associated with $2nb$ non-linear equations, which makes the system underdetermined. The parametrization procedure can be regarded as including another equation to this problem, so the parameter λ can be solved alongside with the EPS states.

Mathematically, this additional equation defines successive solutions of the power flow equations, i.e. sequential points in the PV curve (CHIANG et al., 1995). In general, any extra equation may be employed as a parametric equation, as long as it relates two consecutive solutions of the power flow problem.

Two widely used parametrization techniques will be presented here. They avoid the ill-conditioning of the power flow Jacobian near the MLP, solving possible convergence problems that the traditional power flow formulation may encounter. First, the local parametrization is described, then the arc-length one is presented.

Local parametrization

Given a power flow solution $\hat{x}_1$ at a known loading level λ_1, the idea of the CPFLOW with local parametrization is to find an ensuing solution $(\hat{x}_2, \lambda_2)$ taking a fixed step (Δh) in a given EPS state. This step is attributed to the variable that is more likely to undergo a big change between the two successive solutions $\hat{x}_1$ and $\hat{x}_2$. This selected variable can be a bus voltage magnitude or angle, or even the load parameter λ (CANIZARES; ALVARADO, 1993; AJJARAPU, 2007).

First, it is necessary to estimate how much each variable is expected to change from the known solution to the next one. For such purpose the following linear approximation is employed:

$$0 = \frac{\mathrm{d}\mathbf{f}(\hat{x})}{\mathrm{d}\hat{x}} \Delta\hat{x} + \hat{b}\Delta\lambda \tag{2.9}$$

The derivative term in (2.9) is the Jacobian matrix of the power flow equations. Evaluating such matrix at the known power flow solution $(\hat{x}_1, \lambda_1)$ and remembering that $\hat{b}$ is a known parametric vector, then the aforementioned equality is a linear system composed

by $2nb$ equations and $2nb+1$ variables $(\Delta\hat{x}, \Delta\lambda)$. To solve this system, one arbitrary value is attributed to either $\Delta\lambda$ or one element of $\Delta\hat{x}$ (AJJARAPU, 2007). The choice of the parameter that receives the numerical value is also arbitrary, the only criteria that needs to be met is that the resulting linear system, comprised by $2nb$ equations, has a single unique solution. The numerical result of the linear system for $(\Delta\hat{x}, \Delta\lambda)$ is numerically the tangent vector of the power system equilibrium diagram at the known power flow solution. This way, employing different parameters with different values to solve this linear system, will result in the same tangent vector direction with distinct magnitudes.

As a result of this process the numerical values of $(\Delta\hat{x}, \Delta\lambda)$ are obtained. They are an estimate of how much each state and the loading parameter is expected to change near $\hat{x}_1$. The parameter associated with the greatest variation, i.e. the biggest component of the tangent vector, is selected as the local parameter that will be employed in the continuation step (AJJARAPU, 2007). During the parametrization, the actual numerical values of $\Delta\hat{x}$ and $\Delta\lambda$ are not of any particular interest, the goal is to select the one that have the greatest variation to be the continuation parameter. Nevertheless, the calculated tangent vector carry important information regarding the equilibrium point $(\hat{x}_1, \lambda_1)$ and may be used in other stages of the continuation process.

The selected local parameter will be referred with letter p and it may be the load parameter λ, a voltage magnitude or angle . After it is chosen, the goal of the CPFLOW will be to find a power flow solution $(\hat{x}_2, \lambda_2)$, so that the local parameter meets (2.10).

$$p_2 = p_1 + \Delta h \tag{2.10}$$

Here, p_1 is the value of the local parameter at the power flow solution $(\hat{x}_1, \lambda_1)$ and p_2 will be its value on the next solution to be found $(\hat{x}_2, \lambda_2)$. The step-length Δh is a arbitrary parameter that depends on the type of local parameter that is being used, that is, it can be different if p is the loading parameter, a voltage magnitude or angle. Its value establishes the separation between two successive power flow solutions that are calculated with the continuation method.

It is (2.10) that is included in the set of $2nb$ equations of the power flow problem, making equal the number of variables and equations.

Practical use of the locally parametrized CPFLOW demonstrates that, when the power flow solutions are far from the MLP, the load scalar λ is the selected local parameter, which is numerically equivalent to solving the traditional power flow problem for a given value of λ. However, if the known solution $(\hat{x}_1, \lambda_1)$ is close to the nose point, bus voltages are prone to substantial variations, which results in the selection of the most critical bus voltage as the local parameter. This avoids the ill-conditioned Jacobian matrix problem and allows adequate tracing of SNBs (CANIZARES; ALVARADO, 1993).

The graphical interpretation of one continuation step using local parametrization is presented in Figure 2.5(a), alongside with the arc-length parametrization that will be described in the following topic.

Arc-length parametrization

The goal of the arc-length parametrization is to find the power flow solution $(\hat{x}_2, \lambda_2)$ that is at a distance Δs from the already known solution $(\hat{x}_1, \lambda_1)$. This distance is the euclidean norm in the parametric hyperspace that comprise all EPS states and the load parameter λ. Mathematically this can be written as:

$$\Delta s^2 = \|\hat{x}_2 - \hat{x}_1\|_2^2 + (\lambda_2 - \lambda_1)^2 \tag{2.11}$$

When this parametrization is employed, (2.11) is added to the set of power flow equations. This way, the load flow problem (2.8) can be simultaneously solved for the bus voltages, angles and λ.

Geometrically, the step Δs defines the radius of a hypersphere centered at $(\hat{x}_1, \lambda_1)$. The next solution to be calculated is the intersection between such sphere and the equilibrium points of the power system (CAO; CHEN, 2010). The equivalent in two dimensions of this geometric interpretation is indicated in Figure 2.5(b).

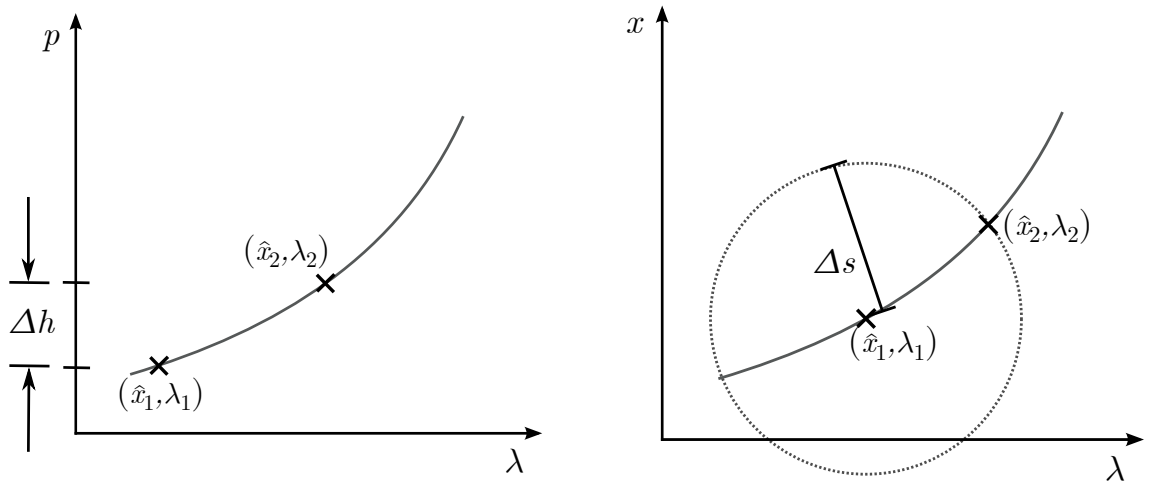

(a) Local parametrization.

(b) Arc-length parametrization

Figure 2.5: Graphic interpretation of one continuation step for the two most commonly employed parametrization types.

Just like the local parametrization, the arc-length one avoids the poor conditioning of the Jacabian matrix near the maximum loadability point, solving the divergence problems of the power flow formulation around this point (CHIANG et al., 1995; CAO; CHEN, 2010).

It is worth pointing out that the arc-length parametrization is computationally more efficient than the local one (CHIANG et al., 1995). It does not require the calculation of tangent vector via the solution of the linear system (2.9), which may be time-consuming for large power systems.

2.3.2 Prediction

The purpose of the prediction stage is to find an approximate solution $(\hat{x}_2', \lambda_2')$, that is close to the next power flow solution $(\hat{x}_2, \lambda_2)$ defined by the parametrization equation

and the continuation step employed. This estimate is calculated based on previously determined power flow solutions and curve fitting techniques.

The most commonly employed predictors are based on linear approximations. They are called tangent and secant predictors and are described in the following sections (CHIANG et al., 1995).

Tangent Predictor

As its name portraits, this predictor employs the tangent vector at the last known power flow solution to predict the next one. In other words, an approximate power flow solution is estimated from the PV curve derivative at the last known solution.

In the local parametrization, the tangent vector was calculate to select the local parameter. In the tangent prediction, the same vector is now used to estimate what will be the states of the power system at the next desired solution. Once again the tangent vector is calculated at the known power flow solution $(\hat{x}_1, \lambda_1)$ with (2.9). This equation is rewritten bellow:

$$0 = \frac{\mathrm{d}\mathbf{f}(\hat{x})}{\mathrm{d}\hat{x}}\Delta\hat{x} + \hat{b}\Delta\lambda$$

As already discussed, to solve this linear system, the power flow Jacobian (derivative term) needs to be evaluated in the known equilibrium point $(\hat{x}_1, \lambda_1)$ and one arbitrary value needs to be applied to one element of $\Delta\hat{x}$ or $\Delta\lambda$. When the linear system is solved, the numeric values of $\Delta\hat{x}$ and $\Delta\lambda$ become known.

With this result and a given continuation step σ, it is possible to estimate the next power flow solution with (2.12).

$$\begin{aligned} \hat{x}'_2 &= \hat{x}_1 + \sigma\Delta\hat{x} \\ \lambda'_2 &= \lambda_1 + \sigma\Delta\lambda \end{aligned} \tag{2.12}$$

Overall, the tangent predictor is employed alongside with the local parametrization. Both this steps require the same tangent vector, which means that it is only necessary to solve the linear system (2.9) once every continuation step and that the predictor itself only requires the operation (2.12) (CANIZARES; ALVARADO, 1993). Nevertheless, this predictor can be employed with any other parametrization technique, even the arc-length one.

The geometric interpretation of the local predictor is available in Figure 2.6(a).

Secant Predictor

This predictor relies on two previously known power flow solutions to perform a linear curve fitting and then estimate the next one. If the known solutions are $(\hat{x}_0, \lambda_0)$ and $(\hat{x}_1, \lambda_1)$, this procedure can be done with (2.13) (CHIANG et al., 1995).

$$\begin{aligned} \hat{x}'_2 &= \hat{x}_1 + \sigma(\hat{x}_1 - \hat{x}_0) \\ \lambda'_2 &= \lambda_1 + \sigma(\lambda_1 - \lambda_0) \end{aligned} \tag{2.13}$$

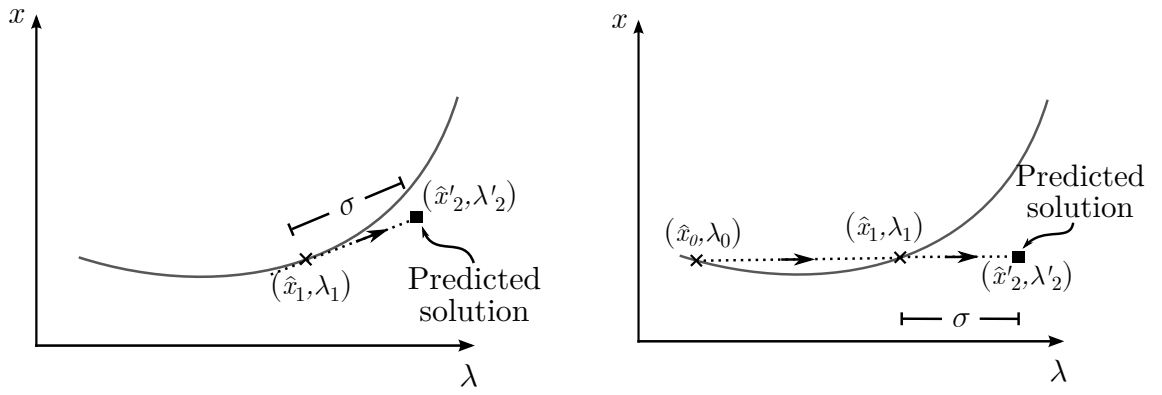

(a) Tangent predictor.

(b) Secant predictor.

Figure 2.6: Graphic interpretation of the two most commonly used predictors.

The secant predictor can be compared with the tangent one in Figure 2.6. This geometric interpretation is done in two dimensions to simplify the analysis, nevertheless it is important to remember that the prediction takes place in the complete state space of the EPS and also includes the load parameter λ.

Looking at the fact that the secant predictor does not need to solve the linear system (2.9), it is computationally faster when compared to the tangent predictor. Due to this advantage, it is commonly employed with the arc-length parametrization, in which case the mentioned linear system does not need to be solved (CHIANG et al., 1995). Its disadvantage is that it requires two previous power flow solutions, while the tangent predictor can achieve the same goal with a single one.

2.3.3 Correction

After the prediction stage finds an approximate equilibrium point of the EPS, the correction stage is designed to enhance the precision of this operation point by solving the power flow equations within the desired accuracy tolerance. In other words, its goal is to solve the non-linear set of equations (2.8) along with the parametric equation to determine bus voltages magnitudes, angles and the loading parameter λ (CANIZARES; ALVARADO, 1993; CHIANG et al., 1995; AJJARAPU, 2007).

In this situation, there are $2nb + 1$ equations and variables that are generally solved with the Newton-Raphson method. The starting point of the numeric procedure is the approximate solution obtained in the prediction stage. Since this result is usually close to the actual power flow solution, the Newton's method converges in few iterations (CANIZARES; ALVARADO, 1993; CHIANG et al., 1995; YORINO; LI; SASAKI, 2005).

The predictor employed curve fitting approximations and it is not capable to account for possible discontinuities that may be present in power system equilibrium diagrams, as is the case of generators Q-limits. It is the corrector that is responsible to consider such constraints and other possible discontinuities. This is achieved within the Newton's numeric procedure with conditions that guarantee that possible limits are not violated.

As a result of that, when any discontinuity is met, the predictor worsen its precision and more iterations are needed in the correction stage (CHIANG et al., 1995).

The two dimensional graphic interpretation of both the prediction and corrector stages are available in Figure 2.7. It is worth pointing out, that the solution that is found after the corrector depends on the parametrization and the continuation step employed.

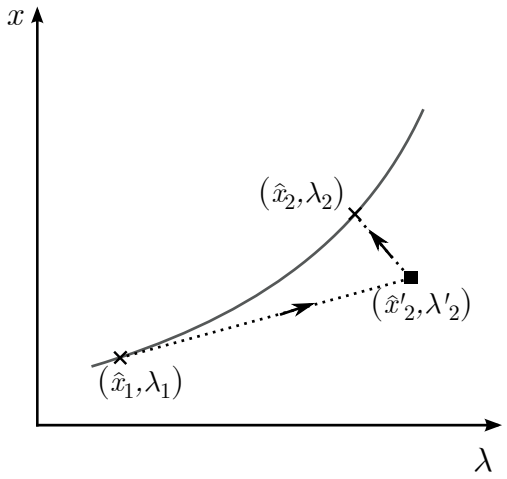

Figure 2.7: Geometric interpretation of the prediction and correction stages of one continuation step.

2.3.4 Step-Length Control

The continuation step-length Δh or Δs of the parametrization step and σ of the prediction one impacts the computational efficiency of the continuation method. Small steps lead to good prediction and consequently few corrector iterations, however the number of power flow solutions required to trace the PV curve up until the MLP increases significantly. If the continuation step-length is too big the opposite happens: less power flow solutions are calculated, but the number of iterations in each correction stage is increased (CHIANG et al., 1995).

Overall, employing a small step length is a safe solution to avoid divergence of the corrector, if the continuation step is too big the prediction may be too far from the actual power flow solution, which in extreme cases may cause divergence of the corrector. This is especially true when EPS equilibrium discontinuities are considered.

When dealing with power flow equations and PV curves, the adequate step length would be bigger in the flat portion of the equilibrium diagram, where the load is relatively low and the states have an approximately linear behavior. Near the MLP this is not true anymore and small steps should be employed so the nose of the PV curve accurately traced and convergence problems are avoided. Implementing this logic during the execution of the CPFLOW is not a simple task, since the voltage profile of the system is not known prior to the execution of the continuation method (CHIANG et al., 1995).

A simple way to implement a flexible step-length control is proposed by (AJJARAPU, 2007), where the continuation step is calculated depending on how many iterations the corrector took to converge for the previous solution. This method is indicated in (2.14).

$$\sigma_{new} = \sigma_{old} \frac{N_{des}}{N_{ite}} \tag{2.14}$$

In this equation, the step length σ increases if the number of corrector iterations N_{ite} is smaller than the desired number N_{des}. The opposite happens when the corrector takes several iterations to converge. Ajjarapu (2007) suggests that 6 iterations should be used as the desired value. However, this choice depends on the power system under analysis.

Other step-length control techniques are available in the literature, this one was selected merely to exemplify the logic behind their formulation.

2.3.5 CPFLOW Implementation and Evolution

The complete CPFLOW successively execute the prediction and correction steps, which results in several power flow solutions for different values of the loading parameter λ that compose the PV curve. As input, it requires one power flow solution, the load growth direction and the static models for power system equipment. In most applications the lower portion of the PV curve is not needed for analysis, in such case the continuation method can halt when the MLP is reached. Algorithm 1 depicts the general implementation of the CPFLOW.

Algorithm 1 *Continuation Power Flow (CPFLOW)*

Step 1: Insert EPS data, its current load, and expected growth direction;
Step 2: Solve the traditional power flow problem for the base case load to obtain the first point of the PV curve;
Step 3: Execute the predictor;
Step 4: Execute the corrector to find another point of the PV curve;
Step 5: Check whether the MLP was reached, if not return to Step 3.

The first time that the prediction stage is performed (*Step 3*), there is only one known power flow solution available. This precludes the utilization of the secant predictor, therefore the tangent one needs to be applied.

The CPFLOW is a robust technique capable to trace PV curves solving the numerical problems related to the ill-conditioned power flow jacobian matrix when the system load is close to the MLP. In the correction stage the Q-limits of the generators can be included, so their effect are considered in the stability analysis. Overall, this method is widely applied to perform static VSA of electric power systems and it has become the standard for comparison when new techniques are proposed in this area (LI; CHIANG, 2008b; CAO; CHEN, 2010).

Besides its advantages, the CPFLOW usually requires the execution of the Newton–Raphson method several times before the MLP is reached. For this reason, it may not

comply with computational requirements of real time applications or ones that require the stability assessment of several EPS configurations, as it is the case of contingency analysis (MANSOUR et al., 2013; YORINO; LI; SASAKI, 2005; JIA; JEYASURYA, 2000). For this reason, several studies deal with the computational efficiency of the CPFLOW. Alongside with time performance, many researchers study the negative effect of Q-limits on the MLP. Interest lie on how to identify such points especially when they cause a bifurcation and how these discontinuities influence the CPFLOW execution.

That is the case of Cao and Chen (2010), they employed arc-length parametrization with the step-length control presented in (2.14) to make the continuation method computationally faster. The authors mentioned that the ideal corrector iterations number should be within two and four. They also proposed the repetition of continuation steps with reduced step-lengths when the system is apparently close to a SIB caused by a Q-limit. With this method it is possible to identify the SIB alongside with the generator that caused it, however, for such purpose it requires a few extra continuation steps.

Taylor and Irving (2008) also employed arc-length parametrization. They proposed that the continuation step Δs should be selected in order to predict which is the next generator that will reach its Q-limit. After estimating which is this generator, the proposed method employs a few continuation steps to find the power flow solution where this limit is met. This is done repetitively until the MLP. According to the authors, this method can estimate the VSM using half of the continuation steps that the traditional CPFLOW would require.

Yorino, Li and Sasaki (2005) enhanced the work of Hiskens and Chakrabarti (1996). They proposed a parametrization that is based on generators Q-limits. After the predictor and corrector, the method results in the next power flow solution where one generator reaches its reactive limit. With this method, all Q-limits that happen before the MLP are calculated. The number of continuation steps required is equal to the number of such constraints, which can be significantly lower than the standard CPFLOW. The main contribution of this paper is that the continuation step is automatically selected to be equal to a continuous portion of the PV curve, i.e. the arc between two discontinuities. Due to its contribution regarding non-smooth characteristics of the PV curve, this method will be described in details in Section 2.4.

Besides these studies that worked mainly with the performance of the CPFLOW, some researches dealt with the robustness of such method. Even though it is considered a robust technique and has been widely used to assess the VSM of electric power system, in some situations the CPFLOW may experience convergence difficulties. Since such situations are of particular interest in this dissertation, these problems are described in the following section alongside with important contributions made by researchers in this area.

2.3.6 Convergence Problems of the CPFLOW

According to Zhao and Zhang (2006), under certain circumstances the CPFLOW is expected to fail when tracing EPS equilibrium diagrams. Its corrector may diverge either before or after the nose of the PV curve, which means that it may compromise an adequate estimate of the VSM.

There are two main types of convergence problems that the continuation power flow may experience: one caused by inadequate prediction and/or step-length size and another due to the parametrization employed (ZHAO; ZHANG, 2006; NETO; ALVES, 2010).

The first problem is a direct outcome of an inaccurate prediction. For the corrector to converge the initial guess of bus voltages magnitudes and angles need to be within the convergence neighbourhood of the desired power flow solution. In other words, the predicted solution should not lie too far from the equilibrium point that satisfies the parametric equation, otherwise divergence may happen when trying to find this point with numerical procedures (SUNDHARARAJAN et al., 2003; XU; WANG; AJJARAPU, 2012).

One situation that may yield poor prediction accuracy is when inadequately big continuation steps are used. By its nature, this problem can be easily solved with a proper step-length selection and control. However, it can be significantly aggravated when equilibrium discontinuities are considered. Predictors are not capable to account for the effect of such power system sudden changes, in which situation they may result in poor approximations that, in extreme cases, may cause divergence of the corrector (XU; WANG; AJJARAPU, 2012). As a consequence of equilibrium discontinuities, simply reducing the step-length may not solve divergence problems.

The second problem is related with the parametrization employed. Two important aspects need to be analysed here: (i) whether the inclusion of the parametric equation in the power flow problem solves the ill-condining of the power flow jacobian matrix near the MLP and (ii) if there is a power flow solution that satisfies the parametric equation. Both this situations are directly related to the parametrization process and are independent of the step-length used (ZHAO; ZHANG, 2006).

Convergence problems may arise with both local and arc-length parametrization and there is no consensus whether which one is more robust. Chiang et al. (1995), Li and Chiang (2008c) openly defend the arc-length parametrization. They argue that even with inaccurate predictors this parametrization can reach convergence, which means that bigger continuation steps can be taken. Indeed such parametrization is widely employed, examples of its application can be seen in (FLUECK; DONDETI, 2000; LI; CHIANG, 2008a; CAO; CHEN, 2010). On the other side, Ajjarapu (2007), Alves et al. (2000), Canizares and Alvarado (1993) support the local parametrization, attesting that power systems with local voltage instability characteristics may experience divergence when arc-length parametrization is used.

The local voltage instability mentioned is characterized when only a few buses of the

power system suffer unbounded voltage drop, while others can keep their magnitude. In this situation, some buses have the traditional PV curve profile (Figure 2.8(a)), while for others the lower portion of the PV curve have a similar slope to the upper one (Figure 2.8(b)) (ZHAO; ZHANG, 2006).

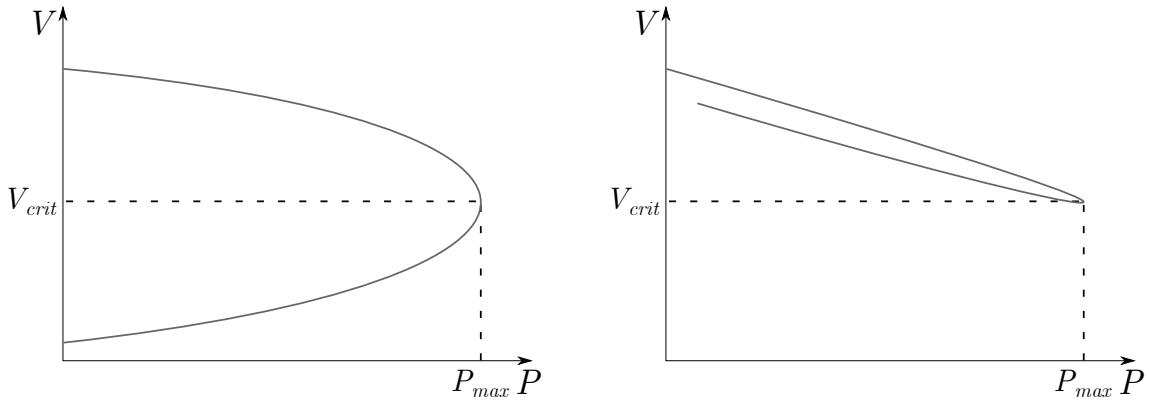

(a) Bus prone to voltage drop. (b) Bus capable to withstand voltage drop.

Figure 2.8: Voltage profile of different buses in a power system that displays local voltage instability phenomena.

This inclined acute angle in the voltage profile of some buses can indeed cause convergence problems for the arc-length parametrized CPFLOW due to ill-conditioning of its Jacobian matrix (ZHAO; ZHANG, 2006; NETO; ALVES, 2010). Nevertheless, the local parametrization may also go through divergence in this situation if an inadequate load parameter is selected. For example, suppose that the selected local parameter is the voltage magnitude of the bus with a profile similar to that of Figure 2.8(b), then, the corrector may try to find a power flow solution for a non-existing value of such voltage, i.e. a value smaller than V_{crit}. In this case, there is no power flow solution that satisfies the parametric equation and the continuation method diverges.

For the author of this dissertation, there is not a obvious choice between this two parametrizations to assure convergence of the CPFLOW.

In fact, Zhao and Zhang (2006) acknowledged the difficulties and advantages of the two traditional parametrization techniques presented here. These authors ended up proposing that these parametrizations should be used interchangeably, whenever one fails the other should be employed. In case of divergence, they go even further, proposing that distinct EPS states should also be tested as the local parameter.

Since the parametrization dictates the convergence of the continuation method, some studies propose new parametrizing equations to solve possible divergence of the CPFLOW. For instance, Neto and Alves (2010) parametrize the PV curve with the slope of one straight line in the plane of the load parameter λ and the sum of bus voltage magnitudes. Alves et al. (2000) use the total active power loss of the EPS as the parameter for the continuation process.

To deal with possible convergence problems related with inadequate continuation step-lengths and poor prediction, Xu, Wang and Ajjarapu (2012) proposed a convergence monitor for the first iteration of the correction stage, which is used to select an adequate continuation step. The authors went further to include in the predictor an estimate to whether there is PV curve discontinuity before the next power flow solution. If that is true, then the step length is significantly reduced to avoid problems caused by poor prediction due to the non-smoothness of the EPS equilibrium diagram.

Besides the aforementioned work, Yorino, Li and Sasaki (2005) also dealt with discontinuities that exists in PV curves, particularly the generators Q-limits. Since this work is the basis for future discussions it deserves its own section.

2.4 Q-limit Guided CPFLOW Proposed by Yorino et al. (2005)

Yorino, Li and Sasaki (2005) proposed a predictor/corrector scheme to find the power flow solutions at which generators reach their reactive limits as the load increases in a given direction. The method calculates the successive Q-limits that happen in the PV curve prior to the MLP. First, it is predicted what is the next generator that will reach its reactive constraint. Then, the power flow solution where such limit is reached is calculated via a correction stage. Just like the conventional CPFLOW, this method is based on the repetition of a predictor and a corrector.

The prediction and correction stages proposed will be described in the following sections along with a mathematical procedure designed to identify when a Q-limit causes instability, i.e. when they are responsible for a Structure Induced Bifurcation (SIB).

2.4.1 Prediction

Differently from the conventional CPFLOW, the predictor is designed to estimate what is the next generator that will find its Q-limit, then at which load level this happens and, finally, the EPS bus voltages and angles at this point. For this purpose a linear predictor is employed based on the tangent vector calculated with the linear system (2.9), that is rewritten bellow:

$$0 = \frac{\mathrm{d}\mathbf{f}(\hat{x})}{\mathrm{d}\hat{x}}\Delta\hat{x} + \hat{b}\Delta\lambda$$

The procedure to solve this system was already described in Section 2.3 and it will not be repeated here. It is important to remember that it results in the tangent vector $(\Delta\hat{x}, \Delta\lambda)$ of the EPS equilibrium diagram at a known power flow solution $(\hat{x}_1, \lambda_1)$.

Using another linear approximation it is possible to determined what is the expected variation in the reactive power generated by each unit:

$$\Delta Q_{Gi} = \frac{\mathrm{d}Q_{Gi}(\hat{x}, \lambda)}{\mathrm{d}\hat{x}}\Delta\hat{x} + \frac{\mathrm{d}Q_{Gi}(\hat{x}, \lambda)}{\mathrm{d}\lambda}\Delta\lambda \tag{2.15}$$

where, $Q_{Gi}(\hat{x}, \lambda)$ is the traditional power flow equation that relates the generator i reactive power injection with the EPS states. The derivative of such equation can be easily calculated and when it is evaluated at the known solution $(\hat{x}_1, \lambda_1)$ it allows the estimation of ΔQ_{Gi}. This value needs to be calculated for every generator that can meet its reactive power constraint.

After this approximation, it is possible to predict what is the generator that is closer to its reactive limit. This is done by calculating the linear distance between the known power flow solution and the Q-limit with (2.16).

$$\sigma_i = \frac{Qmax_{Gi} - Q_{Gi}(\hat{x}_1, \lambda_1)}{\Delta Q_{Gi}} \tag{2.16}$$

Here, $Qmax_{Gi}$ is the maximum reactive power output of generator i. Note that, σ_i represents the linear distance between the given power flow solution and the point where generator i will reach its limit. If the reactive power variation (ΔQ_{Gi}) is small, then the Q-limit point is expected to be far, whereas if the reactive power generation Q_{Gi} is close to $Qmax_{Gi}$, then such constraint point is expected to be near the known solution.

It is reasonable to assume that the generator associated with the smallest value of σ_i is the one that is closer to reach its limit. It is worth pointing out that this is based on a linear approximation, which can not guarantee that the correct Q-limit is identified.

The power system bus associated with the smallest value of σ_i is selected, so its voltage magnitude can be used as the local parameter in the correction stage. After this selection, such bus will be referred as the pivot bus and indicated with the latter p.

After the next Q-limit is identified and the pivot bus is selected, the predictor proceeds to estimate at which loading level λ and EPS states this happens. For this purpose, the continuation step-length employed will be the value of σ_i associated with the pivot bus.

$$\sigma = \min_{i \in G} \sigma_i \tag{2.17}$$

In this equation, the set G comprises all generators that could reach their reactive power limit. With this continuation step the estimated power system states can be calculated with the linear approximation used in the tangent prediction (2.12) and is repeated bellow:

$$\hat{x}'_2 = \hat{x}_1 + \sigma\Delta\hat{x}$$
$$\lambda'_2 = \lambda_1 + \sigma\Delta\lambda$$

In the situation where the Q-limits are the only discontinuities considered in the EPS equilibrium diagram, if the next generator Q-limit is correctly foresaw, then the predicted

power system states are expected to be accurate, since there is no discontinuity between the known solution and the desired one. This contributes to reduce the number of iterations required by the corrector and may enhance its chance to converge. In this situation, the continuation step is automatically selected to be the length of the smooth arc of the EPS equilibrium diagram.

After the pivot bus is selected and the predicted states are calculated, the procedure moves over to the correction stage.

2.4.2 Correction

The main objective here is to find the power system states where the predicted generator reaches its Q-limit. The power flow solutions are solved with the Newton-Raphson method starting from the predicted voltages and angles $(\hat{x}'_2, \lambda'_2)$ and resulting in the equilibrium point where the pivot bus changes from PV to PQ type $(\hat{x}_2, \lambda_2)$.

This is possible noticing that at the constraint point, where the generator at bus p meets its maximum reactive power supply, the pivot bus satisfies simultaneously the conditions of a PV and a PQ bus. Mathematically this means that:

$$\begin{aligned} V_p^{set} - V_p &= 0 \\ Qmax_{Gp} - Q_{Gp} &= 0 \end{aligned} \tag{2.18}$$

where V_p^{set} is the specified voltage level for the generator p when it is modelled as a PV bus and $Qmax_{Gp}$ is its maximum reactive capability.

To find the point where these two equations are satisfied, the generator bus is considered to be of PQ type with reactive power injected equal to $Qmax_{Gp}$ and the power flow solutions are simultaneously solved with equation:

$$V_p^{set} - V_p = 0 \tag{2.19}$$

This is the parametric equation of the method proposed by Yorino, Li and Sasaki (2005) and it is conceptually similar to the one utilized in the locally parametrized CPFLOW. However, here, such equation is employed to find the power flow solution where the predicted generator reaches its Q-limit.

2.4.3 Identification of Structure Induced Bifurcation

Since the method described here finds the discontinuities caused by generators constraints, Yorino, Li and Sasaki (2005) go on to propose a mathematical algorithm to identify if a particular Q-limit causes instability, meaning if such point is a SIB.

To achieve such purpose, two conditions that characterize if a power flow solution lie in the stable or unstable portion of the PV curve are employed. For that, these conditions use the tangent vector $(\Delta\hat{x}, \Delta\lambda)$ and ΔQ_{Gp}.

They are based on the simple consideration that, in the upper and stable portion of the PV curve, the inequalities (2.20) need to be satisfied at least for generators that are expected to reach their Q-limits. After the MLP, the slope of the PV curve is expected to change for such buses, therefore the two inequalities are not satisfied anymore, which characterizes equilibria in the bellow and unstable part of the PV curve.

$$\begin{aligned} \Delta V_p &\leq 0 \\ \Delta Q_{Gp} &\geq 0 \end{aligned} \tag{2.20}$$

Those inequalities can be easily justified for stable equilibria. If a generator is going to reach its reactive constraint, then its reactive power is expected to increase as the load grows, while its bus voltage is held constant ($\Delta Q_{Gp} > 0$ and $\Delta V_p = 0$). If it has already met its limit, then it is not capable to increase its reactive power supply nor to control its bus voltage, which is expected to fall when λ increases ($\Delta V_p < 0$ and $\Delta Q_{Gp} = 0$).

After the correction stage finds a power flow solution $(\hat{x}_2, \lambda_2)$, two conditions are performed to identify if this power flow solution is a SIB. The first condition is related to whether the system equilibrium is stable after the Q-limit happened. The second condition evaluates the equilibrium points prior to the generator constraint.

Condition 1

For this test, the power flow equations employed are the ones when the pivot bus is set to be of PQ type, which represents the power system after the Q-limit. Here, the voltage inequality in (2.20) is tested, since the reactive supply of the unit under analysis is held constant. Therefore, the EPS equilibrium points ensuing the Q-limit are stable if $\Delta V_p < 0$.

To calculate this voltage variation, the tangent vector $(\Delta\hat{x}, \Delta\lambda)$ to the power flow solution $(\hat{x}_2, \lambda_2)$ needs to be calculated. This is done solving the linear system in (2.21), remembering that the procedure to do so was already described in Section 2.3.1.

$$0 = \left.\frac{\mathrm{d}\mathbf{f}(\hat{x})}{\mathrm{d}\hat{x}}\right|_{(\hat{x}_2,\lambda_2)}^{p \text{ is PQ}} \Delta\hat{x} + \hat{b}\Delta\lambda \tag{2.21}$$

ΔV_p is one component of the state vector $\Delta\hat{x}$ that is calculated with the above linear system. To asses whether such voltage magnitude is increasing or decreasing all that is necessary is to observe what is the sign of ΔV_p.

Considering that the load is growing ($\Delta\lambda > 0$) and remembering that such linear approximation characterizes the power system after the Q-limit happened, then if ΔV_p is negative the power flow solutions after $(\hat{x}_2, \lambda_2)$ lie in the upper portion of the PV curve, otherwise they are in the bellow one. Two possibilities arise in the latter case: the Q-limit is responsible to cause a bifurcation or the equilibrium point associated with it is unstable.

This means that (2.22) is a necessary but not sufficient condition for the Q-limit to be a SIB. This inequality and the whole procedure described to test it comprise Condition 1

to assess if the power flow solution under analysis is a bifurcation.

$$\Delta V_p > 0 \tag{2.22}$$

Condition 2

This condition deals with the power system configuration right before the unit meets its Q-limit. This means that the power flow equations are constructed considering such generator as a PV bus. This time the reactive power inequality in (2.20) is under analysis, since the generator bus voltage is constant.

For this condition, the linear system used to calculate the tangent vector is (2.23).

$$0 = \left.\frac{\mathrm{d}\mathbf{f}(\hat{x})}{\mathrm{d}\hat{x}}\right|^{p \text{ is PV}}_{(\hat{x}_2,\lambda_2)} \Delta\hat{x} + \hat{b}\Delta\lambda \tag{2.23}$$

Even though they are similar, this linear system is slightly different than the one of Condition 1. One equation of the power flow model changes. In the previous formulation, the pivot bus (p) was considered a PQ bus; now it is a PV one. This yields a different power flow jacobian and consequently a distinct tangent vector $(\Delta\hat{x}, \Delta\lambda)$.

This time the interest does not lie in a voltage variation, but rather in a reactive power one. This can be calculated from the tangent vector with equation (2.24), which was rewritten from (2.15).

$$\Delta Q_{Gp} = \left.\frac{\mathrm{d}Q_{Gp}}{\mathrm{d}\hat{x}}\right|^{p \text{ is PV}}_{(\hat{x}_2,\lambda_2)} \Delta\hat{x} + \left.\frac{\mathrm{d}Q_{Gp}}{\mathrm{d}\lambda}\right|^{p \text{ is PV}}_{(\hat{x}_2,\lambda_2)} \Delta\lambda \tag{2.24}$$

Once again considering that the load is growing before the Q-limit is reached ($\Delta\lambda > 0$), then the reactive power supplied by this generator is expected to raise ($\Delta Q_{Gp} > 0$) if the equilibrium before the power flow solution $(\hat{x}_2, \lambda_2)$ is stable. This situation happens in two possible scenarios: (i) the point $(\hat{x}_2, \lambda_2)$ itself is a stable equilibrium or (ii) the Q-limit associated with it causes a SIB. If $\Delta Q_{Gp} < 0$, then the critical point has passed and the power flow solution under analysis is an unstable one.

As a consequence of that, a necessary but not sufficient condition for a SIB is:

$$\Delta Q_{Gp} > 0 \tag{2.25}$$

This inequality together with the procedure to reach it compose Condition 2 to assess if a Q-limit is a SIB.

Summary of Conditions 1 and 2

Condition 1 deals with the power flow solutions that immediately follow the calculated Q-limit in $(\hat{x}_2, \lambda_2)$, while Condition 2 is associated with the equilibrium points immediately before such solution.

If (2.22) is true, then the power flow solutions after the Q-limit are in the unstable portion of the PV curve. If (2.25) is true, then the equilibria before this constraint is stable. This interpretation is graphically represented in Figure 2.9.

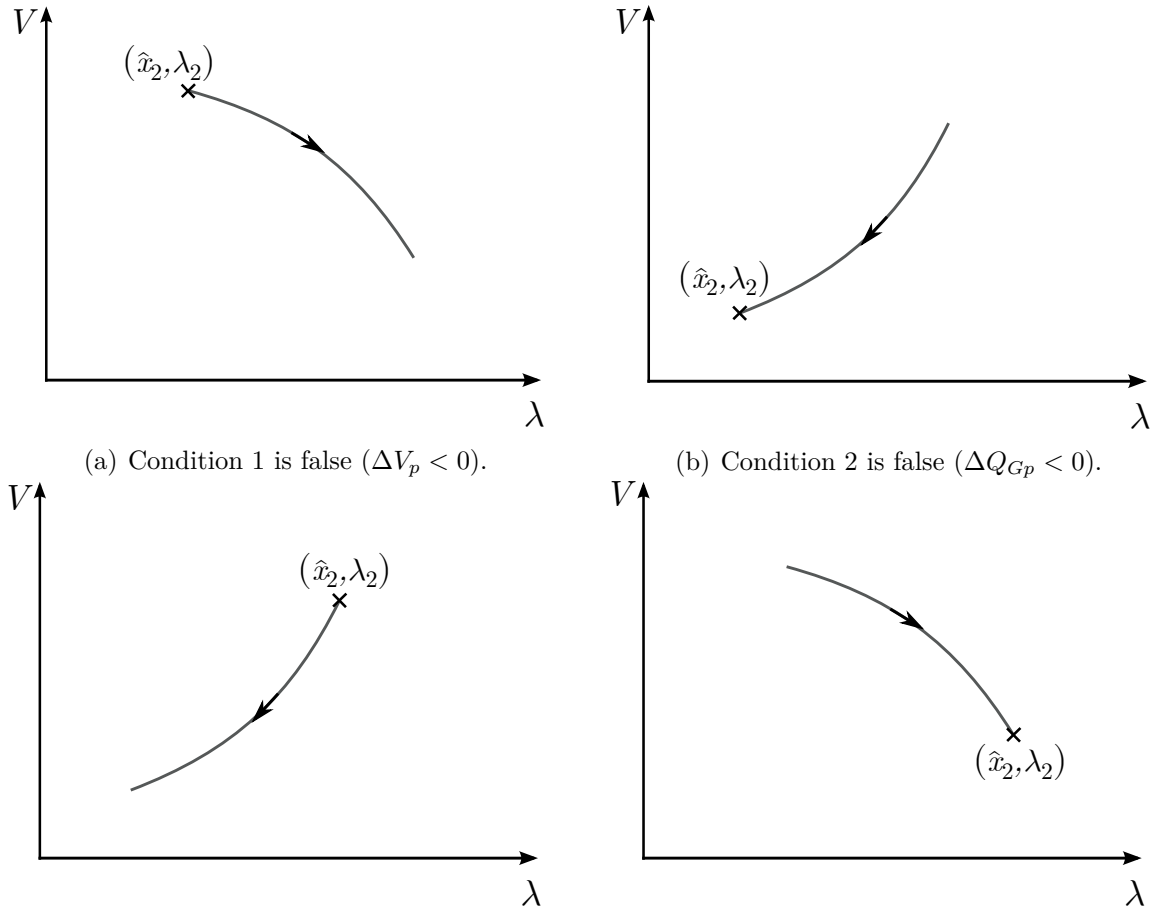

(a) Condition 1 is false ($\Delta V_p < 0$).

(b) Condition 2 is false ($\Delta Q_{Gp} < 0$).

(c) Condition 1 is true ($\Delta V_p > 0$).

(d) Condition 2 is true ($\Delta Q_{Gp} > 0$).

Figure 2.9: Graphical interpretation of the conditions proposed to identify if a Q-limit is a structure induced bifurcation.

From this analysis, it is possible to conclude that if Conditions 1 and 2 are simultaneously satisfied, then the power flow solution $(\hat{x}_2, \lambda_2)$, where the generator at the pivot bus reaches its Q-limit, is a Structure Induced Bifurcation (SIB).

2.4.4 Implementation and General Aspects of the Method Proposed by Yorino et al. (2005)

Just like any continuation method, the general idea of the procedure described here is to repeat the predictor and corrector until the MLP is reached. This method successively finds the PV curve points where generators reach their reactive limits.

Two main drawbacks of this procedure directly follow its main characteristic. First, when the power system is subject to a SNB, it is not capable to trace the voltage profile near the MLP, since Q-limits may not be available in this region. Second, if the EPS have few generators prone to meet their Q-limits, then continuation steps become big and the

predictor may be prohibitively inaccurate. In the extreme case where no generators reach their constraint, the method is bound to diverge in its the first continuation step.

The second problem is innate to Yorino's method and when it arises other techniques need to be applied. The first problem is solved by the author: the method is designed to execute standard techniques to find the MLP (like the traditional CPFLOW) after an unstable Q-limit equilibrium point, that is not a SIB, is found. This procedure and the general implementation of this method are indicated in Algorithm 2.

Algorithm 2 *Procedure to find Q-limits as Proposed by Yorino (2005)*

Step 1: Insert EPS data, its current load, and expected growth direction;
Step 2: Solve the traditional power flow problem for the base case load to obtain the first point of the PV curve;
Step 3: Execute the predictor;
Step 4: Execute the corrector to find a generator Q-limit;
Step 5: Check Condition 1: if false return to Step 3, if true continue to Step 6;
Step 6: Check Condition 2: if false jump to Step 7a, if true jump to Step 7b;
Step 7a: Run the traditional CPFLOW to find the SNB between the last two Q-limits;
Step 7b: The last Q-limit is identified as a SIB.

This method can be interpreted as a locally parametrized CPFLOW, where the local parameter is selected accordingly to the generators reactive power limits.

In the opinion of the author of this dissertation, the most striking contribution of this method is that the continuation step is automatically selected to be the length of one smooth arc of the PV curve. In other words, if the predictor correctly estimates each one of the Q-limits, then the power flow solutions found are the discontinuities in the EPS equilibrium diagram. In this situation, every interval between two solutions is necessarily continuous and smooth. With this, the predictor is expected to be accurate and the corrector is unlikely to diverge, which is particularly true if a power system is subject to the occurrence of several Q-limits not far from each other.

2.5 Final Remarks

The general ideas of the method designed by Yorino, Li and Sasaki (2005) will be the base of the proposed technique to handle sudden load variations in EPS equilibrium diagrams. The traditional CPFLOW described here is the standard technique to perform VSA in a static framework and will serve for comparison purposes to evaluate the adequacy of the method proposed in this dissertation.

Chapter 3

Sudden Load Variations on Static Voltage Stability Analysis

A bulk power system comprises a wide range of devices that influence its steady state behavior. During PV curve tracing, as the load increases some of these devices may suddenly change their parameters according to the EPS states. This is the case of OLTC transformers, switchable shunt capacitors, excitation limiters of generators and ULS protection schemes (XU; WANG; AJJARAPU, 2012). Those examples were not selected randomly, they represent discrete changes in the system that, in turn, cause discontinuities in its equilibrium diagram. This means that they are responsible to modify the PV curves, so they are not the basic smooth and continuous curves expected.

Of the given examples, switchable capacitors, OLTCs and load shedding schemes are capable to increase bus voltages and may contribute to increase the MLP. However, generator excitation limiters have the opposite effect and may even cause voltage instability.

When using the CPFLOW, such discrete controls are considered during the corrector stage, where conditional tests are employed to verify at every iteration whether or not controlled variables reach specified limits (ALVES et al., 2000). For example, whenever a generator supplies more reactive power than its Q-limit, then the bus type is switched from PV to PQ type.

The prediction stage is based on curve fitting approximations and, therefore, cannot take into account discrete changes on EPS parameters. Therefore, these controls worsen the accuracy of the predicted solution and increase the number of iterations required by the corrector of the CPFLOW.

Continuation methods are formally proposed to trace solutions of a set of non-linear smooth equations while one of its parameter varies continuously. When the aforementioned sudden parametric changes are considered, the power flow equations change whenever a limit is reached. This makes the PV curve non-smooth and discontinuous.

Although this could be a problem, these changes do not present major difficulties to the traditional CPFLOW. It is common practice to include them during VSA of a power

system. Their main practical consequence is an increase of iterations required by the corrector to converge.

Nevertheless, this chapter will evidence that when the system undergo severe discrete variations, the discontinuities derived from it can cause convergence problems for the CPFLOW. This may be the case of sudden load variations that power systems may face. Practical examples studied in the following chapters will be the undervoltage mandatory disconnection of DG units and Undervoltage Load Shedding (ULS).

Besides these two applications, the discussion in this chapter is suitable to evaluate the impact of any discrete load step in transmission systems caused by undervoltage protection schemes. It particularly focuses on situations when demand switching is distributed throughout the network due to local voltage measurements. Hopefully, the numerical results available in the next two chapters will evidence the usefulness of the discussion provided here.

In the literature, Zhao and Zhang (2006), Neto and Alves (2010) studied possible convergence problems that the traditional CPFLOW may experience. Both of them go on to propose particular parametrization techniques to enhance the convergence rate of the continuation method. However, they do not include any discontinuity that may be present in the PV curve. Alves et al. (2000), went a little further comparing several parametrization techniques while accounting for the generator reactive limits and OLTCs, but this work fails to deliver a complete analysis of the effects of these sudden changes on the convergence of the continuation technique employed.

The work presented by Li and Chiang (2008b) dealt with non-linear characteristic of loads and its effect on PV curves. Nonetheless, the author refrained from considering sudden change in EPS demand, which still results in continuous equilibrium diagrams.

Regarding discontinuities caused by contingencies, it is possible to mention the papers of: Flueck and Dondeti (2000), Sundhararajan et al. (2003), Song, Baik and Lee (2006). The last authors developed a convergence monitor to assess whether or not it is possible to obtain power flow solutions for the incomplete system, starting from the complete network solution. Sundhararajan et al. (2003), Flueck and Dondeti (2000) employed a continuation method that uses a smooth change in the tripped line parameter to track the post-contingency configuration. Although not originally proposed to asses the effect of load steps in PV curves, conceptually those papers could be employed to do so. Their main inconvenience is that they need to be applied for one known parametric system discontinuity. Therefore, they are not suitable to achieve the objectives of this work, that concern successive and distributed load discrete changes throughout the transmission system.

Perhaps the method proposed by Yorino, Li and Sasaki (2005), described in Section 2.4,is the most appropriate technique to deal with discrete system changes while tracing PV curves. It finds successive discontinuities in the Jacobian of the power flow equations, i.e.

in the derivative of EPS equilibria. This is essentially different from sudden load changes that cause discontinuities in the power system voltages and angles.

Finally, the paper that is closer to the problem under study here, was done by Xu, Wang and Ajjarapu (2012). They considered simultaneously switching capacitors and generator Q-limits, selecting adequate continuation step-lengths to avoid possible convergence problems. However, this work did not provide a detailed analysis of the effect of sudden parametric variations in the CPFLOW performance and robustness, particularly in scenarios where such discontinuities are severe.

In this chapter, a qualitative description of the PV curve discontinuities caused by sudden load variations will be provided in section 3.1. After, a parametrization technique will be proposed to deal with such discontinuities in section 3.2. Finally, in section 3.3, the final remarks of this chapter are presented.

3.1 PV Curve Discontinuities Produced by Sudden Load Variations

Considering three discrete load levels at a particular bus of a transmission system, which will be referred as low, medium and high. As obvious as it may be, it is necessary to point out that the low level power consumption is smaller than the medium one that, in turn, is lower than the high one. In static analysis, the highest demand levels are expected to have smaller voltage magnitudes and MLP, effect that is illustrated in Figure 3.1.

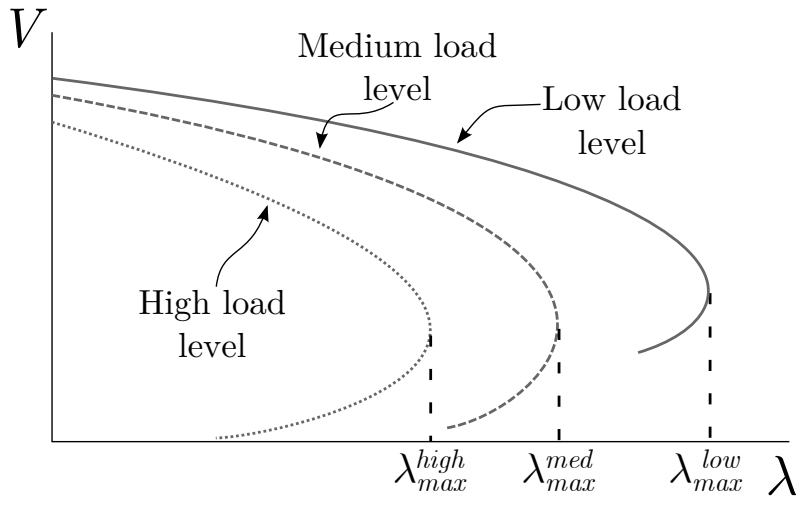

Figure 3.1: PV curve effect of three different discrete load levels at a particular transmission system bus.

If load switching occurs between these three levels due to an undervoltage protection scheme, then the power system equilibrium point will experience a jump between PV curves, which characterizes state discontinuities. This effect is illustrated in Figure 3.2, considering that first the load suddenly increases from the medium level to the high one

and then it reduces to the low one at. Suppose that, at the bus under consideration, this is possible because a generator is disconnected when its voltage magnitude reaches V_{off1} and afterwards some load is shed at the voltage V_{off2}. The equilibrium diagram of the EPS is now given by the solid curve and is inherently discontinuous due to the undervoltage load switching.

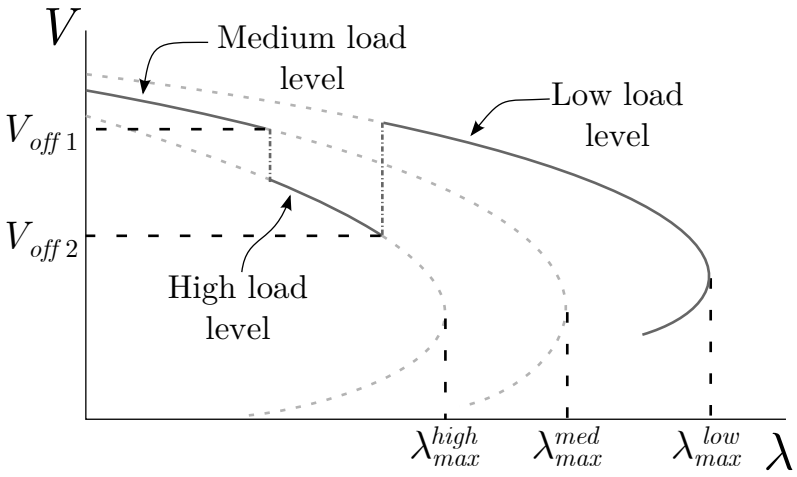

Figure 3.2: Discontinuities in power systems equilibrium diagrams caused by sudden changes in load. When the bus voltage magnitude reaches V_{off1} load is switched on, when this value is V_{off2} it is switched off.

Although these discontinuities are essentially load variations for the bulk power system, they do not take place in the abscissa of the equilibrium diagram that represents the system loading. That happens because the scalar λ relates the base case loading to the load of the whole system. In other words, as λ varies the system demand changes at all buses accordingly to the growth direction $\hat{b}$, just like it was described in Section 2.2. A load switching at a single bus does not entail a change in any other part of the system nor in the loading parameter λ. Referring to the formulation of Section 2.2, what is modified is the base case demand at the bus that experiences the sudden change, that is, P_{L0k} and Q_{L0k}, where k is the referred bus. While the rest of the system does not undergo a load variation, the parametric modification at a single bus is responsible to change the power system states causing the discontinuities observed.

When the base case load changes, one important aspect of PV curve interpretation is also modified. A EPS with a known base case loading, that is subject to a different scenario of undervoltage load switching, may end up supplying a different total power for the same values of λ. This happens because the base case of the system may have been modified, which would result in a distinct relation between λ and the total load connected. During the PV curve scrutiny this means that the same value of λ may be related to a different total load supplied, i.e. that the relationship between λ and the total active load is not monotonic.

This can be easily understood considering that a single load is turned on at a particular value of λ. Since the system demand in any other bus does not change, then λ is still

constant. However, the total load connected to the system was increased, due to the load that was switched on. This means that the scalar λ is equal right before and after the demand is modified, regardless of the fact that for these two points the total active load connected to the system changed.

This aspect will be discussed further in the following chapters that present numerical results.

The impact of load discrete variations on the MLP could be evaluated effortlessly, if the loads that are turned on/off were known beforehand. Unfortunately, when the undervoltage protections schemes are distributed around the power system, such information is not available prior to the PV curve tracing, which will depend on the effect of these protections. This is the case of the two numerical examples given in the following chapters: they are the mandatory disconnection of distributed generators and disperse undervoltage load shedding.

As a result of that, these undervoltage protection schemes need to be contemplated during the execution of the continuation power flow, like it is already done with generator reactive power limits, OLTCs and switchable shunt capacitors.

The traditional parametrization techniques employed in the CPFLOW are capable to deal with the discontinuities caused by Q-limits of generators (CHIANG et al., 1995). Such constraints cause structural changes in the Jacobian of the power flow equations that, in turn, are responsible for a sudden modification in the derivative of the PV curve. This is in nature different from the load switches that originate discontinuities in EPS states.

Much more similar to sudden load changes are the discontinuities caused by OLTCs and switchable shunt capacitors. Their effect can also be studied with traditional CPFLOW, just like it was done by Alves et al. (2000), Xu, Wang and Ajjarapu (2012). Although structurally similar to the discontinuities under analysis here, they are expected to be quantitatively different, which is particularly true when big blocs of loads are expected to be turned on and off.

Before moving on to propose a parametrization technique capable of handling the discontinuities caused by severe load switching, it is necessary to anticipate whether the traditional CPFLOW is capable to deal with them.

For the local parametrization, it was seen that the correction step solves the power flow equations in such a way that the local parameter steps Δh from the previously known equilibrium point.

This parametrization should not entail any convergence difficulty while the continuation parameter is λ, since there is a power flow solution for every value it can assume before the MLP, as can be seen in Figure 3.3 whether the load is stepping up or down. Independently of the discontinuity there is always a available power flow solution for the continuation method to converge to.

However, near the nose of the PV curve the adequate load parameter is either a bus

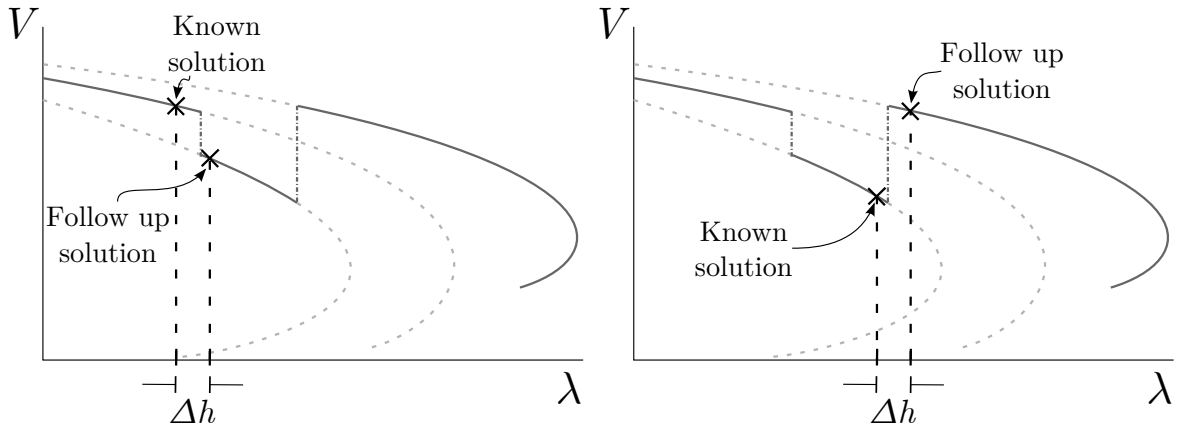

(a) Load stepping up. (b) Load stepping down.

Figure 3.3: Qualitative continuation step when the local parametrization is employed while the local parameter is the system loading (λ).

voltage magnitude or angle. This case is illustrated in Figure 3.4 and its analysis is divided whether the load steps up or down.

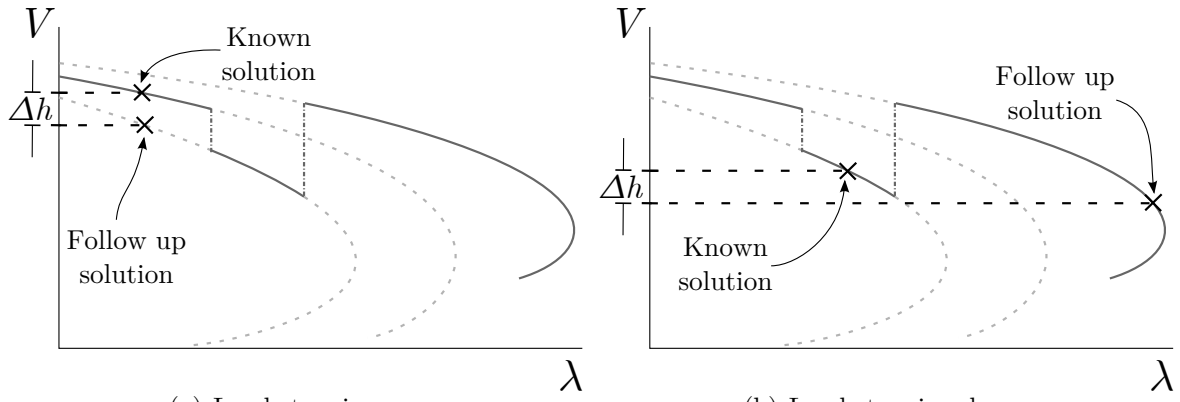

(a) Load stepping up. (b) Load stepping down.

Figure 3.4: Qualitative continuation step when the local parametrization is employed while the local parameter is a power system state.

The first case can be seen in Figure 3.4(a). Depending on the continuation step (Δh) there is a chance that the corrector looks for a solution between the curves where the system is with and without the load. In this situation, the solution that satisfies the parametric equation lies in the portion of the PV curve that does not illustrate the actual voltage profile of the system, i.e. the solid trace. Although this is not ideal, it allows the continuation process to proceed towards the MLP. A worse situation could be caused by the inaccuracy of the predictor, since curve fitting techniques could not possibly predict the follow up solution. In extreme cases this could lead to divergence of the corrector.

Further observing Figure 3.4(a) it is possible to expect that these problems could be solved by increasing the continuation step. This is not ideal because an adequate step size is system dependent and it is generally unknown before executing the CPFLOW. Besides that, big steps worsen the predicted solution which can also lead to divergence.

The second case, when the load steps down, is shown in Figure 3.4(b). This time, if the

corrector converges, the power flow solution can only lie in the solid trace that comprises the EPS equilibria. Nevertheless, the parametric equation is designed to reduce the bus voltages magnitude, which disguises the actual voltage rise caused by the sudden load reduction. Furthermore, this discontinuity may also cause divergence of the corrector due to the predictor accuracy, since it is not capable to anticipate the load switch nor its effect on EPS states.

Converge problems may also happen when the arc-length parametrization is employed, a situation that is illustrated in Figure 3.5, whether the load steps up or down.

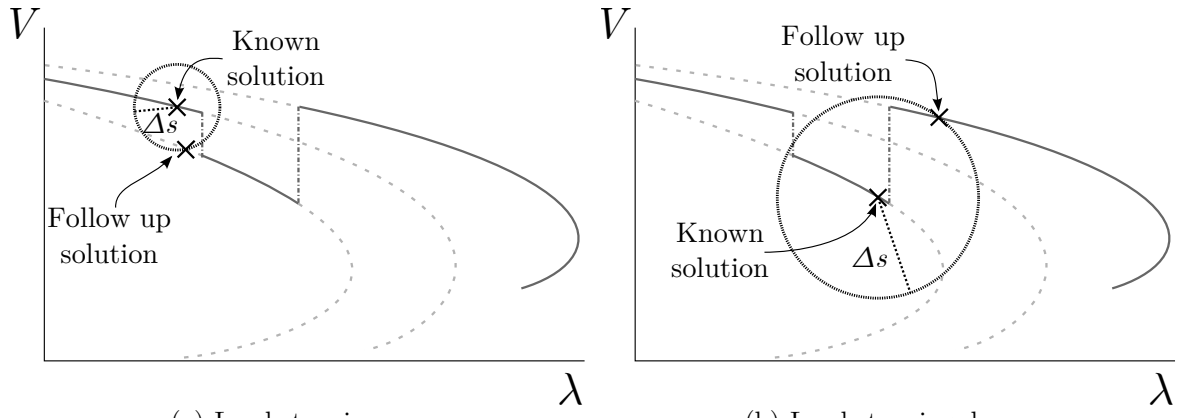

(a) Load stepping up. (b) Load stepping down.

Figure 3.5: Qualitative continuation step when the arc-length parametrization is employed.

This time as well, corrector divergence may follow from poor prediction accuracy caused by the discontinuity.

When the load steps up, depending on the continuation step Δs, the power flow solutions that satisfy the parametric equation may not be located in the actual voltage profile of the system. In this case, the continuation method can proceed to find the MLP, however the PV curve does not depict the equilibrium points of the EPS anymore.

A more critical problem could happen if the continuation step Δs is too small. This situation is indicated in Figure 3.6, where it is noticeable that there is no power flow solution that satisfy the arc-length parametric equation. The lack of available solution would inevitably entail divergence of the correction stage.

Just like the local parametrization, the convergence problems mentioned here could be solved if the continuation step is big enough. However, the adequate arc-length depends on the problem under analysis and it is unknown a priori.

From this discussion it is possible to conclude that discontinuities caused by sudden load variations disqualify the traditional concept that smaller continuation steps are more robust than bigger ones. Nevertheless, large steps may not be a viable solution to assure convergence, after all they worsen the predicted solution accuracy, a circumstance that is magnified by the fact that the predictor is not capable to account for these discontinuities.

With that in mind, to study the effect of sudden load variations, the CPFLOW requires an adequate selection of the continuation step to avoid convergence problems. This choice

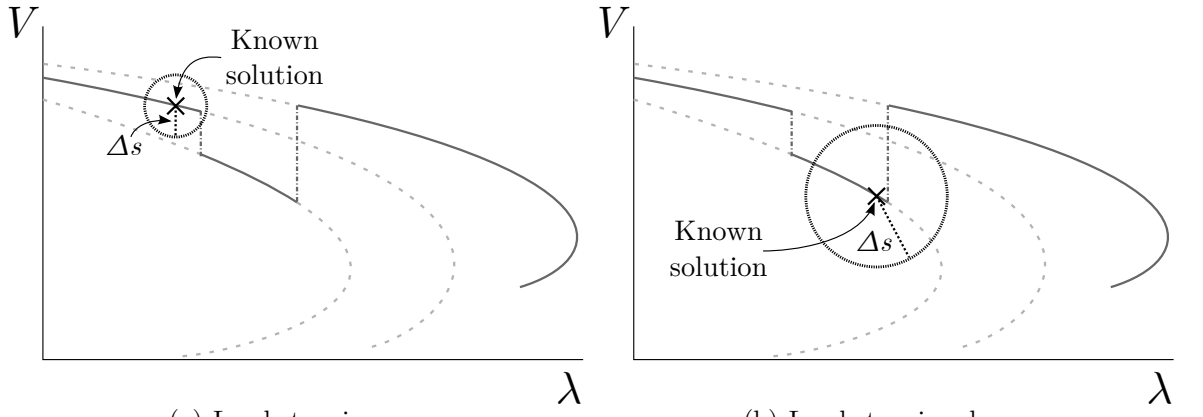

(a) Load stepping up. (b) Load stepping down.

Figure 3.6: Qualitative continuation step when the arc-length parametrization is employed. The arc-length (Δs) is so small that there is no power flow solution that satisfies the parametric equation, which causes divergence of the CPFLOW.

is complex and it depends on the power system under analysis and on the size of the load blocks that are turned on/off.

In extreme situations, there may not be a step length suitable to trace PV curves considering the discontinuities under analysis. This would happen when such discontinuities are big enough to require continuation steps so large that the whole continuation process is rendered impossible due to lack of prediction precision. This indicates that the traditional CPFLOW may be inadequate to study the load sudden changes mentioned here.

The convergence problems foresaw here will be verified in the following chapters that present numerical results.

3.2 Proposed Predictor/Corrector Scheme to Handle Sudden Load Variations

The Q-limit guided continuation method proposed by Yorino, Li and Sasaki (2005) is the conceptual basis for the Predictor/Corrector Scheme proposed here to deal with sudden load variations. Perhaps the main insight of the referred paper is to predict the next discontinuity that will be present in the PV curve and set the continuation step to find such point. In this case, it is improbable that the continuation process will find convergence problems due to equilibrium discontinuities, since two successive power flow solutions will likely be separated by a continuous arc of the curve.

This idea will be employed to handle the sudden load variations that are the subject of this research. However, it should be emphasised that these discontinuities are in nature different from the ones studied by Yorino, Li and Sasaki (2005). Their main technical contributions are adapted to the necessities of the applications desired in this dissertation.

As a result, this section describes a predictor/corrector scheme that aims to successively find the equilibrium points of EPSs right before and right after the occurrence of a load

switching caused by undervoltage protection schemes. This procedure is divided into four parts as follows:

- ❏ Load Switching Prediction
- ❏ Correction Stage I - Pre load switching
- ❏ Correction Stage II - Post load switching
- ❏ Identification of MLP and bifurcation type

Each part will be described separately in the following subsections.

3.2.1 Load Switching Prediction

The goal of this stage is to anticipate what is the next load discontinuity that happens as the load grows and at which power system states it takes place. For that, a linear approximation based on the tangent vector is employed.

As it was done in Section 2.3.1, the tangent vector of the PV curve at a known power flow solution $(\hat{x}_1, \lambda)$ is calculated with equation (2.9), which is rewritten bellow:

$$0 = \frac{\mathrm{d}\mathbf{f}(\hat{x})}{\mathrm{d}\hat{x}}\Delta\hat{x} + \hat{b}\Delta\lambda$$

As already mentioned, to solve this linear system the Jacobian (derivative term) is evaluated at the given equilibrium point and an arbitrary value is attributed to the load parameter or a state variation $(\Delta\hat{x}, \Delta\lambda)$. This value only influences the magnitude of the tangent vector and not its direction. With that, the linear system can be solved for $\Delta\hat{x}$ and $\Delta\lambda$.

Afterwards, for each bus that contains an undervoltage protection capable to switch loads on or off, the linear distance between the known equilibrium to the point where the protection trips is estimated with (3.1).

$$\sigma_i = \frac{V_i - V_i^{pick}}{\Delta V_i} \tag{3.1}$$

In this equation, V_i^{pick} is the undervoltage pick-up value that would trigger load switching in bus i and V_i is the actual bus voltage magnitude at the know power flow solution $\hat{x}_1$. At last, ΔV_i is the component of the tangent vector $\Delta\hat{x}$ that corresponds to the bus voltage under analysis. The calculated value σ_i is an estimate of the distance that bus i is from triggering its undervoltage protection. From this interpretation, the next load discontinuity in the PV curve will be the one associated with the smallest value of σ_i. This will be the selected continuation step.

$$\sigma = \min_{i \in L} \sigma_i \tag{3.2}$$

In (3.2) L is the set of load buses that employ undervoltage protection schemes. The bus that is associated with the smallest continuation step (σ) will be further used in the correction stages indicated by letter p and referred as pivot bus.

After the pivot bus and the continuation step-length are determined, EPS states can be estimated from the tangent vector. These predictions $(\hat{x}'_2, \lambda'_2)$ serve as the starting point for the correction stage to find a power flow solution.

$$\begin{aligned} \hat{x}'_2 &= \hat{x}_1 + \sigma\Delta\hat{x} \\ \lambda'_2 &= \lambda_1 + \sigma\Delta\lambda \end{aligned} \tag{3.3}$$

The geometric interpretation of this predictor is indicated in Figure 3.7 whether load steps up or down.

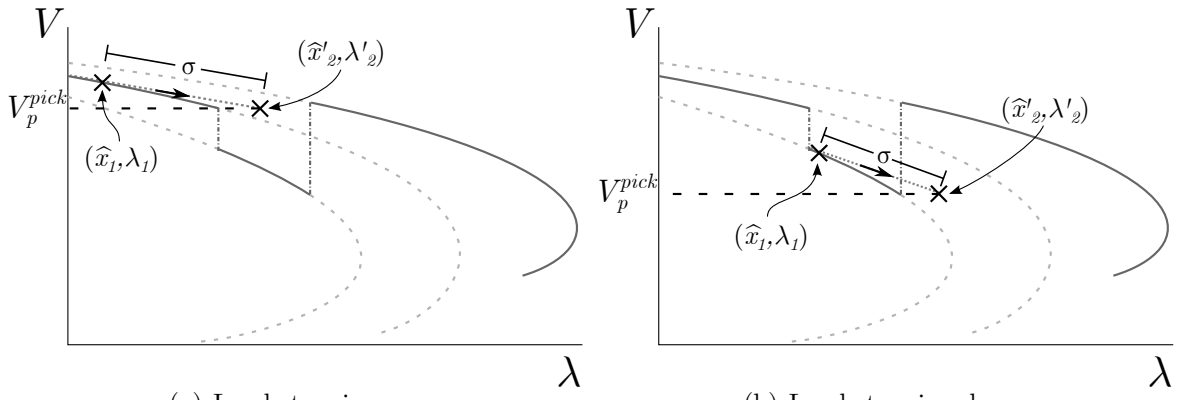

(a) Load stepping up. (b) Load stepping down.

Figure 3.7: Graphical representation of the predictor that estimates what is the next load discontinuity in the PV curve and estimates at which EPS voltages and angles it happens.

Because the predictor relies in a linear approximation and the power flow equations are in nature non-linear, there is no guarantee that the selected pivot bus really corresponds to the next load discontinuity in the PV curve. This means that the power flow solver, i.e. the correction stage, should not ignore the undervoltage protection schemes that exist in the EPS. At every numeric iteration, the corrector should verify whether any undervoltage pick-up happens, in which case its effect ought to be considered. This is similar to what is traditionally done to account for Q-limits in power flow solvers. The implication of prediction errors will be addressed again in the description of the correctors and its practical consequences will be studied in the numerical results.

3.2.2 Correction Stage I - Pre Load Switching

The goal of this stage is to calculate the power flow solutions within the desired accuracy to find the EPS equilibrium point right before the predicted load switching takes place. To achieve that, the power flow problem formulation is augmented with the parametric equation that sets the pivot bus voltage magnitude equal to its undervoltage protection setting. That is:

$$V_p - V_p^{pick} = 0 \tag{3.4}$$

The augmented power flow set of equations is solved with the Newton-Raphson method, resulting in the EPS states together with the load parameter $(\hat{x}_2, \lambda_2)$. This is equivalent

to executing a continuation step using local parametrization, where the local parameter is set to be the pivot bus voltage magnitude. Notice that the continuation step-length is automatically dimensioned to find the discontinuity, as a result of (3.2).

The starting point of the numerical method employed here is the power system states predicted with (3.3). The outcome of this corrector is indicated in Figure 3.8.

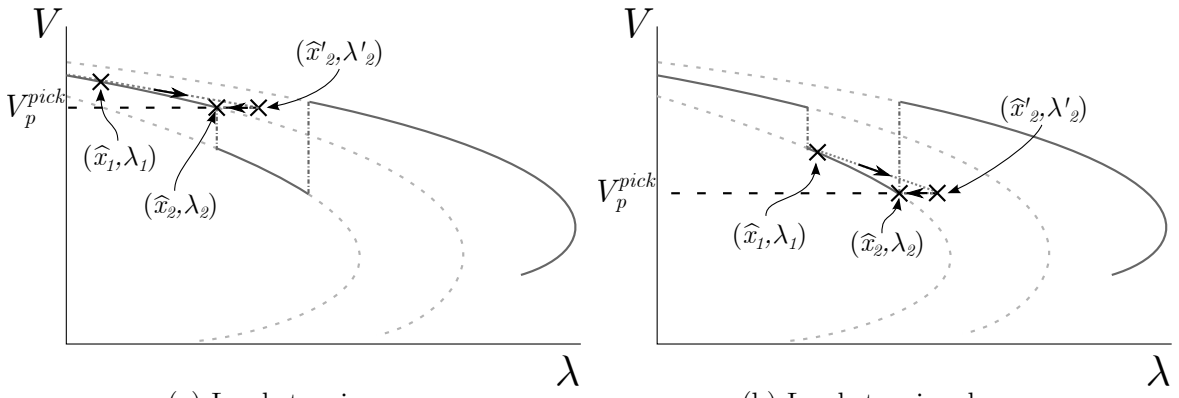

(a) Load stepping up. (b) Load stepping down.

Figure 3.8: Graphical representation of Corrector I that solves the power flow equations for the equilibrium point right before the predicted load switching happens.

Since there is no certainty if the pivot bus is the next one to go through a sudden load variation, the corrector should still account for all other undervoltage protection schemes present throughout the power system. During each iteration of the Newton-Raphson method, bus voltages magnitudes need to be observed to check whether any other protection is activated. When that happens the respective loads should be turned on or off accordingly.

3.2.3 Correction Stage II - Post Load Switching

A second corrector is necessary to find the power flow solution right after the load discontinuity takes place. This is different from what was done by Yorino, Li and Sasaki (2005) to find Q-limits that cause a discontinuity in the derivative of the EPS equilibrium states. These means that these limits are responsible to make the PV curve non-smooth but continuous, i.e. the equilibrium states immediately before and after the constraint do not change.

Prior to this correction stage, it is not feasible to employ a predictor. This happens because it deals with the actual occurrence of the discontinuity, i.e. a jump between two PV curves. In this situation, approximations based on curve fitting techniques are not expected to be very accurate, even though their application is not technically impossible.

Sundhararajan et al. (2003) claims that after a sudden variation of power injection, the power flow solution will most likely lie in the vicinities of the equilibrium point that existed prior to this change. This justifies not using a predictor and employing the power flow solution of Corrector I as the seed of the numeric method employed in Corrector II.

With that in mind, the correction stage II will employ the Newton-Raphson method to find the equilibrium point of the EPS right after the sudden load variation anticipated by the predictor. The initial guess for this numeric method will be the solution of the first corrector.

Just like in the previous corrector, it is important to include in this stage all undervoltage protection schemes that exist in the power system. This is required to attain possible undervoltage pick-ups that may take place between the pre and post sudden change in load.

In Corrector II, the parametric equation employed is different whether the load is suddenly increased or reduced, as will be depicted in the following subsections.

Sudden load reduction

It was mentioned in Section 3.1 that right after a sudden load variation, the parameter λ does not change and that the discontinuity is observed in the system voltages and angles. This fact can be well depicted if λ is selected as the local parameter. This means that the power flow equations need to be solved simultaneously with the following parametric equation:

$$\lambda - \lambda_2 = 0 \tag{3.5}$$

where λ_2 is the load parameter that was obtained from the corrector stage I.

After executing the Newton-Raphson method, the EPS equilibrium calculated will be $(\hat{x}_3, \lambda_3)$. The parametric equation employed guarantees the load parameter before and after the sudden load variation will be the same, that is $\lambda_3 = \lambda_2$. This characterizes correctly the nature of the discontinuity under analysis. The geometric interpretation of this corrector stage is illustrated in Figure 3.9.

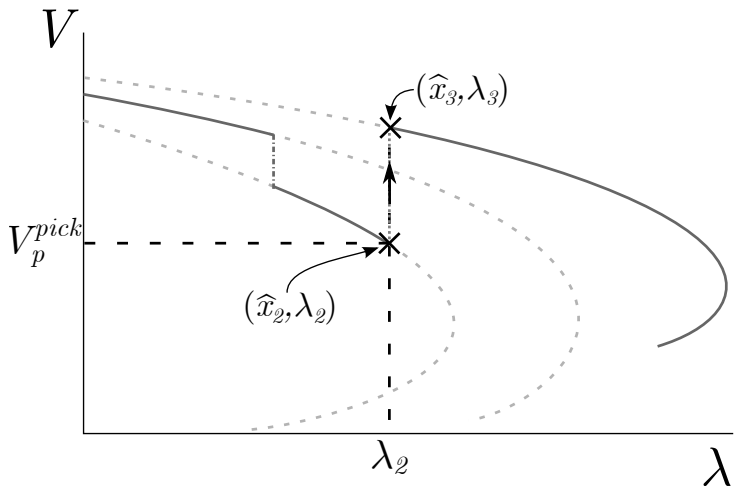

Figure 3.9: Graphical representation of Corrector II that solves the power flow equations for the equilibrium point right after a predicted load reduction happens.

The parametric equation employed is mathematically equivalent to solve the power flow equations at the load level λ_2. As a consequence of that, if this given load level is close to

the MLP, then this corrector may experience convergence problems due to ill-conditioning of its Jacobian matrix. Although this is technically possible it is improbable, because the discontinuity under analysis is a load reduction responsible to increase the power system MLP and distance it from λ_2.

To be fair, the parametrization employed here does not guarantee the convergence of the corrector and contributes negatively to the robustness of the method. However, at least for the practical application in this dissertation (Undervoltage Load Shedding (ULS)), no significant problems were observed in the tested examples. In this situation, the goal of the load discontinuities is to increase the VSM. If divergence arises for a given load that is shed, then the effect of such disconnection is inadequate to increase the MLP significantly and other ULS scheme should be employed.

Sudden load increase

After a discrete load increase, a reduction in the VSM is expected. Therefore, the reasoning that supported the use of λ as the local parameter is not valid anymore and other parametrization equation needs to be employed.

In the Corrector I, the pivot bus voltage magnitude was used for that purpose and for simplicity reasons it is employed once more here. This time, the goal is to obtain a EPS equilibrium point after the load switching under analysis takes place.

The parametric equation employed in this stage is (3.6), where $V_p(\lambda_2)$ is the voltage magnitude of the pivot bus at the solution of Corrector I.

$$V_p - V_p(\lambda_2) = 0 \tag{3.6}$$

To be thorough, the voltage $V_p(\lambda_2)$ is an element of the state vector $\hat{x}_2$ and, due to the parametric equation employed in Corrector I (3.4), it is equal to V_p^{pick}. Geometrically this can be seen in Figure 3.10.

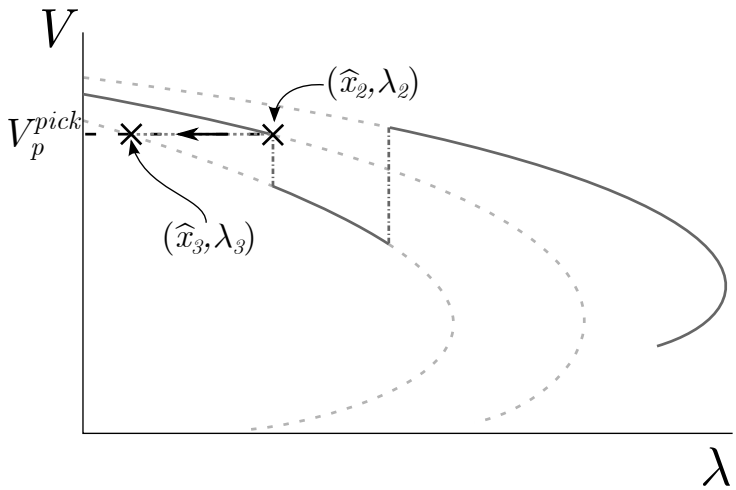

Figure 3.10: Graphical representation of Corrector II that solves the power flow equations for the equilibrium point right after a predicted load increase happens.

With this parametrization, a power flow solution is found keeping the pivot bus voltage magnitude constant after its load is suddenly increased. To attain such equilibrium point, the total load of the system is reduced, i.e. λ decreases, as can be seen in Figure 3.10. The resulting power flow solution does not lie in the system equilibrium diagram. Nevertheless, it allows the predictor/corrector procedure to continue and the next load discontinuity to be found. In fact, this reduction in load may contribute to the robustness of the method, since it can increase the distances between the calculated power flow solution and the MLP.

After a given load is suddenly increased, bus voltages are expected to drop. This reduction can cause pick-up of other undervoltage protection schemes and, consequently, more load discrete steps may follow the first one. Using as example the undervoltage mandatory disconnection of distributed generators, after one unity is disconnected from the power system, bus voltages may fall leading to the trip of other units.

The reduction of λ, caused by the parametrization proposed here, facilitates the understanding of these successive load steps. It essentially isolates each discontinuity, decreasing the system load after each sudden step up in demand. As will be seen in the numerical results, this contributes to assure that only the predicted load switching happens in a single continuations step, separating this discontinuity from other ones that would directly result from it.

This parametrization does not disregard the possible cascading effect caused by sudden load increases (generation disconnections) due to undervoltage protections, where one load stepping up triggers another one to do the same. When this happens, the second discontinuity will lie in the portion of the PV curve where the load parameter is smaller than the one that originated the first sudden load change.

To clear up, Figure 3.11 exhibit such circumstance. Suppose that a load is stepping up (ΔL_1) at $(\hat{x}_a, \lambda_a)$. If it did not cause another undervoltage protection pick-up, then it would make the system move to operating point $(\hat{x}'_a, \lambda'_a)$. However, suppose that this voltage level will also trigger another load to step up (ΔL_2) making the actual equilibrium of the system to be $(\hat{x}''_a, \lambda''_a)$.

What the proposed parametric procedure does first is to find the power flow solution $(\hat{x}_b, \lambda_b)$ after ΔL_1 as a result of Corrector II. At this equilibrium point, bus voltages are not expected to have deviated significantly from their pre-swithiching value $(\hat{x}_a, \lambda_a)$, which means that it is highly unlikely that any other undervoltage pick-up happened. Afterwords, the predictor goes on to estimate what is the next undervoltage pick-up and Corrector I is designed to find at which point it occurs. As a result, the power flow solution found is $(\hat{x}_c, \lambda_c)$. The voltage at this point is higher then the one that would have followed the first load switching ΔL_1 at $(\hat{x}_{a'}, \lambda_{a'})$. This means that the second discontinuity ΔL_2 will result directly from the first one ΔL_1. In fact, this will be true if the latter solution lies somewhere in the red portion of the PV curve in Figure 3.11.

To be fair, the solution found after this procedure would be $(\hat{x}_c, \lambda_c)$ and not $(\hat{x}''_a, \lambda''_a)$

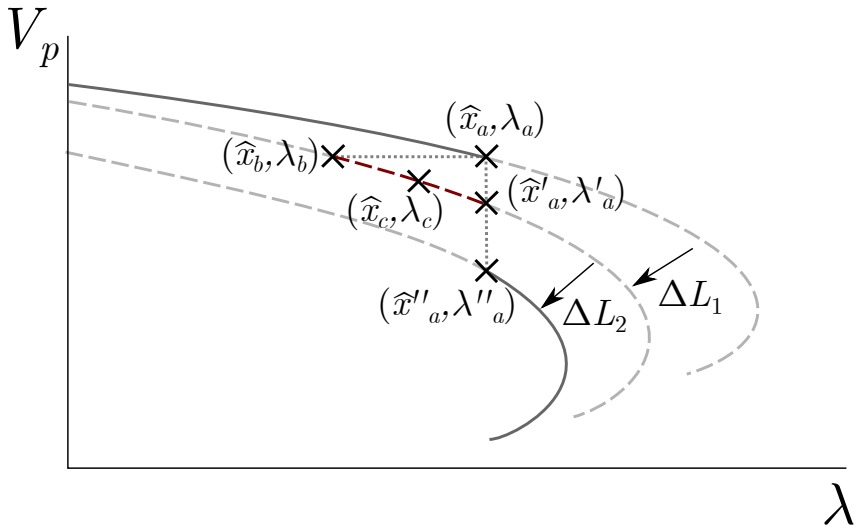

Figure 3.11: Cascading loads stepping up (generation disconnections) due to undervoltage protection schemes as attained by the proposed predictor/corrector scheme. The red portion of the PV curve represents the locus of power flow solutions where discontinuity ΔL_2 is caused by the predecessor variation ΔL_1.

which is the system equilibrium state that would follow ΔL_1. The solution found may not represent the system voltage profile, but it allows to predictor/corrector scheme to continue and depicts the order of the cascading events.

Notice that this procedure is expected to isolate each discrete change in one single continuation step. This can strengthen the robustness of the method, because it allows the continuation steps to gradually find load discontinuities. Meanwhile, the traditional CPFLOW would have to deal with a big discontinuity caused by cascading sudden load variations.

It is necessary to point out that there is no mathematical guarantee that no parametric variation would take place between the solutions of Correctors I and II and that each load discontinuity will be found one by one. This reinforces the need to consider in every correction stage all undervoltage protection schemes and their respective consequences in the power system load.

3.2.4 Identifying the MLP and Bifurcation Type

Executing the predictor and both correctors repetitively will compute the successive load discontinuities that the power system is subject to. However, the operator is generally interested in the maximum loadabiltiy point of the transmission network. Unless one of the load discontinuities causes instability, the proposed predictor/corrector scheme should be aided with another tool to find the MLP.

The tangent vector to the PV curve can be used to identify whether or not the MLP has passed, that is, if a given power flow solution lies in the stable upper portion of the PV curve or in the unstable lower one (CHIANG et al., 1995; CAO; CHEN, 2010; ZHAO; ZHANG,

2006). Considering this, after every correction step, the tangent vector to the calculated equilibrium is used to assess if an unstable point was found.

Just to remember, the tangent vector is calculated solving the linear system (2.9), which is rewritten bellow, as described in Section 2.3.1.

$$0 = \frac{\mathrm{d}\mathbf{f}(\hat{x})}{\mathrm{d}\hat{x}}\Delta\hat{x} + \hat{b}\Delta\lambda$$

Undervoltage protection schemes will actuate in buses where the voltage is decreasing when the load parameter is increasing. As a consequence of that, the tangent vector component related to the pivot bus voltage magnitude and the load parameter should have opposite signs, as long as the equilibrium point under analysis is in the upper part of the PV curve. Therefore if their signs are equal this indicates that the power flow solution is an unstable equilibrium. This is carried out with following criteria:

$$\mathrm{sign}(\Delta V_p) = \mathrm{sign}(\Delta\lambda) \tag{3.7}$$

where $\Delta\lambda$ and ΔV_p are components of the tangent vector $(\Delta\hat{x}, \Delta\lambda)$.

This criteria is mathematically equivalent to Condition 1 of the method proposed by Yorino, Li and Sasaki (2005) that is described in Section 2.4.3. The only difference is that, now, it is applied to the bus that goes through a load switching instead of a Q-limit.

When (3.7) is satisfied, the proposed method should stop solving the power flow equations and an algorithm should be employed to identify the bifurcation type to which the system is subject.

This stopping criteria can be overlooked after Corrector II if the load is suddenly reduced. In this case, one bus demand steps down while the loading parameter λ is held constant. Therefore the EPS equilibrium is not expected to become unstable.

It was seen in Chapter 2 that besides the common Saddle-Node Bifurcation (SNB), the power flow equations are also subject to Structure Induced Bifurcation (SIB) caused by the reactive limit of power systems generators.

When the load suddenly steps up, it can also cause instability. This is particularly true when cascading load increases or generator losses take place (KUNDUR et al., 2004). This instability is caused by a parametric discrete change in the EPS, which is similar to the bifurcation that results from a Q-limit. In this sense, the bifurcation caused by a load switching is also referred as SIB. However, the term Limit Induced Bifurcation should not be used in this situation, since a limit is not actually met.

When the stopping criteria (3.7) is met, two conditional tests are employed to identify if the MLP is a saddle-node bifurcation or a structure induced one. These conditions are summed up in Figure 3.12, where $\hat{x}_{sup}$ and $\hat{x}_{bel}$ are the last power flow solutions calculated that lie in the superior and inferior portion of the PV curve respectively. $\hat{x}_{maj}$ is the power flow solution that corresponds the highest value of the loading parameter λ.

Condition I deals with the situation where one load increase or generation disconnection prompts instability. In this case, the last two power flow solutions found ($\hat{x}_{sup}$ and $\hat{x}_{bel}$)

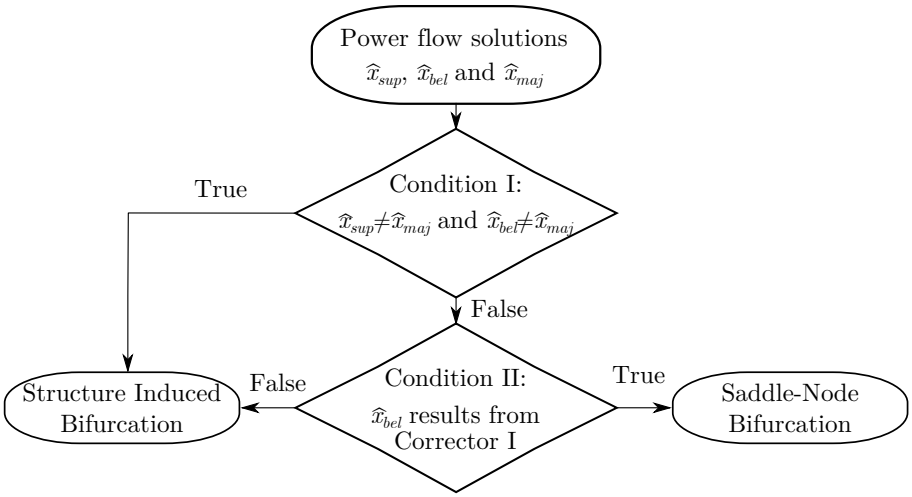

Figure 3.12: Conditions to identify whether the power system under analysis is subject to a saddle-node bifurcation or a structure induced one. The latter being caused by a sudden load variation.

are not the ones that correspond to the biggest load level ($\hat{x}_{maj}$) due to Corrector B, that reduces the load parameter λ. This can be understood with Figure 3.13, if the solution $\hat{x}_{bel}$ is an unstable equilibrium point, then the discontinuity that led to this point (ΔL_1) is responsible to cause instability. In other words, if an unstable power flow solution is found for a load level smaller than a previous sudden load variation, then the EPS equilibrium right before such discontinuity ($\hat{x}_{maj}$) is a SIB.

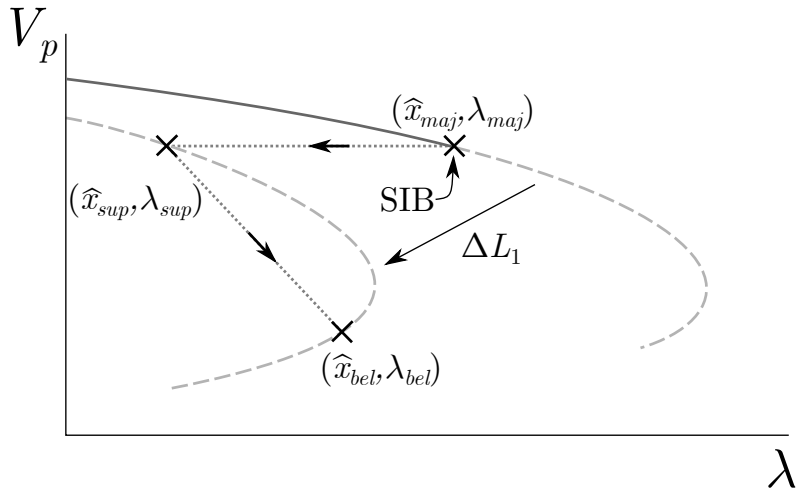

Figure 3.13: Scenario when Condition I is satisfied and one load switching is identified as a Structure Induced Bifurcation (SIB).

Condition II contrasts whether the unstable equilibrium ($\hat{x}_{bel}$) is a result of Corrector I or II. The first case is in Figure 3.14, where it is possible to see that the bifurcation happened between two load discontinuities in a continuous arc of the PV curve. As a result of that, between these two solutions there is necessarily a SNB. This is certainly true if the last power flow solution found did not flag the existence of another load discontinuity. In the situation where this is not true, the system should be further analysed. Nevertheless,

this is highly unlikely and, therefore, it was not treated in the proposed method.

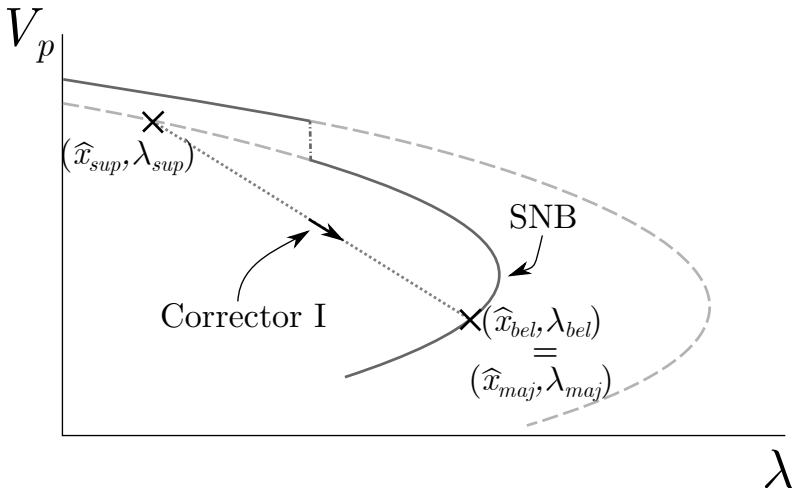

Figure 3.14: Scenario when Condition II is satisfied and a Saddle-Node Bifurcation (SNB) is identified.

Whenever the SNB is encountered another method should be employed to accurately find the MLP, since the parametrization described here only searches for discontinuities. For this purpose, the last stable equilibrium is used as the stating point of the traditional CPFLOW (or any other method that can find SNBs) to estimate the MLP.

The proposed parametrization is expected to assure that the portion of the PV curve to be traced with the CPFLOW is continuous, since it connects two consecutive discontinuities, therefore convergence problems are not likely to occur.

Still discussing Condition II, consider now that the solution found in the lower portion of the PV curve is a result of Corrector II, just like it is indicated in Figure 3.15. In this case, it is clear that the discontinuity under analysis (ΔL_1) is responsible for the unstable equilibrium found.

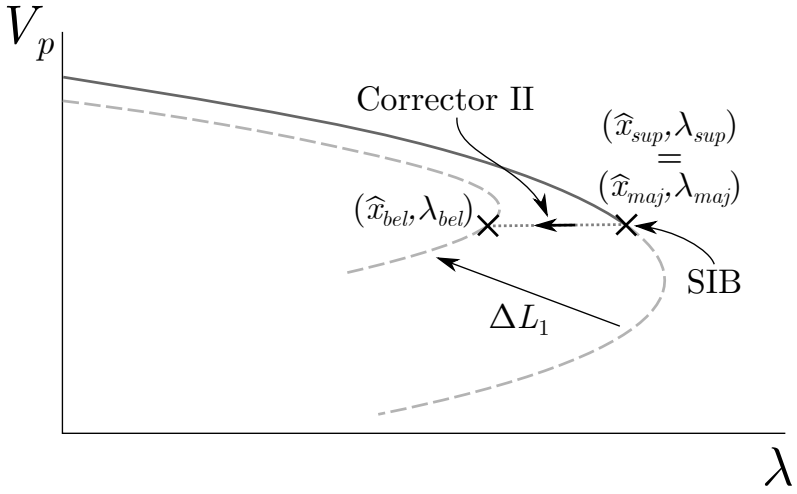

Figure 3.15: Scenario when Conditions I and II are not satisfied and one load switching is identified as a Structure Induced Bifurcation (SIB).

The two conditions proposed here do not require any additional calculation and are capable of identifying the bifurcation type that the EPS under analysis experiences. Furthermore, in the case where a SIB happens, it is possible to single out which load sudden variation caused it.

3.2.5 Complete Iterative Predictor/Corrector Scheme to Handle Sudden Load Variations

The bifurcation identification process, the stopping criteria, the proposed predictor and both correctors can be bundled together to comprise an iterative method capable of estimating the effect of sudden load variations on the voltage stability margin of power systems.

The predictor and both correctors described here are capable to successively find load discontinuities caused by undervoltage protection schemes. After each power flow solution is calculated, the tangent vector is used to evaluate the stopping criteria. Finally, from two conditions it is possible to identify the bifurcation type that happened. This whole process is schematically described in the flowchart available in Figure 3.16.

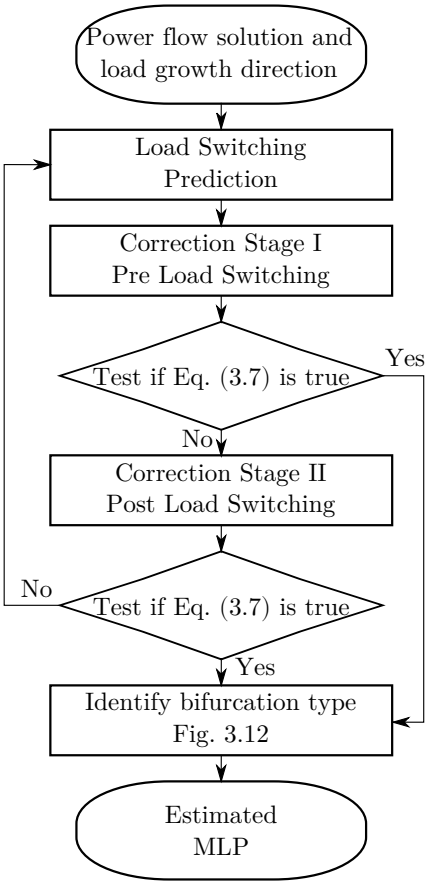

Figure 3.16: Flowchart of the proposed predictor/corrector scheme capable to identify sudden load variations caused by undervoltage protection schemes and to estimate their impact in the maximum loadability point of power systems.

In principle, this whole process could be seen as a locally parametrized continuation method whose step-length is automatically selected to be equal to the next continuous arc of the EPS equilibrium diagram. This means taking large steps in the portion of the curve where the power system is not subject to parametric discrete changes and smaller ones when they take place in close proximity.

The author refrains from referring to the proposed algorithm as a continuation method, despite having its four basic parts: parametrization, prediction, correction and step-length control. This is done for two main reasons: first, the method does not trace the EPS equilibrium diagram (PV curve), which means that voltage profiles do not result from it. Second, there is no rigorous justification to employ continuation methods with discontinuous functions and the proposed algorithm is designed to deal with discontinuities.

This method is expected to work well if the EPS is subject to successive load discontinuities that are not far from each other. Otherwise, it may derive prohibitively long step-lengths that could compromise the prediction accuracy and prevent convergence of the power flow solver.

It is important to state that the proposed method can be executed together with the traditional CPFLOW according to specific necessities of power utilities, including in this standard VSA tool another capability that may broaden its applicability.

The proposed algorithm can also be simultaneously implemented with the method proposed by Yorino, Li and Sasaki (2005) that is described in Section 2.4. In this case it is possible to identify whether the next equilibrium discontinuity is a generator Q-limit or a sudden load variation to find the power flow solution where it happens.

3.3 Example of Application for the Proposed Predictor/Corrector Scheme

To elucidate any unclear aspects regarding the proposed Predictor/Corrector algorithm, it was employed to obtain two load discontinuities that were introduced in the IEEE 14 bus test system. The data regarding this EPS is available in (IEEE, 1993).

In bus 14 two undervoltage protection schemes were included to cause sudden parametric variations in load. First the load steps up, event caused by a unit disconnection at the referred bus due to an undervoltage protection pick-up at 0.9 pu. As a result of this trip, the base case load at bus 14 (P_{L014}) goes from 22.35 MW to 29.8 MW. Afterwards, half of this load is shed as a consequence of another undervoltage protection set at 0.8 pu, which results in a total load at bus 14 of 14.9 MW.

These events amount to three possible configurations for the IEEE 14 bus test system: (i) the complete network, (ii) the network without the disconnected generator and (iii) the network without this unit after load shedding occurs. Each of these configurations

can be associated with one PV curve for the EPS under analysis, which are presented in Figure 3.17.

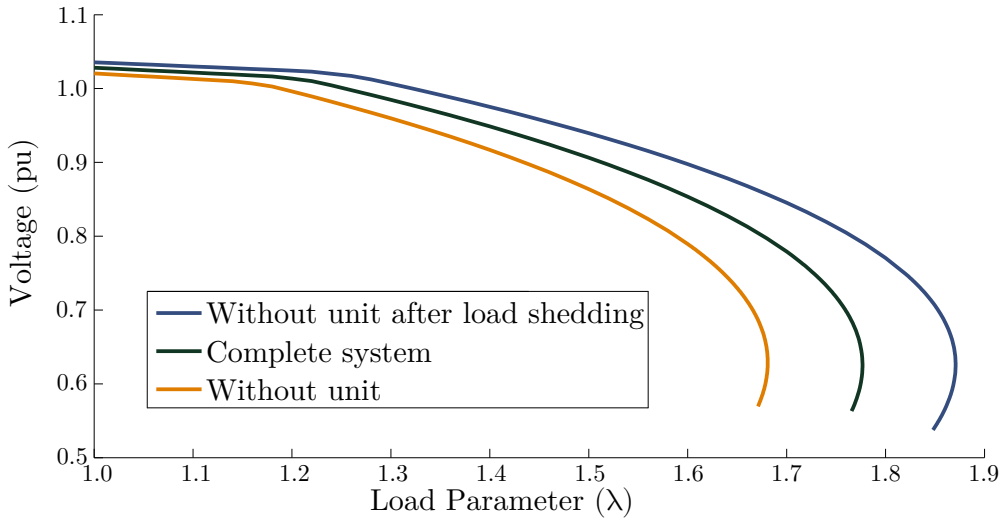

Figure 3.17: Bus 14 voltage profile of the IEEE 14 bus test system considering the three configurations that this system is subject to, as a result of sudden variations in load.

As a result of the two load discontinuities considered, the voltage profile of the power system becomes the solid curve indicated in Figure 3.18.

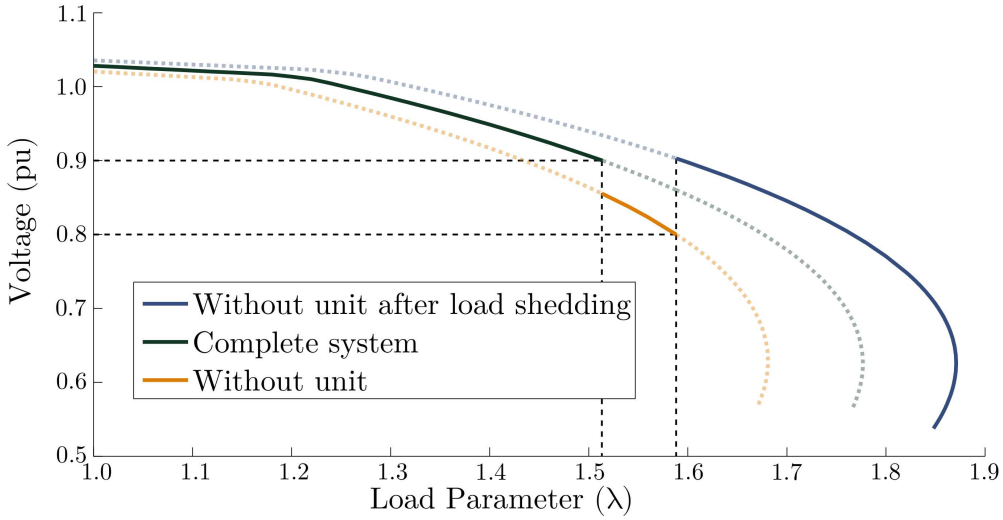

Figure 3.18: Bus 14 voltage profile of the IEEE 14 bus test system that results from two sudden load variations.

The power flow solutions calculated with the proposed predictor/corrector scheme are indicted in Figure 3.19 and numbered according to the order that they are attained. Solution number 1 is the known equilibrium point required prior to the execution of the proposed method. Solutions 2 and 4 are calculated with Corrector I and they comprise the power system equilibrium right before the respective load discrete change happened.

Finally, Solutions 3 and 5 results from Corrector II, when the load steps up and down respectively.

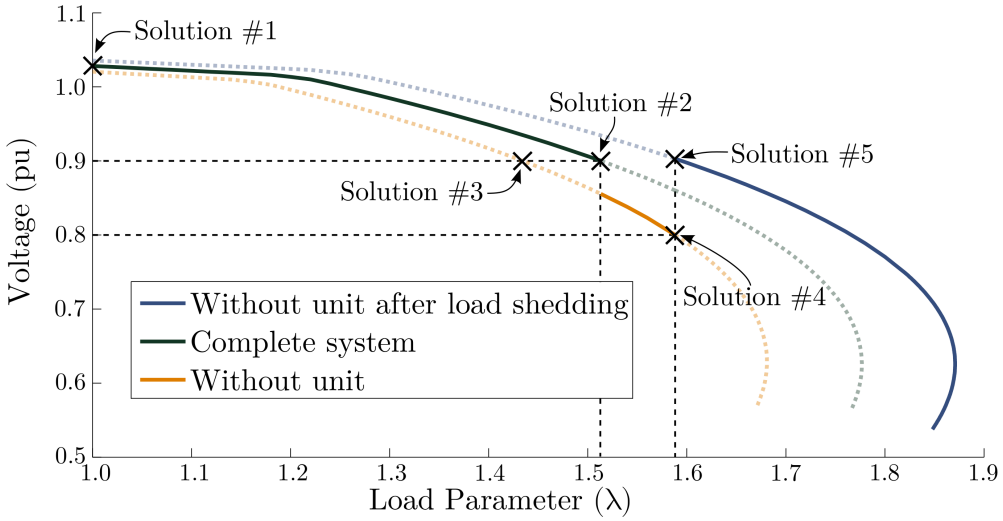

Figure 3.19: Equilibrium solutions obtained with the proposed method to characterize the sudden variations in load that took place in the IEEE 14 bus test system.

Solution number 3 does not lie in the actual equilibrium diagram of the EPS under question, however it allows the predictor/corrector procedure to continue.

Since the MLP is not caused by a load discontinuity, it is not calculated with the proposed method alone. In this situation the method would identify a SNB, therefore the CPFLOW should be employed after the last discontinuity was found.

When implemented alongside with the Q-limit guided continuation power flow proposed by Yorino, Li and Sasaki (2005) and described in Section 2.4, the proposed predictor/corrector method can identify whether the next discontinuity is a reactive power limit or a load switching and then encounter the equilibrium point where it happens. For the IEEE 14 bus test system, this procedure resulted in the sequence of discontinuities presented in Table 3.1.

Table 3.1: Sequence of discontinuities calculated with the proposed predictor/corrector method for the IEEE 14 bus test system.

Discontinuity	Bus	System Loading (λ)
Q-limit	3	1.1970
Q-limit	6	1.2186
Q-limit	8	1.2669
Q-limit	2	1.2670
Load step up	14	1.5133
Load step down	14	1.5933

3.4 Final Remarks

The proposed predictor/corrector scheme is not expected to replace the traditional CPFLOW or any other standard VSA tool. Its applicability is restricted to analyse the effect of sudden load variations caused by undervoltage protection schemes on the static voltage stability of EPSs. This method was designed specifically to deal with the discontinuities caused by such parametric variations, in which case it is expected to perform better than the CPFLOW.

In this sense, this procedure can be used as a complementary tool to the CPFLOW enhancing it with new features that could broaden its applicability.

It is also reasonable to expect that the ideas presented here could be useful to deal with other equilibrium discontinuities that power systems may encounter.

However, it is essential to point out that there is no mathematical guarantee that the proposed method will converge when dealing with sudden load changes. In other words, it is not a definite solution to analyse such discontinuities and further studies could be done in this area.

Chapter 4

Case Study on Distributed Generation Mandatory Disconnection

One sudden load variation that is dispersed throughout power system and can negatively impact its voltage stability is the mandatory disconnection of Distributed Generation (DG) units (VIAWAN, 2008; WALLING; MILLER, 2002; LONDERO; AFFONSO; NUNES, 2009; YANG et al., 2013).

There is no consensus regarding the definition of DG. However, such paradigm is usually described as small power generation units connected close to EPS loads (OWENS, 2014; WADE, 2006). This dissertation uses the definition that comprises the Brazilian legislation, where Distributed Generators are electric power units connected directly to distribution systems, as long as they are not hydroelectric plants with installed capacity bigger than 30 MW nor thermal plants with efficiency lower than 75% (PRESIDÊNCIA DA REPÚBLICA, 2004).

Government financial support to expand the use of renewable sources and the electricity market deregulation created a favourable scenario to increase investments in distributed generation (XAVIER DIAS; BOROTNI; HADDAD, 2004). Owens (2014) mentions that out of the total word wide installed capacity, the DG penetration increased from 21% in 2000 to 39% in 2012. Data collected by WADE (2006) show that more than 30% of the total installed power in several European countries is characterized as DG. In Brazil, it is estimated that this value was equal to 4.4% in 2006 and has grown to about 8% in 2015 (SANTOS, 2015).

Distributed generators can reduce distribution and transmission power losses, can contribute to increase the participation of renewable energy sources in the electricity market and can increase the efficiency of the electric generation process (WALLING et al., 2008; ABRI; MEMBER; ATWA, 2011; BOLLEN; HASSAN, 2011). Even though these units are essentially beneficial to EPSs, distribution utilities are concerned with possible adverse effects that they may have on protection coordination, stability and voltage control (WALLING et al., 2008; YANG et al., 2013; LONDERO; AFFONSO; NUNES, 2009).

Distribution networks are generally planned and operated with unidirectional power flow and passive loads. With the penetration of DG units this paradigm changes and the network becomes active creating technical difficulties that need to be addressed by distribution utilities (WALLING et al., 2008).

To mitigate possible adverse effects of DG units, such generators are required to be disconnected whenever there is a fault or disturbance in the feeder to which they are connected. This ensures proper performance of the feeder protection and control and prevents islanded operation of DG.

Usually, for such purposes, distribution utilities require under/overvoltage and under/overfrequency protection schemes at the DG Point of Common Coupling (PCC) (BLACKBURN; DOMIN, 2006; CHEN; MALBASA; KEZUNOVIC, 2013). The main goal of these protections are:

1. If a fault occurs in a feeder with a distributed generator, then this unit needs to be disconnected to assure that it does not contribute to the fault current nor it compromises the feeder protection actuation.
2. Dynamic oscillations that DG units may cause in distribution systems need to be isolated, so the unit does not compromise the energy quality at the consumer end.
3. Islanded operation need to be prevented in most situations to assure safe automatic breaker reclosing and to guarantee complete control of the feeder de-energization by the utility. This is necessary for the safety of utility employees and consumers.

In some cases, the stipulated protection settings are quite restrictive and inadvertent disconnections are not uncommon (WALLING; MILLER, 2002; CHEN; MALBASA; KEZUNOVIC, 2013). The trip of a distributed generator as a direct consequence of such protection schemes, or any other utility requirement, is what is refereed in this work as DG mandatory disconnection.

When assessing the static voltage stability of EPSs, it is expected that DG units contribute to increase the system VSM. In static models, DG is portrayed as a negative power injection and, as such, it lessens the transmission lines loading increasing the system stability margin (ABRI; MEMBER; ATWA, 2011). However, as the load grows, the system voltages tend to decline, even in distribution substation buses. These voltages may reach levels that could cause pick-up of undervoltage protections located at the DG PCC and consequently promote the trip of such units. This is equivalent to stepping the load up and may decrease the VSM and even cause instability.

The effect of distributed generators on both transmission and distribution voltage stability was studied by Yang et al. (2013), Londero, Affonso and Nunes (2009), Abri, Member and Atwa (2011), Zhao et al. (2015). However, these authors did not consider the undervoltage protection of DG units, neglecting their potential negative effect in EPSs.

In the studies of Walling and Miller (2002), Chen, Malbasa and Kezunovic (2013), the DG mandatory disconnection was considered during dynamic simulations. Walling and

Miller (2002) demonstrated that inadvertent undervoltage trip of a DG unit may cause instability in bulk power systems. In the work of Chen, Malbasa and Kezunovic (2013), a transmission system MLP was estimated with successive, slow and small increments in its load. This study concluded that for high DG penetration levels mandatory disconnection of these units may cause a significant reduction in the VSM.

These studies demonstrated that inadvertent trip of DG units may cause voltage stability problems. However, to the extent of the knowledge of the author, there is no detailed research in the literature regarding the effect of DG mandatory disconnection during static voltage stability analysis. Notably, DG undervoltage disconnections comprises the kind of discontinuity that could be studied with the predictor/corrector scheme proposed in the previous chapter.

The undervoltage protection of DG units is the utility requirement that is most likely to cause stability problems under a static framework. Particular undervoltage settings defined by Brazilian distribution utilities are presented in Table 4.1. Notice that the time delay of such protections are not presented, because they are not relevant during static analysis.

Table 4.1: Undervoltage setting at the DG point of common coupling as required by Brazilian distribution utilities.

Distribution Utility	Federation State	Undervoltage Pick-up	Reference
COPEL	Paraná	0.95	(COPEL, 2014)
CELESC	Santa Catarina	0.85	(CELESC, 2014)
ELEKTRO	São Paulo	0.80	(ELEKTRO, 2013)
CEMIG	Minas Gerais	0.80	(CEMIG, 2011)

These requirements attest that DG units may be subject to inadvertent disconnections and it is reasonable to expect that such events can negatively impact the VSM. This is particularly true for the very restrictive requirement of COPEL.

The main goal of this chapter is to quantify the effect that DG mandatory disconnections have in the VSM of bulk power systems. At the same time, it will demonstrate a practical application of the predictor/corrector algorithm proposed in this dissertation, demonstrating its strengths and drawbacks.

Before actual numerical results are shown, a distribution system model is described in Section 4.1. This model makes it possible to consider the DG undervoltage protection schemes during the VSA of transmission systems. The effect of DG disconnections is quantitatively depicted in Section 4.2 for two test systems. These results were obtained with the proposed predictor/corrector scheme. The final remarks of this chapter are available in Section 4.3.

4.1 Distribution System Model with DG for Voltage Stability Assessment of Transmission Systems

In order to predict the mandatory disconnection of distributed generators, it is necessary to estimate the voltage drop from the substation bus associated with the unit to its PCC. This means that distribution feeder models should be included into the bulk power system.

Simultaneous analysis of transmission and distribution systems is difficult for two main reasons: (i) these systems have different topological structures, impedance parameters and voltage levels; (ii) they are operated and planned by different companies that usually exchange little information (ZHAO et al., 2015). Therefore, including distribution feeder models into the static analysis of a transmission network is a cumbersome task that involves several uncertainties.

The feeder voltage drop and consequently the DG undervoltage protection actuation depends on the power injected by such unit, the feeder impedance parameters, its automatic voltage control and the system loading level. In general, this information is not available to transmission system utilities, therefore simplifying hypotheses are necessary to account for DG mandatory disconnection during the voltage stability assessment of a large EPSs.

Here, three hypotheses are made based on general characteristics of distribution systems instead of specific data that would probably be unknown to the transmission system operator.

- ❏ Hypothesis 1: Substations are equipped with an On-load Tap Changer (OLTC). This transformer automatically increases the substation bus voltage in order maintain distribution feeders in adequate voltage levels. Therefore, it is expected that the OLTC has already achieved its maximum control limit before any DG disconnection takes place.
- ❏ Hypothesis 2: DG units supply only active power to the distribution system and this injection is independent of the voltage magnitude at the PCC.
- ❏ Hypothesis 3: DG units connected to a given substation can be divided into three groups according to the voltage drop from the substation to their PCC. The first group is close to the substation and is not subject to voltage drop, the second one is located at a distance from the substation to which the voltage drop is 0.015 pu and, finally, for the third group this value is equal to 0.030 pu.

Hypothesis 1 is realistic and based on the common practice of employing a transformer capable to change its tap under load in distribution substations. This transformer generally monitors and controls a downstream bus voltage. From that, it is reasonable to assume that the control margin of this OLTC has reached its regulation limit before there is pick-up of any DG undervoltage protection. The maximum tap is considered to take place when the voltage ratio is 10% above its nominal value (WALLING et al., 2008).

The second hypothesis regards the frequent use of unity power factor control in

distributed generators (LONDERO; AFFONSO; NUNES, 2009; ABRI; MEMBER; ATWA, 2011; WALLING et al., 2008). In principle, DG units could supply reactive power to the system assisting the feeder voltage control. Nevertheless, this reactive injection needs to be coordinated with the active voltage control designed by the utility, otherwise the DG unit can conflict with other distribution equipment. To assure safe penetration of DG, there are standards that restrict the implementation of active voltage control in such units (WALLING et al., 2008; ABRI; MEMBER; ATWA, 2011). Beyond that, in Brazil DG investors are not financially compensated by their reactive support, so they commonly operate supplying as much active power as possible to maximize their profitability.

The third and last hypothesis requires a higher level of approximation. The alternative to this approach would depend on information regarding distribution systems that is usually unavailable to transmission operators. In this context, including detailed models of distribution feeders would only replace the postulated voltage drops by other unknown parameters and variables of these circuits.

The resulting model from these three hypotheses is indicated in Fig. 4.1.

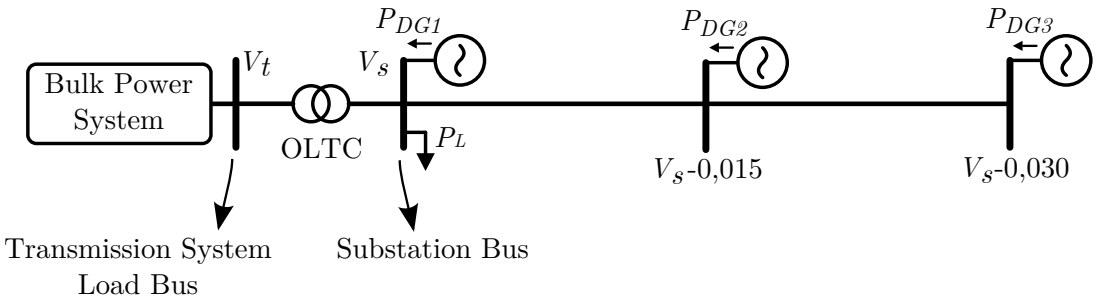

Figure 4.1: Proposed distribution system model to account for DG mandatory disconnection during static voltage stability assessment of bulk power systems.

This model considers that transmission system load buses are distribution substations. Each substation is associated with three groups of distributed generators, which distinguish different distances that DG units may be from the bulk power system. These three groups are individually paired with a distinct feeder voltage drop. Considering this and the OLTC, one DG group will have its associated units tipped due to their PCC undervoltage protection when (4.1) is satisfied.

$$V_t \leq \frac{V_{drop} + V_{prot}}{1.1} \tag{4.1}$$

In this inequality, V_t is the voltage magnitude of an EPS load bus and it corresponds to the high side of a substation OLTC. V_{prot} is the undervoltage pick-up value of the DG PCC protection. Finally, V_{drop} is the feeder voltage drop, which can assume the values of 0, 0.015 or 0.030 pu depending on the DG group under analysis. The denominator is related to the OLTC maximum control margin.

Because of the distribution feeder voltage drop, each DG group undervoltage protection scheme is expected to disconnect their associated units at different load levels.

To exemplify, if the undervoltage protection is set at 0.95 pu for all units associated with a given distribution substation, then the first disconnection will take place at the farthest group when the respective transmission system bus voltage (V_t) reaches 0.894 pu. If the voltage continues to fall, then the mid-distance group will be decoupled from the system when V_t goes under 0.879 pu. Finally, if this voltage magnitude reduces even more, bellow 0.864 pu, then the units near the substation are also disconnected.

4.2 Numerical Results

This section illustrates the application of the proposed predictor/corrector scheme described in Chapter 3 and compares it with the traditional locally parametrized CPFLOW. The local parametrization was selected over the arc-length one due to its similarity with the proposed predictor/corrector algorithm. These two methods were implemented in MATLAB, since commercial software is not designed to account for load discrete variations.

Both the CPFLOW and the proposed predictor/corrector scheme were used to assess the Voltage Stability Margin (VSM) of two power systems: the IEEE 118 bus test system (IEEE, 1993) and the 107 bus reduced Brazilian interconnected system (ALVES, 2007). The IEEE system is a well established reference in static analysis, while the Brazilian system is based on real EPS data and has been thoroughly used by the research group of the author. Table 4.2 summarizes a few characteristics of both these systems. Their complete data, including their one-line diagrams, are available in Appendices A and B.

Table 4.2: General characteristics of both the IEEE 118 bus test system and the reduced interconnected Brazilian system.

	IEEE 118	Brazilian
Number of buses	118	107
PV buses	53	23
PQ buses	64	83
Number of lines	186	170
Load buses	91	39
Total active load (GW)	3.668	12.682

This section will address the effect of the DG mandatory disconnection on the VSM of both test systems mentioned. For that, a few simplifying considerations were made, even though the two methods employed here are not restricted to them. These assumptions are presented in the following list:

1. The load growth was parametrized as described in Section 2.2 considering that K_{Pi}, K_{Qi} and K_{Gi} are all equal to one for every system bus. This means that, load power increases in each bus proportionally to the base case loading with constant power factor. Note that all load data are provided in Appendices A and B. Also, to meet this load increase, generators are dispatched proportionally to their base case active

power injection. This way the generators that were supplying more power to the system in the base case, i.e. the bigger ones, are responsible to take on more load.

2. DG units were included in every load bus according to the model in Figure 4.1. The author recognizes that this is not common. Nevertheless, this assumption is in line with the principle that every load bus is a possible coupling point for DG. It is worth to emphasize that DG penetration data are not available for both test systems under consideration, which makes any allocation of such units arbitrary.
3. The percentage of the total load that is supplied by DG units is called DG penetration level. Three levels were considered during the numerical studies: 10%, 20% and 30%. For example, the total active power injected by DG in the IEEE 118 bus test system is 366.8 MW, when its penetration level is 10%. The lesser penetration level considered (10%) is not far from the DG contribution in Brazil, while the higher one (30%) could be associated with a few European countries.
4. The DG power injection in each load bus was not uniformly distributed throughout the transmission system. If this was the case, big bundles of DG units, whose disconnection could be severe to the system stability, would have been be neglected. The actual power supplied by DG units in each load bus is available in Appendices A and B.
5. In each load bus, the total DG power injection was equally divided between the three voltage drop groups of the proposed distribution system model depicted in Figure 4.1.
6. The power supplied by DG units was fully compensated by an equivalent load increase. In other words, after a DG unit is included, the load in its bus is incremented by the exact the same amount of its injected power. This way the base case does not change from the bulk power system viewpoint no matter the DG penetration level considered and it represents the power system without mandatory disconnection of DG units.
7. All distributed generators have the same undervoltage protection setting at their PCC. The two most stringent undervoltage pick-up values of Table 4.1 were employed separately to obtain the numerical results of this chapter: that is the COPEL setting of 0.95 pu and the CLELESC one of 0.85 pu.
8. The power flow equations are used to represent power system equilibria.
9. The predictor/corrector algorithm described in this dissertation was implemented together with the method proposed by Yorino, Li and Sasaki (2005). Combined they can find the generators reactive power limits as well as the DG disconnection points. Since these two are the only parametric discontinuity types modeled here, the implemented algorithm is expected to successively find all discontinuities that the test systems are subject to.

The three DG penetration levels and the two undervoltage protection settings considered

create several scenarios so it is possible to identify situations where the DG mandatory disconnection is critical to the system stability and situations where it is unimportant.

As mentioned in Chapter 3, the proposed approach to consider discrete load changes does not entail a monotonic relationship between the load parameter λ and the total load connected to the power system. Although this is generally true, the DG mandatory disconnection is an exception to that. In this case, referring to the load parametrization of Section 2.2, the discontinuity is not in P_{L0k} or Q_{L0k} as previously described, but rather in P_{Gk}. To account for DG, P_{DGk} is added to P_{Gk}, representing the DG active power injection. Therefore, the load itself is not subject to discontinuities. What does change when a DG unit trips is P_{DGk} that goes to zero. For the EPS, this looks like a discrete load increase, since the amount of power that needs to be delivered through the transmission system suddenly rises.

This means that, rigorously, the DG mandatory disconnection is mathematically different than the sudden load variations described in the previous chapter. However, in nature, DG units turning off can be perceived as such load discontinuities, therefore the proposed predictor/corrector scheme is adequate to study such phenomena.

What results from this discussion is that, when the DG mandatory disconnection is under analysis, the load parameter λ represents the total active power of the system, i.e. the relationship between λ and the active power consumed in the whole EPS is monotonic.

First, the quantitative effect of the DG mandatory disconnection is studied for the IEEE 118 bus test system. Afterwards, the results regarding the 107 bus Brazilian system are presented.

4.2.1 IEEE 118 bus test system

To define a comparative framework, the numerical results were obtained with the proposed predictor/corrector scheme and the CPFLOW with local parametrization. These methods are considered to have converged, if one unstable equilibrium is found.

The three DG penetration levels and the two undervoltage protection settings considered combine to a total of six scenarios.

DG undervoltage protection set at 0.95 pu

For the three cases where the DG undervoltage protection was set equal to 0.95 pu, the Maximum Loadability Point (MLP) and the Voltage Stability Margin (VSM) are indicated in Tables 4.3 and 4.4, for the CPFLOW and the proposed method respectively. These tables also present the absolute amount of DG that was disconnected in MW and the percentage of the total DG injection that was lost.

With exception of the base case, where the system is not subject to DG mandatory disconnection, the CPFLOW diverged for every scenario considered, i.e. no solution

Table 4.3: Effect of the DG mandatory disconnection in the IEEE 118 bus test system, when the undervoltage protection setting is 0.95 pu. These results are the outcome of the CPFLOW with local parametrization.

DG Penetration level	λ_{max}	VSM (GW)	VSM (%)	DG disconnection (MW)	DG disconnection (%)
0%	2.126	4.13	113%	–	–
10%	2.111	4.07	111%	69	19%
20%	2.085	3.98	108%	123	17%
30%	2.072	3.93	107%	201	18%

Table 4.4: Effect of the DG mandatory disconnection in the IEEE 118 bus test system, when the undervoltage protection setting is 0.95 pu. These results are the outcome of the proposed predictor/corrector scheme.

DG Penetration level	λ_{max}	VSM (GW)	VSM (%)	DG disconnection (MW)	DG disconnection (%)
10%	2.113	4.08	111%	75	21%
20%	2.093	4.01	109%	170	23%
30%	2.073	3.93	107%	279	25%

was found in the inferior portion of the PV curve. The MLP and VSM indicated in Table 4.3 regard the last power flow solution found before divergence of the method. The continuation step-length employed to find such results culminated from several trial and error attempts to make the CPFLOW converge and the actual value selected was the one associated with the higher loading level of the last converged solution.

The proposed predictor/corrector scheme did converge for these three cases. The VSM of both methods are similar, which indicates that the CPFLOW diverged right before the MLP. Prior to the results obtained with the proposed method, it was not possible to be sure whether or not the VSM calculated with the CPFLOW was a precise estimate of the IEEE system stability margin, due to the divergence of the method.

From the result of the proposed scheme, it is possible to affirm that the locally parametrized CPFLOW was not capable to trace the nose of the PV curve for the bifurcation type that this system is subject to.

Even though the MLP estimated with the CPFLOW turned out to be accurate, this was not true for the total amount of DG that was disconnected. This happened because the continuation method diverged right before the nose of the PV curve, missing the units that were tripped near the critical point of the IEEE test system. Assuming that the numerical results obtained from the proposed predictor/corrector procedure are accurate, the error caused by the divergence of the CPFLOW reached 27% regarding the amount of DG that is disconnected prior to MLP.

The outcome of the proposed predictor/corrector scheme also comprises the sequence of discontinuities to which the power system equilibrium diagram is subject to. Between the

reactive power limits and the DG mandatory disconnections, more than 200 discontinuities take place in the IEEE 118 test system prior to the MLP, when the undervoltage setting is equal to 0.95 pu for the three DG penetration levels considered.

First, for ease of analysis, only the last 20 discontinuities of the case where the DG penetration level is equal to 10% are indicated in Table 4.5.

Table 4.5: Sequence of the last 20 discontinuities of the IEEE 118 bus test system equilibrium diagram. The undervoltage protection setting of DG units is equal to 0.95 pu and the DG penetration level is 10%.

Discontinuity	Bus	Voltage drop DG group	System Loading (λ)	Cascading Events
DG	34	3	2.0971	Isolated
DG	3	3	2.0975	A
DG	2	3	2.0968	
DG	18	3	2.0964	
DG	1	1	2.0968	
DG	45	2	2.0980	Isolated
DG	96	2	2.1008	Isolated
DG	84	2	2.1012	Isolated
DG	36	2	2.1040	B
DG	35	2	2.1028	
DG	33	1	2.1035	
Q-limit	54	–	2.1054	Isolated
DG	13	2	2.1065	Isolated
DG	117	2	2.1087	Isolated
DG	15	2	2.1113	Isolated
DG	19	1	2.1115	C
DG	3	2	2.1108	
DG	2	2	2.1108	
Q-limit	113	–	2.1130	Isolated
Q-limit	10	–	2.1132	Isolated

Notice that two types of discontinuity are considered: the reactive power limit of generators and the DG undervoltage mandatory disconnection. As discussed in Chapter 3, the load reduction that is observed in successive DG disconnections is a consequence of Corrector II that reduces λ to assure solvabitilty of the power flow equations. From the discussion of Section 3.2.3, if a discontinuity takes place in a load level smaller than a previous disconnection, then the second parametric change is a direct consequence of the first one. With that in mind, all discontinuities can be separated into blocks that group cascading events. This is indicated in the last column of Table 4.5, where it is possible to notice isolated events, that do not cause any other discontinuity, and cascading ones, where the first disconnection is responsible for the ones comprised in the same event.

For example, in event A, the trip of DG units located in group 3 of bus 3 is responsible to reduce power system bus voltages to the extent of causing the disconnection of three other DG groups located at buses 2, 18 and 1. The same interpretation is valid for the cascading events indicated as B and C.

The traditional CPFLOW does not provide such detailed information regarding equilibria discontinuities. At most, it can provide which discrete parametric change happened between two calculated power flow solutions. In such case, obtaining the actual sequence of DG disconnections would require very small continuation steps which could yield convergence problems, as described in the previous chapter.

Besides indicating the sequence of discontinuities, the proposed method can also identify the bifurcation type of the MLP. As a result of the proposed stopping criteria, the last power flow solution found (Q-limit of Generator 10) was identified to be unstable. From the test proposed by Yorino, Li and Sasaki (2005) described in Section 2.4.3, this solution is classified as a SIB, meaning that instability is a direct consequence of Generator 10 reaching its reactive limit.

This result helps to explain why the locally parametrized CPFLOW diverged. Since the local parameter is selected based on the tangent vector to the PV curve, which can not foresee discontinuities, its choice may be inadequate near the SIB.

The last discontinuities found in the PV curve of the IEEE test system when the DG penetration is equal to 20% and 30% are shown in Tables 4.6 and 4.7 respectively. These results can be interpreted like the ones regarding the DG penetration level of 10%.

When the penetration is equal to 20%, the trip of DG group 2 at bus 13 is responsible to turn off a total of 11 MW of DG, as well as to make two bulk power system generators reach their Q-limits. For the case where the penetration is 30%, an even more severe event happens after the disconnection of DG at bus 3: 78 MW of DG contribution is lost due their mandatory disconnection and four generators reach their limits. This cascading events are so severe that there is no stable equilibrium available to the system operate afterwards.

With these results it is noticeable that as the DG penetration level increases, the disconnection of such units become more severe to the power system. As a result, the EPS becomes more likely to suffer cascading disconnections and consequently structure induced instability.

The last solution indicated in the last line of both Tables 4.6 and 4.7 were identified as unstable equilibria. From Condition I of Section 3.2.4, the first discontinuities of the last event of each table was identified as a SIB. This means that, when the DG penetration is 20%, the disconnection of DG group 1 at bus 36 causes instability. When the penetration is 30%, the same thing can be asserted about DG group 3 at bus 3.

For these two cases, the CPFLOW diverged right before the occurrence of event A, which represents a severe discontinuity in the EPS equilibrium diagram. This demonstrates

Table 4.6: Sequence of the last discontinuities of the IEEE 118 bus test system equilibrium diagram. The undervoltage protection setting of DG units is equal to 0.95 pu and the DG penetration level is 20%.

Discontinuity	Bus	Voltage drop DG group	System Loading (λ)	Cascading Events
Q-limit	4	–	2.0844	Isolated
DG	36	2	2.0851	A
DG	35	2	2.0819	
DG	33	1	2.0848	
DG	3	3	2.0845	
DG	2	3	2.0821	
DG	1	1	2.0826	
DG	96	2	2.0852	Isolated
DG	84	2	2.0880	Isolated
DG	13	2	2.0919	B
DG	15	2	2.0916	
DG	19	1	2.0881	
DG	45	1	2.0870	
Q-limit	54	–	2.0869	
DG	117	2	2.0898	
Q-limit	113	–	2.0904	
DG	34	2	2.0915	
DG	22	1	2.0914	
DG	3	2	2.0916	
DG	2	2	2.0898	
DG	36	1	2.0930	C
DG	35	1	2.0904	
DG	18	2	2.0907	
DG	52	3	2.0888	
Q-limit	10	–	2.0903	

that the traditional continuation method can experience convergence problems due to discrete load changes and may be inapt to consider such events.

Even though the CPFLOW diverged, it got close enough to the MLP, which makes it possible to compare its computational efficiency to the proposed method. The latter solves the power flow problem twice for every load discontinuity, calculating one equilibrium point before the DG is disconnected and one after. In each penetration levels considered, this amounted to almost 200 power flow solutions. With the continuation step-length employed, the CPFLOW resulted in a few more equilibrium points. The case that required less power flow solutions were the one for which the penetration level was equal to 20%, where 219 PV curve points were calculated. This means that the proposed method estimated the MLP a little faster than the traditional CPFLOW. Larger continuation step-lengths could have been employed to reduce the number of power flow solutions required by

Table 4.7: Sequence of the last discontinuities of the IEEE 118 bus test system equilibrium diagram. The undervoltage protection setting of DG units is equal to 0.95 pu and the DG penetration level is 30%.

Discontinuity	Bus	Voltage drop DG group	System Loading (lambda)	Cascading Events
DG	105	3	2.0636	Isolated
DG	96	2	2.0692	Isolated
Q-limit	4	–	2.0701	Isolated
DG	3	3	2.0726	
DG	2	3	2.0686	
DG	1	1	2.0684	
DG	19	1	2.0702	
DG	15	2	2.0672	
DG	34	2	2.0624	
DG	22	1	2.0630	
Q-limit	113	–	2.0673	
DG	13	2	2.0677	
DG	36	1	2.0662	
DG	35	1	2.0619	
Q-limit	54	–	2.0652	
DG	117	2	2.0664	
DG	18	2	2.0663	A
DG	3	2	2.0635	
DG	2	2	2.0600	
DG	15	1	2.0633	
DG	34	1	2.0577	
DG	13	1	2.0588	
DG	14	3	2.0579	
DG	117	1	2.0582	
Q-limit	73		2.0573	
DG	52	3	2.0581	
DG	16	3	2.0582	
DG	3	1	2.0579	
DG	2	1	2.0544	
Q-limit	10	–	2.0537	

the CPFLOW. However, this is not enough to ascertain that this traditional VSA tool is computationally more efficient than the proposed technique. In fact, the CPFLOW commonly requires many dozens of power flow solutions, which makes the 200 equilibrium points calculated by the proposed method a reasonable computational cost to solve the convergence problems that happened with the continuation power flow.

It is necessary to point out that the predictor/corrector scheme was programmed to notify and consider the occurrence of any discontinuity that was not anticipated by the proposed predictor. Yet, this did not happen in any of the scenarios studied above. From that, it is possible to conclude that for the IEEE system, two successive discontinuities

are close to each other. Therefore the linear predictor proposed is accurate enough to adequately foresee the next discontinuity that will happen.

To be fair, two disadvantages of the proposed predictor/corrector scheme need to be mentioned. First, it cannot be used to estimate the power system VSM when the DG mandatory disconnections are not considered. The method only finds parametric discontinuities in EPSs, meaning it can not be employed when such discontinuities do not exist. Second, the proposed correctors go back and forward with the loading parameter λ, so the method does not result in the system voltage profile, i.e. the PV curve is not estimated.

To observe the DG discontinuities, the PV curve obtained with the CPFLOW before it diverged is indicated in Figure 4.2.

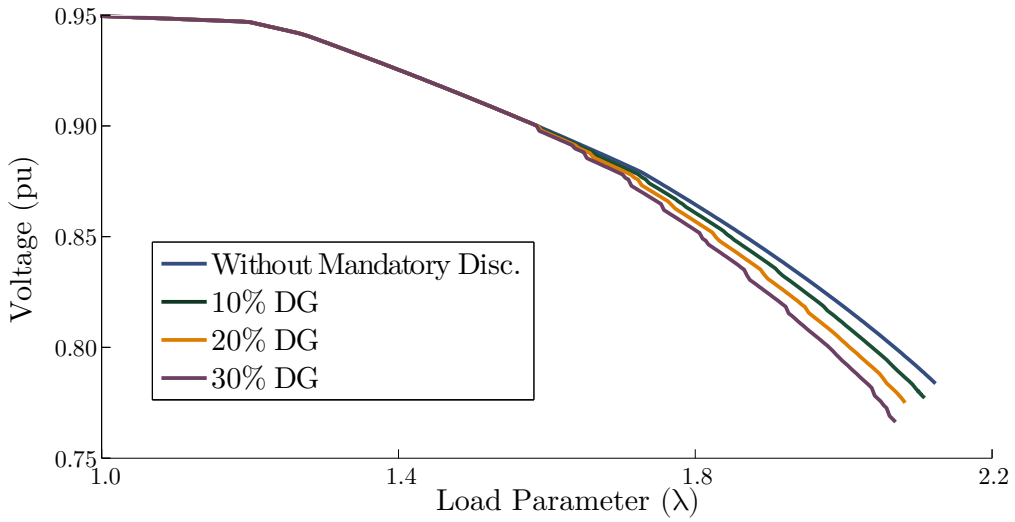

Figure 4.2: Voltage Profile of bus 118 of the IEEE 118 bus test system considering the DG mandatory disconnection with undervoltage protection set at 0.95 pu for three DG penetration levels.

The DG mandatory disconnection does not happen for small load levels, at which bus voltages are close to 1 pu. However, as the load grows, voltages drop and some DG units are disconnected due to their undervoltage PCC protection. With that, the voltage profile of the system deflects down from the base case, where mandatory disconnection is not considered. It is evident in Figure 4.2 that for higher DG penetration levels, the impact of their undervoltage trip is bigger.

Even though the discontinuities caused by DG disconnections are not appreciably big, they are noticeable. This is particularly true for the highest penetration level considered.

Intuitively, it would be expected that high penetration of DG increases the MLP of the system, since a big part of the load would be supplied by nearby units. This is true, but is not observed here because of consideration 6 in page 79. Each DG unit that is included is followed by an equivalent increase in load. As a result of that, the base case of the EPS does not change with different DG penetration levels. Therefore, the only effect of

such units in the system equilibrium diagram is related to their undervoltage mandatory disconnection.

DG undervoltage protection set at 0.85 pu

Reducing the undervoltage protection setting at the PCC of DG units from 0.95 pu to 0.85 pu is expected to significantly diminish the negative effect of their mandatory disconnection in the EPS. The VSMs estimated employing the lessened undervoltage requirement are indicated in Tables 4.8 and 4.9 for the CPFLOW and the proposed predictor/corrector scheme respectively.

Table 4.8: Effect of the DG mandatory disconnection in the IEEE 118 bus test system, when the undervoltage protection setting is 0.85 pu. These results are the outcome of the CPFLOW with local parametrization.

DG Penetration level	λ_{max}	VSM		DG disconnection	
		(GW)	(%)	(MW)	(%)
0%	2.126	4.13	113%	–	–
10%	2.126	4.13	113%	7.1	1.9%
20%	2.126	4.13	113%	14.3	1.9%
30%	2.127	4.13	113%	23.8	2.2%

Table 4.9: Effect of the DG mandatory disconnection in the IEEE 118 bus test system, when the undervoltage protection setting is 0.85 pu. These results are the outcome of the proposed predictor/corrector scheme.

DG Penetration level	λ_{max}	VSM		DG disconnection	
		(GW)	(%)	(MW)	(%)
10%	2.127	4.13	113%	7.1	1.9%
20%	2.127	4.13	113%	14.3	1.9%
30%	2.127	4.13	113%	23.8	2.2%

This time the continuation method converged for all cases, i.e. one unstable equilibrium point was found. With that, the CPFLOW can be used to validate the results obtained with the proposed predictor/corrector procedure. Indeed, they are practically the same both for the stability margin and the amount of DG that is disconnected.

The VSM that resulted from the CPFLOW when the DG penetration level is equal to 30% was slightly bigger than the other cases considered. The reason why this happened is merely numerical. Meaning that, the continuation step employed was able to find a solution that is closer to the PV curve nose.

With the reduced undervoltage protection requirement, very few units are disconnected. The impact of DG mandatory disconnections became insignificant for any practical purpose. Since now the DG blocks that are switched off are small, the IEEE power system is not

prone to cascading disconnections. Consequently, the PV curve discontinuities are not severe enough to yield convergence problems for the continuation method.

For the new protection setting, the proposed method identified that the IEEE test system is subject to a SIB caused by Generator 10 reaching its Q-limit, for the three DG penetration levels considered.

Actually, the Q-limits are essential to the adequate progress of the proposed method. In the three cases, less than six discontinuities resulted from DG disconnections, therefore the successive calculation of Q-limits is what guarantees the accuracy of the predictor stage and the convergence of the proposed correctors. The predictor was able identify consecutive discontinuities and, once again, not even one of them was skipped, situation that would be flagged in the correction stages. Without the Q-limits, the proposed method would most likely have diverged, since the first known power flow solution ($\lambda = 1$) is far from the first DG trip ($\lambda > 2$).

The PV curves obtained when the DG undervoltage protection is equal to 0.85 pu will not be presented here due to their similarity with the base case voltage profile of Figure 4.2. That is the blue curve for the system without mandatory disconnection of DG units.

Partial conclusions

One possible conclusion that can be drawn from all results regarding the IEEE 118 bus test system is that the CPFLOW may be inadequate to assess EPSs voltage stability when the same is subject to cascading DG trips which represent large equilibria discontinuities. This is the exact situation where the DG mandatory disconnection significantly impacts the system. However, when such events are small in size and scarce throughout the bulk power system the opposite is true: the proposed predictor/corrector scheme may go through convergence problems while the CPFLOW would yield adequate results.

4.2.2 107 bus reduced interconnected Brazilian test system

The same six scenarios, regarding different DG penetration levels and undervoltage protection settings, studied with the IEEE test system are repeated for the Brazilian one.

DG undervoltage protection set at 0.95 pu

Starting with the 0.95 pu undervoltage protection requirement for DG units. The VSMs of the reduced Brazilian system obtained with the locally parametrized CPFLOW and the proposed predictor/corrector scheme are presented in Table 4.10 and 4.11 respectively.

For the Brazilian system, the CPFLOW diverged for the three DG penetration scenarios considered. Once again the MLP obtained with this method is not a reliable estimate of the system loadability limit. This is more pronounced for the total amount of DG that is disconnected, where it is evident that the method diverged before any DG is tripped.

Table 4.10: Effect of the DG mandatory disconnection in the 107 bus reduced interconnected Brazilian test system, when the undervoltage protection setting is 0.95 pu. These results are the outcome of the CPFLOW with local parametrization.

DG Penetration level	λ_{max}	VSM (GW)	VSM (%)	DG disconnection (GW)	DG disconnection (%)
0%	1.1149	1.457	11.5%	–	–
10%	1.0891	1.130	8.9%	0	0%
20%	1.0891	1.130	8.9%	0	0%
30%	1.0891	1.130	8.9%	0	0%

Table 4.11: Effect of the DG mandatory disconnection in the 107 bus reduced interconnected Brazilian test system, when the undervoltage protection setting is 0.95 pu. These results are the outcome of the proposed predictor/corrector scheme.

DG Penetration level	λ_{max}	VSM (GW)	VSM (%)	DG disconnection (GW)	DG disconnection (%)
10%	1.0919	1.165	9.2%	0.75	58%
20%	1.0892	1.132	8.9%	1.06	42%
30%	1.0892	1.132	8.9%	1.10	29%

The three scenarios went through convergence problems at the same point as a result of consideration 6 in page 79, which guarantees that the system with different DG penetration levels is the same if no unit is disconnected.

With the Brazilian test system as well, several continuation steps-lengths were employed in an attempt to make the continuation power flow converge.

Once again, the proposed method is not adequate to estimate the MLP for the system without mandatory disconnection of DG units, since, in such case, the PV curve lacks the discontinuities that parametrize the referred method.

The sequence of DG trips and generator Q-limits are presented in Tables 4.12, 4.13 and 4.14 when the penetration level is equal to 10%, 20% and 30% respectively. All these results consider the DG undervoltage protection set at 0.95 pu.

Differently from the IEEE system, the Brazilian one is much closer to its MLP. As a result of that, the latter EPS goes through less discontinuities before the PV curve nose is reached. For this reason, all equilibrium discontinuities that happen in the Brazilian system are indicated in the aforementioned tables.

When the DG penetration level is 10%, there are two cascading disconnections. For the first one, called event A, the disconnection of DG group 3 in bus 1015 causes another trip in bus 939. For the second event, referred as B, the shutdown of DG group 2 located in bus 960 drove the cascading disconnection of eleven DG groups amounting to a loss of 571 MW of generation. This is enough to drive instability since the last solution found, the Q-limit of Generator 16, was identified as an unstable equilibrium via the proposed stopping criteria. Since this unstable point follows the trip of a DG group in bus 960, this

Table 4.12: Sequence of discontinuities of the 107 bus reduced Brazilian test system equilibrium diagram. The undervoltage protection setting of DG units is equal to 0.95 pu and the DG penetration level is 10%.

Discontinuity	Bus	Voltage drop DG group	System Loading (λ)	Cascading Events
DG	960	3	1.0892	Isolated
DG	1015	3	1.0898	A
DG	939	3	1.0895	
DG	834	3	1.0904	Isolated
DG	960	2	1.0919	B
DG	814	3	1.0900	
DG	1015	2	1.0894	
DG	939	2	1.0888	
DG	1504	3	1.0847	
DG	1504	2	1.0766	
DG	1504	1	1.0660	
DG	104	3	1.0575	
DG	138	3	1.0495	
DG	104	2	1.0469	
DG	138	2	1.0382	
DG	104	1	1.0347	
DG	138	1	1.0250	
Q-limit	16	–	1.0171	

incident is classified as a SIB by Condition I of Figure 3.12.

Table 4.13: Sequence of discontinuities of the 107 bus reduced Brazilian test system equilibrium diagram. The undervoltage protection setting of DG units is equal to 0.95 pu and the DG penetration level is 20%.

Discontinuity	Bus	Voltage drop DG group	System Loading (λ)	Cascading Events
DG	960	3	1.0892	A
DG	1015	3	1.0882	
DG	939	3	1.0866	
DG	834	3	1.0841	
DG	1015	2	1.0846	
DG	1504	3	1.0807	
DG	1504	2	1.0571	
DG	1504	1	1.0229	
DG	104	3	0.9897	
DG	104	2	0.9685	
DG	136	3	0.9447	
DG	104	1	0.9356	

When the DG penetration level is either 20% or 30%, the first DG trip happens at

Table 4.14: Sequence of discontinuities of the 107 bus reduced Brazilian test system equilibrium diagram. The undervoltage protection setting of DG units is equal to 0.95 pu and the DG penetration level is 30%.

Discontinuity	Bus	Voltage drop DG group	System Loading (λ)	Cascading Events
DG	960	3	1.0892	A
DG	1015	3	1.0862	
DG	939	3	1.0830	
DG	1015	2	1.0745	
DG	1504	3	1.0692	
DG	1504	2	1.0273	
DG	1504	1	0.9599	
DG	104	3	0.8649	

bus 960 and it is responsible to cause instability. In other words, the fist power injection discontinuity is severe enough to cause cascading shut-downs and finally prevent the system to find a stable equilibrium point. This explains why these two scenarios have exactly the same MLP, that is because the first DG disconnection is a structure induced bifurcation.

In both these cases, the DG disconnections are not progressive and slow as the load grows. They comprise a cascading event, where one disconnection is enough to disturb the EPS to the extent of causing instability. The proposed method satisfactorily depicted this behavior of the Brazilian system, that was overlooked by the traditional CPFLOW.

There are two main reasons why this happened here and not for the IEEE 118 bus test system. First, the Brazilian system operates under a more stressed base case load level, which means that it is closer to its MLP. Second, it has a smaller number of load buses (39 against 91 in the IEEE system). Looking at the fact that the DG power injection is distributed over such buses, the DG groups for the Brazilian system are considerably bigger. Therefore, the impact of their disconnection is expected to be more severe.

Since the CPFLOW diverged before any DG unit is disconnected, the PV curves obtained for all penetration levels coincide with the case where no unit is disconnected. Because it is not possible to observe the DG discontinuities, the PV curves of the Brazilian system will be left out of this text.

DG undervoltage protection set at 0.85 pu

Differently from the IEEE system, reducing the PCC undervoltage protection requirement to 0.85 pu did not solve the divergence problem of the CPFLOW. Once again the continuation method had convergence problems right before the fist DG unit is disconnected, which corroborates the fact that such method may be unsuited to analyse discrete load discontinuities in power system equilibria.

The VSMs estimated with this reduced undervoltage protection requirement are

indicated in Tables4.15 and 4.16 for the two numerical procedures being used in this research.

Table 4.15: Effect of the DG mandatory disconnection in the 107 bus reduced interconnected Brazilian test system, when the undervoltage protection setting is 0.85 pu. These results are the outcome of the CPFLOW with local parametrization.

DG Penetration level	λ_{max}	VSM (GW)	VSM (%)	DG disconnection (GW)	DG disconnection (%)
0%	1.1149	1.457	11.5%	–	–
10%	1.1132	1.435	11.3%	0	0%
20%	1.1132	1.435	11.3%	0	0%
30%	1.1132	1.435	11.3%	0	0%

Table 4.16: Effect of the DG mandatory disconnection in the 107 bus reduced interconnected Brazilian test system, when the undervoltage protection setting is 0.85 pu. These results are the outcome of the proposed predictor/corrector scheme.

DG Penetration level	λ_{max}	VSM (GW)	VSM (%)	DG disconnection (MW)	DG disconnection (%)
10%	1.1132	1.436	11.3%	195	15%
20%	1.1132	1.436	11.3%	312	12%
30%	1.1132	1.436	11.3%	406	11%

Comparing the VSM of the Brazilian system with and without DG mandatory disconnection, the effect of the 0.85 pu undervoltage setting is practically negligible. This means that this softer undervoltage requirement is not expected to cause instability problems.

The Q-limits and DG disconnections identified with the proposed predictor/corrector method are shown in Tables 4.17, 4.18 and 4.19 for the three DG levels considered.

Table 4.17: Sequence of discontinuities of the 107 bus reduced Brazilian test system equilibrium diagram. The undervoltage protection setting of DG units is equal to 0.85 pu and the DG penetration level is 10%.

Discontinuity	Bus	Voltage drop DG group	System Loading (λ)	Cascading Events
Q-limit	919	–	1.1098	Isolated
DG	960	3	1.1132	A
DG	1015	3	1.1120	
DG	939	3	1.1112	
DG	960	2	1.1087	

For the three DG penetration levels studied, an unstable equilibrium resulted from the first disconnection, which happens for DG group 3 at bus 960. From Condition I of Section 3.2.4, this trip is a SIB.

Table 4.18: Sequence of discontinuities of the 107 bus reduced Brazilian test system equilibrium diagram. The undervoltage protection setting of DG units is equal to 0.85 pu and the DG penetration level is 20%.

Discontinuity	Bus	Voltage drop DG group	System Loading (λ)	Cascading Events
Q-limit	919	–	1.1098	Isolated
DG	960	3	1.1132	A
DG	1015	3	1.1101	
DG	939	3	1.1080	
DG	1015	2	1.1011	

Table 4.19: Sequence of discontinuities of the 107 bus reduced Brazilian test system equilibrium diagram. The undervoltage protection setting of DG units is equal to 0.85 pu and the DG penetration level is 30%.

Discontinuity	Bus	Voltage drop DG group	System Loading (λ)	Cascading Events
Q-limit	919	–	1.1098	Isolated
DG	960	3	1.1132	A
DG	1015	3	1.1077	
DG	939	3	1.1038	

The CPFLOW was not capable to find a power flow solution after such discontinuity. The only reason why it accurately calculated the VSM is because it was able to get really close to the EPS equilibrium right before it happened.

Since the first DG unit trip was enough to cause instability for the smallest penetration level studied, any other level bigger than this will have the same stability margin.

For all scenarios considered for the Brazilian system, one DG disconnection was responsible to cause instability. This can be easily justified by the fact that such unit trip happened for loading levels close the what would have been the MLP of the system without DG undervoltage disconnections. This means that the system is in the verge of voltage collapse before the first unit is tripped, when it actually happens it is enough to cause instability.

Partial conclusions

The numerical results obtained from the 107 bus Brazilian test system corroborate the convergence problems that the CPFLOW may experience when analysing the equilibrium discontinuities caused be the mandatory disconnection of DG units. This time as well, these problems were not experienced by the proposed predictor/corrector scheme.

4.3 Final Remarks

The numerical results regarding DG disconnections evidence the fact that the traditional CPFLOW may experience convergence problems when the power system is subject to load discontinuities. This was particularly true when big blocks of DG units were turned off, especially when cascading events took place.

The proposed predictor/corrector scheme proved capable to identify these cascading disconnections, as well as the events that caused instability and the bifurcation type to which the power system was subject to.

The numerical results provided here also depict the limitations of the proposed method. No information is obtained regarding the actual voltage profile of the system and its application may be compromised if the EPS does not go under several successive parametric discontinuities.

Chapter 5

Case Study on Dispersed Undervoltage Load Shedding

Another sudden load variation that is distributed among EPS buses is the Undervoltage Load Shedding (ULS). The parametric discontinuities caused by such phenomena fit the description of load switches that can be readily analysed with the proposed predictor/corrector scheme.

Load shedding is a last resource but effective method to assure that voltage collapse does not happen. It is a corrective measure to restore stability of power systems, if all other possible control actions are unavailable (FENG; AJJARAPU; MARATUKULAM, 1998; AMRAEE et al., 2007; LEFEBVRE; MOORS; CUTSEM, 2003; AFFONSO et al., 2004).

One possible cause of voltage instability is the occurrence of severe contingencies. After an EPS goes through a contingency there are two possible outcomes: (i) an adequate operation point is achieved, but the voltage stability margin is reduced and the system becomes more vulnerable or (ii) instability will occur and corrective actions need to be taken (AFFONSO et al., 2004).

It is common practice in power systems to plan its expansion and operation, so it is capable to supply the load even when a single of its components becomes unavailable. This is known as N-1 criteria, which is based on a deterministic assessment of the EPS behavior after every credible single contingency that the power system may be subject to (KUNDUR et al., 2004). Even though such analysis may comprise several contingencies, it is not capable of considering all possible scenarios.

The main goal of ULS is to avoid instability after the occurrence of severe contingencies that are not included in the deterministic analysis mentioned above. This means that, load shedding is designed for very unlikely scenarios that could be cumbersome to system operation and even cause voltage collapse (TAYLOR, 1992; LEFEBVRE; MOORS; CUTSEM, 2003; MOORS; LEFEBVRE; CUTSEM, 2001; AFFONSO et al., 2004). In this sense, ULS could even be a cost effective measure to prevent the interruption of power supply to critical loads and expensive manufacturing processes (TAYLOR, 1992; BALANATHAN et al., 1998;

AFFONSO et al., 2004). Nevertheless, load shedding is always a last resource and should be carried out if other means like static reactive compensators and switchable shunt capacitors are unavailable or incapable to restore stability (TAYLOR, 1992; TUAN et al., 1994).

To meet its goals ULS should be carefully designed. Two approaches can be distinguished with this purpose: the decentralized and the centralized schemes. The centralized one is based on the status of the complete EPS as measured by the control center. There, the localization and amount of load to be shed is determined via an elaborated set of rules and the instruction to disrupt load is send through communication networks. The local scheme is simpler and based on local measurements of bus voltages that can automatically disconnect their associated loads (AMRAEE et al., 2007). For such purpose, undervoltage protection schemes are usually employed. As a result of them, load is shed if particular bus voltage magnitudes drop bellow some threshold for a given time (CUTSEM; MOORS; LEFEBVRE, 2002; TAYLOR, 1992).

To adequately select the ULS pick-up value, its time delay and location, dynamic simulations should be employed, since they accurately depict the system behaviour after a contingency (LEFEBVRE; MOORS; CUTSEM, 2003; ARNBORG et al., 1997; BALANATHAN et al., 1998). To maintain an EPS stable, ULS should meet two requirements: (i) there must be a new stable equilibrium point for the post-contingency configuration and (ii) the system dynamic trajectory after the disturbance must be inside the region of attraction of such equilibrium (BALANATHAN et al., 1998).

While the second requirement can only be assessed through time domain simulations of the non-linear dynamic model of the EPS, the first one can employ static techniques. During the design of ULS, dynamic simulations can be computationally exhaustive, since one single undervoltage protection configuration should be capable to avoid instability for several scenarios of contingency (LEFEBVRE; MOORS; CUTSEM, 2003).

Therefore, static techniques can and should be used to screen adequate ULS projects to assure the existence of stable equilibrium point after the system goes through a contingency (AFFONSO et al., 2004; TUAN et al., 1994; FENG; AJJARAPU; MARATUKULAM, 1998). After that, dynamic analysis is required to assess whether such equilibrium point is actually reached.

The proposed predictor/corrector scheme is capable to analyse the effect of local ULS within the framework of static studies. It estimates the VSM of a power system subject to ULS when the load grows at given direction. In this case, it also calculates the location and amount of load that is shed for the undervoltage protection schemes employed.

Due to this nature, it can not depict the load shedding that would occur after a contingency takes place, which makes its application in contingency analysis inadequate. The contribution of the proposed method lies in determining how ULS affects the power system when the load increases in a given direction.

One possible practical situation that may benefit from the proposed predictor/corrector

scheme is the undervoltage protection of air conditioners in Dubai (DEWA, 2011; KAROUI et al., 2011). There the Dubai Electricity and Water Authority (DEWA) requires that every chiller should be provided with an undervoltage relay with fixed voltage cut-off set at 0.75 pu and whose time delay should be less than 200 ms (DEWA, 2011). Such requirement was defined precisely to avoid possible blackouts that may result from voltage instability. Since a significant part of the load in Dubai is composed of air-conditioners, their undervoltage protection can remarkably help the system during adverse situations. In this scenario, the proposed method could be used to identify which loads would go under ULS and how this would affect the VSM for a given load growth direction.

Nevertheless, the numerical results presented in this chapter do not comprise the particular features of the ULS in Dubai. In the following sections, the load blocks that are shed are much bigger than a single air conditioner and they should be regarded as a bundle of several loads that are disconnected simultaneously.

In the literature, there are several studies that proposed different techniques to determine the adequate amount of load to be shed to assure that there is a stable equilibrium after critical contingencies (TUAN et al., 1994; FENG; AJJARAPU; MARATUKULAM, 1998; AFFONSO et al., 2004; AMRAEE et al., 2007). These studies employ static techniques, however they do not explain what would be the driving force to make the calculated load shedding possible. In other words, they overlook how the ULS could be practically implemented in power systems and no discussion is presented regarding the application of undervoltage protection schemes for such purpose.

The same gap can be seen in the works of Arnborg et al. (1997) and Balanathan et al. (1998). Those studies argue that the dynamic behavior of the load governs how much of it should be shed. Then, this value is calculated base on the parameters of the load dynamic model. Once again, a practical undervoltage load shedding implementation is not discussed.

Taylor (1992) directly addresses the design of undervoltage protection schemes for load shedding purposes. To define design criteria, the author employs time domain simulations of the EPS after critical disturbances. One important conclusion of such work is that effective undervoltage cut-off relay setting should be within 0.85 pu and 0.92 pu.

In the same line of work it is possible to mention the papers of Moors, Lefebvre and Cutsem (2001), Cutsem, Moors and Lefebvre (2002), Lefebvre, Moors and Cutsem (2003). They designed undervoltage protection schemes to avoid voltage collapse in the Hydro-Québec system. From time domain simulations, five transmission buses were selected to indicate whether the system is going through stability problems. Among other conditions, if the average of the voltage magnitude at these buses is bellow 0.94 pu, then load shedding starts according to a priority list.

Beyond the analysis made by Taylor (1992), Lefebvre, Moors and Cutsem (2003), the predictor/corrector scheme could be employed to assess how the proposed ULS protection

schemes impact the loadability margin of EPS for a given load growth direction. It also obtains the buses where load shedding happens, how much of it is disconnected and the order at which such events take place. All this is done from a static point of view.

It is important to point out that the proposed method is not envisioned to substitute other techniques specifically developed to design ULS. On the contrary, its goal is to contribute with information regarding the effect of the undervoltage protection schemes as the load grows.

To exemplify the application of the proposed predictor/corrector scheme in studies regarding ULS, this chapter will present in Section 5.2 numerical results for the two test systems employed in the previous chapter (the IEEE 118 bus system and the Brazilian reduced one). They are now implemented with undervoltage load shedding instead of DG units. The model of decentralized ULS that is employed in such systems is described in section 5.1.

5.1 Decentralized Undervoltage Load Shedding Model

The proposed predictor/corrector scheme was designed to examine load discontinuities that are dispersed throughout the EPS. That is why it is employed here to deal with decentralized ULS.

To simplify the analysis, the most straightforward undervoltage protection design was implemented based on what was described by Amraee et al. (2007), Tuan et al. (1994), Lefebvre, Moors and Cutsem (2003). Three basic rules define such ULS:

1. If the voltage magnitude at a pre-specified bus reaches a threshold, then a fixed amount of its load is disconnected.
2. At pre-specified load buses, the voltage magnitude is monitored even if load shedding has already happened. If needed, the undervoltage protection may trigger several successive load disconnections at the same location.
3. There is a maximum limit of load that can be shed in each bus. This ensures that crucial loads remain functioning properly.

Three parameters need to be set for this ULS: the undervoltage cut-off value, the time delay and the amount of load to be shed (CUTSEM; MOORS; LEFEBVRE, 2002). Just like with the DG mandatory disconnection, the actual time delay of such protections will not affect the static analysis performed.

5.2 Numerical Results

This time as well, the results obtained with the proposed predictor/corrector method will be compared to the ones from the CPFLOW employing local parametrization. This

parametrization was selected over the arc-length one for the same reason mentioned in the previous chapter, due to its similarity with the proposed algorithm.

The two EPSs under analysis are also the same, that is the IEEE 118 bus test system and the reduced Brazilian interconnected system. They were briefly described in the preceding chapter and their complete characterization is available in Appendices A and B.

The following consideration were made to simplify the analysis regarding ULS. They are not necessary to the application of the proposed method nor the CPFLOW. Hypothesis 1 and 2 were also employed to study the mandatory disconnection of DG units.

1. The load growth was parametrized as described in Section 2.2 considering that K_{Pi}, K_{Qi} and K_{Gi} are all equal to one for every system bus. This means that, load power increases in each bus proportionally to the base case loading with constant power factor. Note that, all load data are provided in Appendices A and B. Also, to meet such load increase, generators are dispatched proportionally to their base case active power injection. This way the generators that were supplying more power to the system in the base case, i.e. the bigger ones, are responsible to take on more load.
2. The power flow equations are used to represent power system equilibria.
3. The undervoltage load shedding pick-up level was set equal to 0.9 pu. At pre-specified load buses, when the voltage magnitude reaches this threshold, 10% of the total load in the associated bus is disconnected. This setting is in accordance with what was proposed by Taylor (1992).
4. The active and reactive components of a load are shed in the same proportion, i.e. the load power factor remains constant after ULS.
5. At the buses where ULS is possible, 40% of the load comprises critical consumers that can not be turned off. That means that 60% of the bus demand may actually be shed.
6. The predictor/corrector algorithm described in this dissertation was implemented together with the method proposed by Yorino, Li and Sasaki (2005). Combined they can find the generators reactive power limits as well as load shedding cause by undervoltage protections. These two are the only parametric discontinuities considered in the EPSs under analysis.

Its essential to point out the relationship between the loading parameter λ and the EPS load when the system is subject to ULS.

As mentioned in Section 3.1, the load discontinuities happen in the parameters P_{L0k} and Q_{L0k} that represent the base case loading of the system. This is precisely how ULS is modeled here. As a result of that, λ cannot be monotonically related to the total active demand of the power system anymore. Depending on the amount and location of load shed, the same value of λ corresponds to different values of total active load.

Nonetheless, such loading parameter λ still represents the EPS demand. For the buses where load shedding does not happen, it still is monotonically related to the power

consumption. Observing that and the fact that the general purpose of ULS is to disconnect a few loads to allow other consumers to be supplied, then the maximum value of λ should still interest operators.

In such case, the value of λ at the MLP should not be interpreted as the total active power in MW that could be supplied by the system, but rather as an indicator of how much load can be connected before it goes through voltage collapse.

The numerical results displayed here consider two configurations of the test systems: (i) with the complete network and (ii) without a critical generator. These scenarios were selected to demonstrate important features of the proposed predictor/corrector algorithm.

5.2.1 IEEE 118 bus test system

For the IEEE system, undervoltage load shedding schemes were implemented in buses 2, 3, 7, 11, 13, 14 and 117. These locations where selected based on the sensitivity analysis performed by Amraee et al. (2007).

Complete network

First, the complete network is analysed and the voltage stability margin of the system with and without ULS can be compared in Table 5.1. This table also depicts the absolute amount of load that is shed and the percentage one relative to the total amount that could be shed (129.6 MW). The numerical values regarding load shedding are referred to the demand of the base case ($\lambda = 1$) and should be compared with it.

Table 5.1: Effect of the undervoltage load shedding in the IEEE 118 bus test system with complete network.

Method	ULS	λ_{max}	VSM		Load Shedding	
			(GW)	(%)	(MW)	(%)
CPFLOW	×	2.126	4.13	113%	–	–
	✓	2.195	4.22	115%	76.2	59%
Proposed	✓	2.193	4.30	117%	33.3	26%

This study has one essential difference when compared with the one regarding DG mandatory disconnection. This time the load discontinuities are beneficial to the voltage stability and the VSM increases for the system with ULS.

For these results, both the CPFLOW and the proposed predictor/corrector scheme converged. The value λ_{max} corresponds to the maximum load parameter where the power flow equations are solved for a stable equilibria. Notice that the biggest value of λ_{max} does not correspond to the maximum VSM anymore. This is a direct consequence of the load shedding itself. For the two methods employed, the system went through different

amounts of shed, which makes their relationship between λ and the total power supplied distinct.

The value of λ_{max} indicates how much further the load can increase at every bus that is not subject to shedding. This is why such loading parameter is still expected to interest power system operators.

The amount of load that is shed was discrepant for the two methods employed. The CPFLOW overestimated such value due to the discrete nature of the continuation process. Two successive power flow solutions are separated by a gap that is determined by the continuation step-length employed. With this method, it is not possible to isolate the events between the last stable solution and the first unstable one. In this interval, there is no certainty whether the load shedding happened before or after the MLP. Since the proposed predictor/corrector scheme individually finds the load discontinuities, it is expected to determine which discontinuities happened prior to the nose of the PV curve, estimating the total ULS more accurately.

The last discontinuities before the MLP calculated with the proposed method are presented in Table 5.2.

Table 5.2: Sequence of last discontinuities calculated with the proposed predictor/corrector method for the complete 118 bus IEEE test system with ULS protection schemes.

Discontinuity	Bus	Load Shedding Stage	System Loading (λ)
Q-limit	65	–	1.8574
Q-limit	46	–	1.9908
ULS	13	1	1.9967
ULS	117	1	2.0293
ULS	13	2	2.0438
ULS	3	1	2.0627
ULS	2	1	2.0910
ULS	13	3	2.0979
ULS	3	2	2.1128
ULS	117	2	2.1235
Q-limit	54	–	2.1253
ULS	2	2	2.1483
ULS	13	4	2.1586
ULS	3	3	2.1710
Q-limit	99	–	2.1778
Q-limit	10	–	2.1906
Q-limit	4	–	2.1934

The different load shedding stages presented in Table 5.2 are related to the repetitive actuation of the ULS protection schemes to maintain bus voltage magnitudes above the threshold value. In each stage, 10% of the load is shed and this may go on until stage number six, which represents the limit before only critical loads are connected to the bus

under question.

The last solution was identified as a SIB with the conditional test proposed by Yorino, Li and Sasaki (2005) and described in Section 2.4.3. Since the ULS raises bus voltage magnitudes, the cascading scenarios observed when analysing the DG mandatory disconnection are practically impossible here.

Regarding the computational efficiency, the CPFLOW took 240 continuation steps before reaching the MLP. This number is depends directly on the step-length utilized and it could have been significantly reduced if a larger value had been employed. The proposed predictor/corrector scheme estimated the same MLP after calculating 55 power flow solutions. Therefore, in this particular scenario, the proposed method proved to be computationally more efficient than the traditional CPFLOW. Overall, this algorithm solves the power flow equations twice for each sudden load variation that takes place before the MLP. This means that, the number of such discontinuities will determine the computational effort required by the method.

The author would like to emphasise that the discontinuity predictor was able to accurately identify the Q-limits and the ULS in the correct order, since the correctors did not flag any skipped discontinuity. As already said, this happened because the discontinuities are successively close to each other and, therefore, the linear predictor employed is accurate enough to select the next one.

Notice that the proposed method was not used to estimate the MLP of the EPS without ULS, in which case the equilibrium diagram may lack enough discontinuities for adequate performance of the algorithm.

Besides that, the predictor/corrector scheme did not obtain the PV curve of the system. Differently from the CPFLOW, that resulted in the voltage profile of bus 14 indicated in Figure 5.1.

In this graphic it is clear that after bus voltages reach small levels, ULS protection schemes start to act, shedding loading to increase the MLP.

Without a critical generator

The second biggest generator (located at bus 80) was selected to be removed over the first one, because the numerical results obtained with this topology demonstrate important features of the proposed method.

For the IEEE system without this unit, the MLP estimated with the CPFLOW and the proposed predictor/corrector scheme are indicated in Table 5.3.

To the precision presented, the two methods employed obtained the same VSM for the IEEE system. They also agreed upon the fact that the MLP is reached before any load is shed. This fact reduces the number of discontinuities in the EPS equilibria, which may interfere with the adequate operation of the proposed method. For the scenarios

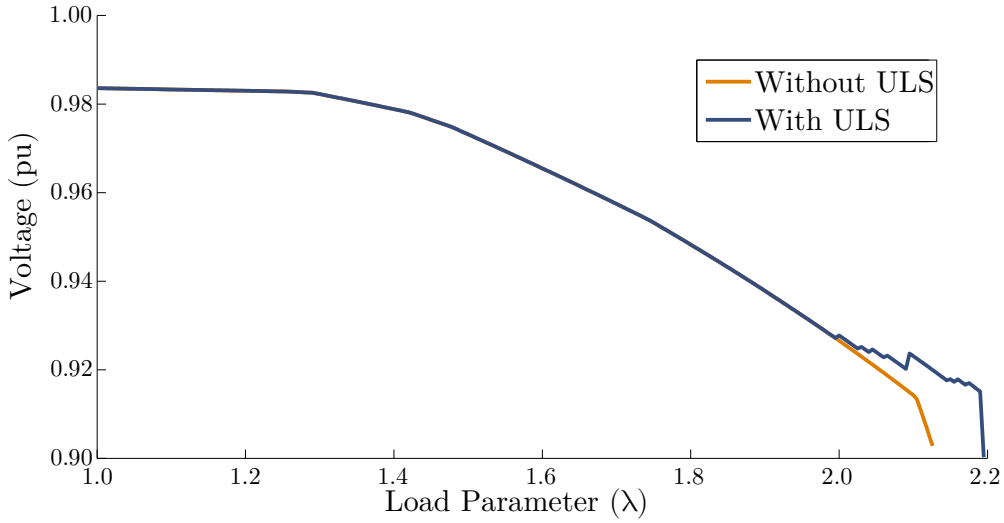

Figure 5.1: Voltage Profile of bus 14 of the IEEE 118 bus test system with and without under voltage load shedding.

Table 5.3: Effect of the undervoltage load shedding in the IEEE 118 bus test system without the generator located at bus 80.

Method	ULS	λ_{max}	VSM		Load Shedding	
			(GW)	(%)	(MW)	(%)
CPFLOW	×	1.935	3.43	93%	–	–
	✓	1.935	3.43	93%	0	0%
Proposed	✓	1.935	3.43	93%	0	0%

considered, this is the first one where actual discontinuities were skipped, that is to say, the predictor incorrectly selected the next one in the equilibrium loci.

This can be seen in the complete set of discontinuities found with the proposed method, which is indicated in Table 5.4.

In these results it is possible to notice that two Q-limits are skipped. To exemplify numerically what this means, pay attention to the reactive limit of Generator 56. After the Q-limit of Generator 100 was calculated, the linear predictor employed foresaw that Generator 15 would reach its limit next. When the correction stage was trying to find the equilibrium point where this actually happens, it identified that Generator 56 had also met its constraint. This means that the reactive limit of Generator 56 lies between the Q-limits of Generators 100 and 15.

It is important to point out that the proposed predictor/corrector scheme considered that generator 56 achieved its operational limit right before Generator 15, i.e. this constraint is not neglected during the estimate of the MLP. Actually, this Q-limit was obtained exactly as the CPFLOW does.

Even though skipped discontinuities do not invalidate the results, they may cause convergence problems for the method. Remember that the main reason why the proposed

Table 5.4: Sequence of discontinuities calculated with the proposed predictor/corrector method for the 118 bus IEEE test system without Generator 80 and with ULS protection schemes.

Discontinuity	Bus	Load Shedding Stage	System Loading (λ)
Q-limit	92	–	1.0090
Q-limit	76	–	1.0633
Q-limit	85	–	1.0956
Q-limit	74	–	1.0974
Q-limit	100	–	1.1149
Q-limit	56	–	Skipped
Q-limit	15	–	1.2214
Q-limit	104	–	1.2309
Q-limit	70	–	1.2423
Q-limit	1	–	1.2858
Q-limit	110	–	1.2969
Q-limit	12	–	1.3085
Q-limit	18	–	1.3170
Q-limit	105	–	1.3178
Q-limit	55	–	1.3488
Q-limit	36	–	1.3529
Q-limit	62	–	1.3965
Q-limit	19	–	1.4055
Q-limit	34	–	1.4221
Q-limit	6	–	1.4820
Q-limit	8	–	1.5874
Q-limit	99	–	1.6705
Q-limit	59	–	1.6891
Q-limit	32	–	1.7308
Q-limit	49	–	1.7613
Q-limit	89	–	1.8885
Q-limit	65	–	1.9084
Q-limit	10	–	1.9136
Q-limit	4	–	Skipped
ULS	13	1	1.9346

scheme avoids divergence is because it is designed to take continuation steps with the same length as a continuous arc of the PV curve. When the predictor skips discontinuities, this is not true anymore and the method is more likely to undergo divergence.

The last power flow solution found with the proposed predictor/corrector method concerns undervoltage load shedding. Remember that the last solution calculated is the first one in the lower and unstable portion of the PV curve. This means that the solved ULS happens after the MLP.

To identify the bifurcation type, Condition I of Figure 3.12 in Section 3.2.4 was not satisfied, while Condition II was met. This means that the proposed method classified the critical point as a SNB. In this case, the CPFLOW is employed to find the MLP starting

from the power flow solution at the Q-limit of Generator 10.

This particular case, where there is a skipped discontinuity between the last stable solution and the first unstable one, lies in the set of scenarios where the proposed method may wrongly identify a SNB. This happens because it is not capable assess whether the Q-limit of Generator 4 is a SIB. This possibility was overlooked in the algorithm used to identify the bifurcation type and it constitutes a gap in the proposed method.

Since the IEEE system without Generator 80 does not go under ULS before the MLP, its PV curve will not be presented here.

5.2.2 107 bus reduced interconnected Brazilian test system

For the Brazilian system, ULS protection schemes were set in buses 138, 140, 536, 1015 and 1504. They were selected based on simple trial and error tests, so that load shedding increases as much as possible the MLP.

Complete network

First, the VSM of the complete Brazilian network was assessed with the locally parametrized CPFLOW and the proposed predictor/corrector scheme. The results obtained are indicated in Table 5.5.

Table 5.5: Effect of the undervoltage load shedding in the 107 bus reduced Brazilian test system with complete network.

Method	ULS	λ_{max}	VSM		Load Shedding	
			(GW)	(%)	(MW)	(%)
CPFLOW	×	1.1149	1.457	11.5%	–	–
	✓	1.1389	1.538	12.1%	196	19%
Proposed	✓	1.1389	1.539	12.1%	196	19%

In this situation the CPFLOW and the proposed method obtained the same results, which helps to validate the technique described in this dissertation. Nevertheless, the CPFLOW was unable to find a solution in the unstable portion of the PV curve, i.e. it diverged. The proposed technique went further, identifying that the Q-limit of Generator 904 caused a SIB. This indicates that the local parametrization was unable to deal with this bifurcation and divergence happened right before it. This can be attributed to an inadequate selection of the local parameter near the discontinuity that caused the bifurcation.

While the ULS allowed a noticeable rise in the loading parameter λ_{max}, this was not so significant for the actual VSM. While the increase in λ_{max} allows the load to grow further, this is achieved through the expense of intentional load shedding, that reduces the total

active demand of the system. Both parameters may interest EPS operators due to their different interpretation.

The sequence of ULS and Q-limits obtained with the proposed method are presented in Table 5.6. In this case, two ULS stages were skipped by the linear predictor. It is worth pointing out that, although this is not ideal, it did not cause divergence of the method nor it greatly compromised its performance.

Table 5.6: Sequence of discontinuities calculated with the proposed predictor/corrector method for the complete 107 bus Brazilian reduced test system with ULS protection schemes.

Discontinuity	Bus	Load Shedding Stage	System Loading (λ)
ULS	1015	1	1.0866
ULS	1015	2	1.0875
ULS	1015	3	1.0884
ULS	1015	4	1.0893
ULS	1015	5	Skipped
ULS	1015	6	Skipped
ULS	140	1	1.1003
ULS	1504	1	1.1239
ULS	140	2	1.1277
Q-limit	919	–	1.1232
Q-limit	904	–	1.1390

The last discontinuity calculated was identified as a SIB with the conditions of Section 2.4.3 proposed by Yorino, Li and Sasaki (2005). This means that, Generator 904 causes instability when it reaches its reactive limit.

Even though the CPFLOW diverged, it did so after all load shedding takes place. Therefore, the PV curves obtained with it depict the effect of the ULS. This can be seen in the voltage profile of bus 976 shown in Figure 5.2.

For small loading levels no load shedding occurs and the PV curves with and without ULS coincide. As voltage magnitudes reduce, some loads are disconnected which resulting in a increased MLP.

Without a critical generator

Disconnecting the biggest generator of the Brazilian system (Generator at bus 810) and performing the same stability analysis, the results obtained are indicated in Table 5.7.

One more time, the CPFLOW diverged. The results of the proposed predictor/corrector scheme indicate that the convergence problem happened right before the first ULS occurs. This suggests that such divergence is a direct consequence of a load discontinuity.

As a consequence of that, not only when loads are stepping up (DG mandatory disconnection) that divergence may arise in the CPFLOW. When it suddenly steps down, the same problem may occur.

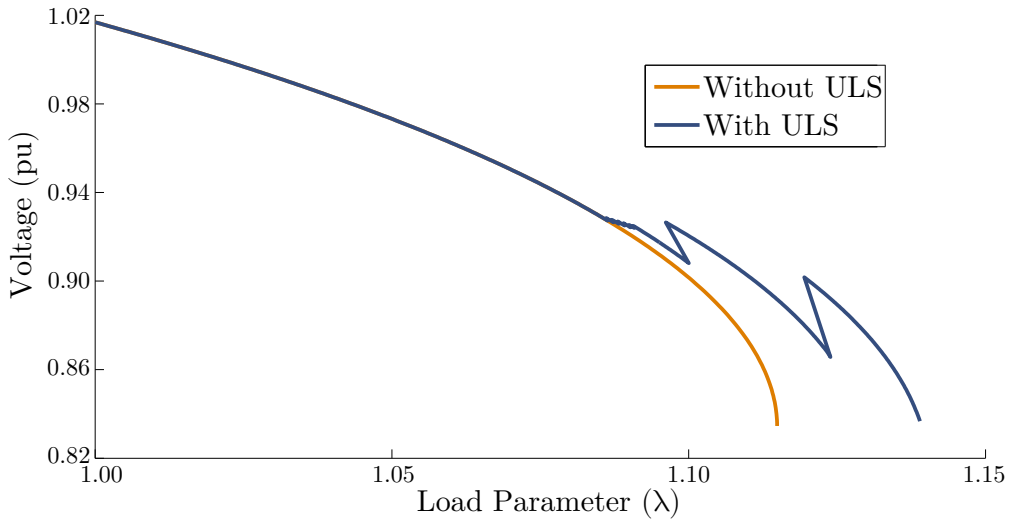

Figure 5.2: Voltage Profile of bus 976 of the 107 bus Brazilian reduced test system with and without under voltage load shedding.

Table 5.7: Effect of the undervoltage load shedding in the 107 bus reduced Brazilian test system without the generator located at bus 810.

Method	ULS	λ_{max}	VSM		Load Shedding	
			(GW)	(%)	(MW)	(%)
CPFLOW	×	1.1088	1.380	10.9%	–	–
	✓	1.0774	0.981	7.7%	0	0%
Proposed	✓	1.1812	1.867	14.7%	365	36%

The sequence of discontinuities that the Brazilian system undergo as obtained by the proposed method are indicated in Table 5.8.

Once more the predictor proposed skipped two discontinuities. However, this did not entail any problems to the adequate execution of the method. Remembering that the skipped events are not neglected, they are recognized during the correction stages and included in the analysis.

The Q-limit of Generator 904 was identified to lie in the unstable portion of the PV curve, meeting the stopping criteria of the method. This point did not satisfy the criteria of a SIB presented in Section 2.4.3, which means that the actual MLP of the system lies between the last two discontinuities calculated. In this situation, the critical point is classified as a SNB.

After the proposed algorithm attained the bifurcation type, it needs the aid of the CPFLOW to reach the MLP. The latter was employed between the last two power flow solutions found, starting from the Q-limit of Generator 925. Since there is no other discontinuity between these two equilibria, the continuation method is not expected to go through convergence problems. An unstable point was found in few iterations, characterizing the convergence of the method. This procedure was responsible for the

Table 5.8: Sequence of discontinuities calculated with the proposed predictor/corrector method for the 107 bus Brazilian reduced test system without Generator 810 and with ULS protection schemes.

Discontinuity	Bus	Load Shedding Stage	System Loading (λ)
ULS	140	1	1.0777
ULS	140	2	1.1043
ULS	1504	1	1.1281
ULS	140	3	1.1345
Q-limit	919	–	1.1503
ULS	1504	2	1.1546
ULS	1015	1	1.1572
ULS	1015	2	1.1584
ULS	1015	3	1.1595
ULS	1015	4	1.1607
ULS	1015	5	Skipped
ULS	1015	6	Skipped
ULS	1504	3	1.1662
ULS	140	4	1.1702
Q-limit	925	–	1.1810
Q-limit	904	–	1.1812

MLP presented in Table 5.7.

Since the CPFLOW alone diverged before any ULS happened and the proposed method did not provide the voltage profile of the system, in this scenario there are no PV curves demonstrating the effect of load shedding in the voltage profile of the EPS.

5.3 Final Remarks

To study undervoltage load shedding, the proposed predictor/corrector algorithm yielded better results than the CPFLOW. This demonstrates that the former method may be more adequate to analyse sudden load changes and their discontinuities in power system equilibria.

These numerical results also indicate that CPFLOW divergence may occur due to sudden load reductions. In the previous chapter, this problem resulted from big blocks of load stepping up (cascading DG disconnections). This illustrates that it is not the direction of the sudden load changes that is responsible for the observed convergence problems, but rather the nature of the load discontinuities under question.

With respect to the advantages and disadvantages of the proposed method, the results here are consonant with the ones presented in the previous chapter. The proposed predictor/corrector scheme is capable to estimate the MLP of the system, classify the bifurcation type and individually identify the discontinuities in its equilibrium diagram.

However, the two main limitations of the method can also be perceived: (i) it does not obtain the voltage profile of the EPS under analysis and (ii) its utilization may be impaired if the system is not subject to successive discontinuities that are relatively close to each other.

Chapter 6

Conclusion

The EPS state discontinuities produced by sudden load variations were responsible to cause convergence problems for the traditional CPFLOW. This evidences that this approach may be inadequate to evaluate the MLP of power systems when they are subject to parametric changes in demand.

In this dissertation a predictor/corrector scheme was specifically designed to deal with the load steps under question. From the numerical results presented, it proved capable to estimate the MLP of power systems under sudden load variations, as well as to individually identify such discontinuities in its equilibrium diagram.

Employing the proposed method, it was possible to quantify the effect of DG mandatory disconnections and ULS in the VSM of the power systems under analysis. This algorithm also identified the instability mechanism that was responsible to deprive the EPSs from a stable equilibrium point, i.e. the bifurcation type that happened.

Furthermore, the numerical results obtained from the proposed scheme yielded important information about the equilibrium diagrams of EPSs subject to sudden load variations, like the cascading disconnections of DG units. This, in turn, even helped to diagnose the reasons for divergence of the CPFLOW.

Despite having presented promising results, the proposed predictor/corrector algorithm should only be employed to manage equilibrium discontinuities caused by sudden parametric variations in load. In other words, its applicability is restricted to EPSs that go through such discontinuities, in which case the method is expected to be more robust than the CPFLOW. If that is not true, then its usage may be infeasible.

This is why this procedure should not be considered to replace the traditional CPFLOW or any other standard VSA tool. On the contrary, it should be regarded as a complementary technique, that could enhance the CPFLOW with new features to broaden its applicability.

It is necessary to emphasize that there is no mathematical proof assuring the robustness of the proposed method when dealing with sudden load changes. However, it converged for every numerical scenario analysed in this dissertation. Further experience with this technique may provide situations where divergence will arise. This means that, the research

described here does not comprise a definite solution to analyse the effect of sudden load variations on the static voltage stability of EPSs.

With this is mind, further studies are required in this field of research. Among them, it is possible to point out:

1. In the numerical results presented, the proposed predictor/corrector scheme was simultaneously executed with the Q-limit guided continuation power flow proposed by Yorino, Li and Sasaki (2005). Similarly, the traditional CPFLOW could incorporate the proposed method to avoid possible convergence problems due to parametric discontinuities.
2. It is possible to employ different techniques to go from one equilibrium point before a sudden variation in load to another one after it happened. In the proposed method this is done with Corrector II that follows Corrector I. In this line of research it is possible to include a predictor before Corrector II or even to take several continuation steps between these two equilibrium points.
3. The main ideas that based the proposed method could be useful to deal with other equilibrium discontinuities that power systems may be subject to.

The research that culminated in this dissertation also produced three conference papers. Two of them were already published, while one has been accepted. They are indicated below:

COLOMBARI, Luan F. S.; MANSOUR, Moussa R.; RAMOS, Rodrigo A.; ALBERTO, Luís Fernando C. A. A Fast Method for Load Margin Estimation Considering the Reactive Power Generation Limits. **IEEE Power Energy Society General Meeting**, 2016, Boston, MA, USA.

COLOMBARI, Luan F. S.; MANSOUR, Moussa R.; DOS SANTOS, Jhonatan A.; DOTTA, Daniel; RAMOS, Rodrigo A. Efeito do Desligamento Mandatório de Unidades de Geração Distribuída na Curva PV De Sistemas De Transmissão. **Congresso Brasileiro de Automática**, 2016, Vitória, ES, Brazil.

COLOMBARI, Luan F. S.; BENTO, Murilo E. C.; DOS SANTOS, Jhonatan A.; RAMOS, Rodrigo A. Procedure to Account for DG Mandatory Disconnection During Voltage Stability Assessment. **IEEE Power Energy Society PowerTech**, 2017, Manchester, England.

Bibliography

ABRI, R. S. A.; MEMBER, S.; ATWA, Y. M. Distributed Generation Placement and Sizing Method to Improve the Voltage Stability Margin in a Distribution System. In: **2nd International Conference on Electric Power and Energy Conversion Systems (EPECS)**. Sharjah: [s.n.], 2011. p. 1–7.

AFFONSO, C. M.; SILVA, L. C. P. da; LIMA, F. G. M.; SOARES, S. Mw and mvar management on supply and demand side for meeting voltage stability margin criteria. **IEEE Transactions on Power Systems**, 2004. v. 19, n. 3, p. 1538–1545, Aug 2004. ISSN 0885-8950.

AJJARAPU, V. **Computational Techniques for Voltage Stability Assessment and Control**. 1. ed. Boston, MA: Springer US, 2007. (Power Electronics and Power Systems). ISBN 978-0-387-26080-8.

ALVES, D. A.; SILVA, L. C. P. da; CASTRO, C. A.; COSTA, V. F. da. New parameterization schemes for the continuation load flow. In: **International Conference on Electric Utility Deregulation and Restructuring and Power Technologies**. London: [s.n.], 2000. p. 4–7. ISBN 078035902X.

ALVES, W. F. **Proposição de Sistemas–Teste para Análise Computacional de Sistemas de Potência**. Tese (Mestrado) — Universidade Federal Fluminense, 2007.

AMRAEE, T.; RANJBAR, A.; MOZAFARI, B.; SADATI, N. An enhanced under-voltage load-shedding scheme to provide voltage stability. **Electric Power Systems Research**, 2007. v. 77, n. 8, p. 1038 – 1046, 2007. ISSN 0378-7796.

ANDERSON, P. M.; FOUAD, A. A. **Power System Control and Stabilityl**. 2. ed. New York, NY: Wiley-IEEE Press, 2002. ISBN 9780471238621.

ARNBORG, S.; ANDERSSON, G.; HILL, D. J.; HISKENS, I. A. On undervoltage load shedding in power systems. **International Journal of Electrical Power & Energy Systems**, 1997. v. 19, n. 2, p. 141 – 149, 1997. ISSN 0142-0615.

BALANATHAN, R.; PAHALAWATHTHA, N. C.; ANNAKKAGE, U. D.; SHARP, P. W. Undervoltage load shedding to avoid voltage instability. **IEE Proceedings - Generation, Transmission and Distribution**, 1998. v. 145, n. 2, p. 175–181, Mar 1998. ISSN 1350-2360.

BALU, N.; BERTRAM, T.; BOSE, A.; BRANDWAJN, V.; CAULEY, G.; CURTICE, D.; FOUAD, A.; FINK, L.; LAUBY, M. G.; BRUCE, W.; WRUBEL, J. N. On-Line Power System Security Analysis. **Proceedings of the Institution of Electrical Engineers**, 1992. v. 80, n. 2, p. 262–280, 1992.

BIJWE, P.; KOTHARI, D.; KELAPURE, S. An efficient approach for voltage security analysis and enhancement. **International Journal of Electrical Power & Energy Systems**, 2000. v. 22, n. 7, p. 483–486, out. 2000. ISSN 01420615.

BLACKBURN, J. L.; DOMIN, T. **Protective Relaying, Principles and Applications**. 3. ed. Boca Raton, FL: Taylor & Francis, 2006. ISBN 9781574447163.

BOLLEN, M.; HASSAN, F. **Integratiion of Distribution Generation in the Power System**. 1. ed. Hoboken, New Jersey: John Wiley & Sons, 2011. ISBN 9780470643372.

CANIZARES, C. A.; ALVARADO, F. L. Point of collapse and continuation methods for large AC/DC systems. **IEEE Transactions on Power Systems**, 1993. v. 8, n. 1, p. 1–8, 1993. ISSN 08858950.

CAO, G. Y.; CHEN, C. Novel Techniques for Continuation Method to Calculate the Limit-induced Bifurcation of the Power Flow Equation. **Electric Power Components and Systems**, 2010. v. 38, n. 9, p. 1061–1075, 2010. ISSN 1532-5008.

CELESC. **I–432.0004 – Requisitos para a conexão de Micro ou Minigeradores de Energia ao Sistema Elétrico da CELESC Distribuição**. [S.l.], 2014.

CEMIG. **ND 5.31 – Requisitos para a conexão de Acessantes Produtores de Energia Elétrica ao Sistema de Distribuição CEMIG – Conexão em Média Tensão**. [S.l.], 2011.

CHEN, P.; MALBASA, V.; KEZUNOVIC, M. Analysis of Voltage Stability Issues with Distributed Generation Penetration in Distribution Networks. In: **North American Power Symposium (NAPS)**. Manhattan, KS: [s.n.], 2013. ISBN 9781479912551.

CHIANG, H. D.; FLUECK, A. J.; SHAH, K. S.; BALU, N. CPFLOW: A practical tool for tracing power system steady-state stationary behavior due to load and generation variations. **IEEE Transactions on Power Systems**, 1995. v. 10, n. 2, p. 623–634, 1995. ISSN 08858950.

CHIANG, H. D.; WANG, C. S.; FLUECK, A. J. Look-ahead voltage and load margin contingency selection functions for large-scale power systems. **IEEE Transactions on Power Systems**, 1997. v. 12, n. 1, p. 173–180, 1997. ISSN 08858950.

CHICONE, C. **Ordinary Differential Equations with Applications**. 1. ed. New York, NY: Springer, 1999. 21–23 p. ISBN 0-387-98535-2.

COPEL. **NTC 905200 – Acesso de Micro e Minigeração Distribuída ao Sistema da COPEL**. [S.l.], 2014.

CUTSEM, T. V.; MOORS, C.; LEFEBVRE, D. Design of load shedding schemes against voltage instability using combinatorial optimization. In: **2002 IEEE Power Engineering Society Winter Meeting. Conference Proceedings (Cat. No.02CH37309)**. [S.l.: s.n.], 2002. v. 2, p. 848–853 vol.2.

CUTSEM, T. V.; VOURNAS, C. **Voltage Stability of Electric Power Systems**. 4. ed. Norwell: Kluwer Academic Publishers, 2003. ISBN 0792381394.

DOBSON, I.; LU, L. Voltage collapse precipitated by the immediate change in stability when generator reactive power limits are encountered. **IEEE Transactions on Circuits and Systems I: Fundamental Theory and Applications**, 1992. v. 39, n. 9, p. 762–766, 1992.

DUBAI ELECTRICITY AND WATER AUTHORITY. **DEWA Regulations for Electrical Installations – U.V.(Under Voltage) Relay for Chiller Equipment/Plant**. [S.l.], 2011. Disponível em: <https://www.dewa.gov.ae/en-/consultants-and-contractors/policies-and-regulations/circulars-and-forms/dewa-circulars>.

ELEKTRO. **ND.64 - Conexão entre Microgeração Distribuída em Baixa Tensão e a Rede de Distribuição da ELEKTRO.** [S.l.], 2013.

FENG, Z.; AJJARAPU, V.; MARATUKULAM, D. J. A practical minimum load shedding strategy to mitigate voltage collapse. **IEEE Transactions on Power Systems**, 1998. v. 13, n. 4, p. 1285–1290, Nov 1998. ISSN 0885-8950.

FLUECK, A. J.; DONDETI, J. R. A New Continuation Power Flow Tool for Investigating the Nonlinear Effects of Transmission Branch Parameter Variations. **IEEE Transactions on Power Systems**, 2000. v. 15, n. i, p. 223–227, 2000.

GAO, B.; KUNDUR, P.; MORISON, G. K. Towards the Development of a Systematic Approach for Voltage Stability Assessment of Large-Scale Power Systems. **IEEE Transactions on Power Systems**, 1996. v. 11, n. 3, p. 1314–1324, 1996.

HISKENS, I.; CHAKRABARTI, B. Direct calculation of reactive power limit points. **International Journal of Electrical Power & Energy Systems**, 1996. v. 18, n. 2, p. 121–129, fev. 1996. ISSN 01420615.

ILLINOIS INSTITUTE OF TECHNOLOGY POWER GROUP. **One-line Diagram of IEEE 118-bus Test System**. [S.l.], 2003. Disponível em: <http://www.al-roomi.org-/multimedia/Power_Flow/118BusSystem/IEEE118BusSystemA.jpg>.

INSTITUTE OF ELECTRICAL AND ELECTRONICS ENGINEERS (IEEE). **Power Systems Test Case Archive**. [S.l.], 1993. Disponível em: <https://www.ee.washington-.edu/research/pstca/>.

JIA, Z.; JEYASURYA, B. Contingency Ranking for On-Line Voltage Stability Assessment. **IEEE Transactions on Power Systems**, 2000. v. 15, n. 3, p. 1093–1097, 2000.

KAROUI, K.; JEBRIL, Y. A.; IBRAHIM, A. I.; SHABAN, S. A.; DESSI, S. A. A. Load model development based on monitoring and laboratory staged testing. In: **2011 IEEE GCC Conference and Exhibition (GCC)**. [S.l.: s.n.], 2011. p. 661–664.

KUNDUR, P. **Power System Stability and Control**. 1. ed. New York, NY: McGraw-Hill, 1994. ISBN 007035958X.

KUNDUR, P.; PASERBA, J.; AJJARAPU, V.; ANDERSSON, G.; BOSE, A.; CANIZARES, C.; HATZIARGYRIOU, N.; HILL, D.; STANKOVIC, A.; TAYLOR, C.; Van Cutsem, T.; VITTAL, V. Definition and Classification of Power System Stability. **IEEE Transactions on Power Systems**, 2004. v. 19, n. 2, p. 1387–1401, 2004.

LEFEBVRE, D.; MOORS, C.; CUTSEM, T. V. Design of an undervoltage load shedding scheme for the hydro-quebec system. In: **2003 IEEE Power Engineering Society General Meeting (IEEE Cat. No.03CH37491)**. [S.l.: s.n.], 2003. v. 4, p. 2036 Vol. 4.

LI, H.; HAQ, E.; ABDUL-RAHMAN, K.; WU, J.; CAUSGROVE, P. On-line voltage security assessment and control. **International Transactions on Electrical Energy Systems**, 2014. v. 24, n. 11, p. 1618–1631, nov. 2014. ISSN 20507038.

LI, S.-h.; CHIANG, H.-d. Continuation Power Flow With Nonlinear Power Injection Variations : A Piecewise Linear Approximation. **IEEE Transactions on Power Systems**, 2008. v. 23, n. 4, p. 1637–1643, 2008.

LI, S. H.; CHIANG, H. D. Look-ahead Q-constrained load margin for large-scale power systems. **2008 IEEE Power and Energy Society General Meeting – Conversion and Delivery of Electrical Energy in the 21st Century**, 2008. n. 1, p. 1–6, 2008.

_____. Nonlinear predictors and hybrid corrector for fast continuation power flow. **IET Generation, Transmission & Distribution**, 2008. v. 2, n. 3, p. 341–354, 2008.

LONDERO, R. R.; AFFONSO, C. M.; NUNES, M. V. A. Impact of Distributed Generation in Steady State , Voltage and Transient Stability – Real Case. In: **IEEE Bucharest Power Tech Conference**. Bucharest, Romania: [s.n.], 2009. p. 1–6. ISBN 9781424422357.

MANSOUR, M. R. **Método Rápido para Análise de Contingências e Seleção de Controles Preventivos no Contexto de Estabilidade de Tensão**. Tese (Doutorado) — Universidade de São Paulo, 2013.

MANSOUR, M. R.; ALBERTO, L. F. C.; RAMOS, R. A. Preventive Control Design For Voltage Stability Considering Multiple Critical Contingencies. **IEEE Transactions on Power Systems**, 2015. PP, n. 99, 2015.

MANSOUR, M. R.; GERALDI, E. L.; ALBERTO, L. F. C.; RAMOS, R. A. A New and Fast Method for Preventive Control Selection in Voltage Stability Analysis. **IEEE Transactions on Power Systems**, 2013. v. 28, n. 4, p. 4448–4455, 2013. ISSN 0885-8950.

MOLZAHN, D. K.; LESIEUTRE, B. C.; CHEN, H. Counterexample to a Continuation-Based Algorithm for Finding All Power Flow Solutions. **IEEE Transactions on Power Systems**, 2013. v. 28, n. 1, p. 564–565, 2013.

MOORS, C.; LEFEBVRE, D.; CUTSEM, T. V. Load shedding controllers against voltage instability: a comparison of designs. In: **2001 IEEE Porto Power Tech Proceedings (Cat. No.01EX502)**. [S.l.: s.n.], 2001. v. 2, p. 6 pp. vol.2–.

NETO, A. B.; ALVES, D. A. Técnicas de parametrização global para o fluxo de carga continuado. **Revista Controle & Automação**, 2010. v. 21, n. 4, p. 323–337, 2010.

OPERADOR NACIONAL DO SISTEMA (ONS). **ONS apresenta relatório final sobre blecaute de 2009**. [S.l.], 2009. Disponível em: <http://www.ons.org.br-/newsletters/informativos-/nov2009/06-materia01.htm>.

_____. **Submódulo 23.3 – Diretrizes e Critérios para Estudos Elétricos**. [S.l.], 2011.

OWENS, B. **The Rise of Distributed Power.** General Electric Ecomagination. [s.l.], 2014.

PRESIDÊNCIA DA REPÚBLICA. **Decreto Num. 5163**. [S.l.], 2004. Disponível em: <http://www.planalto.gov.br/ccivil_03/_Ato2004-2006/2004/Decreto-/D5163compilado.htm>.

SANTOS, J. A. **Análise da Estabilidade de Tensão de Sistemas de Energia Elétrica Considerando a Influência da Desconexão Mandatória de Geradores Síncronos Distribuídos**. Tese (Qualificação de doutorado – não publicado) — Universidade de São Paulo, 2015.

SAUER, P. W.; PAI, M. A. Power system steady-state stability and the load-flow Jacobian. **IEEE Transactions on Power Apparatus and Systems**, 1990. v. 5, n. 4, p. 1374–1383, 1990.

SONG, H.; BAIK, S. D.; LEE, B. Determination of load shedding for power-flow solvability using outage-continuation power flow (OCPF). **IEEE Proceedings - Generation, Transmission and Distribution**, 2006. v. 153, n. 3, p. 321–325, 2006.

SUNDHARARAJAN, S.; PAHWA, A.; STARRETT, S.; KRISHNASWAMI, P. Convergence Measures for Contingency Screening in Continuation Power Flow. In: **IEEE PES Transmission and Distribution Conference and Exposition**. Dallas, TX: [s.n.], 2003. v. 1, p. 169–174.

TAYLOR, C. W. Concepts of undervoltage load shedding for voltage stability. **IEEE Transactions on Power Delivery**, 1992. v. 7, n. 2, p. 480–488, Apr 1992. ISSN 0885-8977.

TAYLOR, G.; IRVING, M. A novel Q-Limit guided Continuation Power Flow method. **2008 IEEE Power and Energy Society General Meeting Conversion and Delivery of Electrical Energy in the 21st Century**, 2008. p. 1–7, 2008.

TUAN, T. Q.; FANDINO, J.; HADJSAID, N.; SABONNADIERE, J. C.; VU, H. Emergency load shedding to avoid risks of voltage instability using indicators. **IEEE Transactions on Power Systems**, 1994. v. 9, n. 1, p. 341–351, Feb 1994. ISSN 0885-8950.

VAN CUTSEM, T.; GLAVIC, M.; ROSEHART, W.; SANTOS, J. A.; CANIZARES, C.; KANATAS, M.; LIMA, L.; MILANO, F.; PAPANGELIS, L.; RAMOS, R. A.; TAMIMI, B.; TARANTO, G. N.; VOURNAS, C. **Test Systems for Voltage Stability and Security Assessment (IEEE PES Technical Report (TR-19) of the PSDP Task Force on Test Systems for Voltage Stability)**. [S.l.], 2015.

VIAWAN, F. A. **Voltage Control and Voltage Stability of Power Distribution Systems in the Presence of Distributed Generation**. Tese (Doutorado) — Chalmers University of Tecnology, 2008.

WALLING, R. A.; MILLER, N. W. Distributed Generation Islanding – Implications on Power System Dynamic Performance. In: **IEEE Power Engineering Society Summer Meeting**. Chicago, IL, USA: [s.n.], 2002. v. 1, p. 92–96. ISBN 078037519X.

WALLING, R. A. R.; SAINT, R.; DUGAN, R. C.; BURKE, J.; KOJOVIC, L. A. Summary of Distributed Resources Impact on Power Delivery Systems. **IEEE Transactions on Power Delivery**, 2008. v. 23, n. 3, p. 1636–1644, 2008.

WORLD ALLIANCE OF DECENTRALIZED ENERGY (WADE). **World Survey of Decentralized Energy**. [S.l.], 2006.

XAVIER DIAS, M. V.; BOROTNI, E. C.; HADDAD, J. Geração Distribuída no Brasil: Oportunidades e Barreiras. **Revista Brasileira de Energia**, 2004. v. 11, n. 2, p. 1–11, 2004.

XU, P.; WANG, X.; AJJARAPU, V. Continuation power flow with adaptive stepsize control via convergence monitor. **IET Generation, Transmission & Distribution**, 2012. v. 6, n. 7, p. 673–679, 2012.

YANG, J.; LI, G.; WU, D.; SUO, Z. The Impact of Distributed Wind Power Generation on Voltage Stability in Distribution Systems. In: **IEEE PES Asia-Pacific Power and Energy Engineering Conference (APPEEC)**. Kowloon: IEEE, 2013. ISBN 9781479925223.

YORINO, N.; LI, H. Q.; SASAKI, H. A Predictor/Corrector Scheme for Obtaining Q-Limit Points for Power Flow Studies. **IEEE Transactions on Power Systems**, 2005. v. 20, n. 1, p. 130–137, 2005. ISSN 0885-8950.

ZHAO, J.; FAN, X.; LIN, C.; WEI, W. Distributed Continuation Power Flow Method for Integrated Transmission and Active Distribution Network. **Journal of Modern Power Systems and Clean Energy**, 2015. Springer Berlin Heidelberg, v. 3, n. 4, p. 573–582, 2015. ISSN 2196-5420.

ZHAO, J.; ZHANG, B. Reasons and Countermeasures for Computation Failures of Continuation Power Flow. In: **2006 IEEE Power Engineering Society General Meeting**. Montreal, Quebec: [s.n.], 2006. ISBN 1424404932.

Appendices

APPENDIX A

IEEE 118 Bus Test System

The data regarding the IEEE 118 bus test system was obtained in IEEE (1993). The per-unit base power is equal to 100 MW and the voltage base value is indicated in Table A.2 alongside with other bus data. The bus voltage magnitudes and angles presented in this table correspond to the power flow solution of the base case scenario, for which the power system load can be seen in the same table. The DG power injection in each bus is presented when the penetration level is equal to 10%. For the two other DG penetration analysed (20% and 30%), the active injection is proportional to the value mentioned. The transmission network parameters are available in Table A.3 according to the model of Figure A.1. The symbols utilized in these tables are defined in Table A.1. Finally, the one-line diagram of the system is available in Figure A.2.

Table A.1: Definition of symbols available in Appendices A and B.

Symbol	Description	Unit
ID	Identification number of a given bus	-
Type	Bus type in the power flow problem formulation	-
From	Bus where the line originates	-
To	Bus where the line arrives	-
V_{base}	Per-unit base voltage	kV
V	Voltage magnitude	pu
θ	Voltage angle	degrees
P_g	Active power supplied	pu
Q_g	Reactive power supplied	pu
Q_{max}	Maximum limit of reactive power supply	pu
Q_{min}	Minimum limit of reactive power supply	pu
V_{set}	Control reference of bus voltage magnitude	pu
P_l	Active power consumption	pu
Q_l	Reactive power consumption	pu
P_{gd}	DG injected power	pu
B_{sh}	Shunt reactor or capacitor	pu
R	Line resistance	pu
X	Line reactance	pu
B	Line shunt susceptance	pu
Tap	Transformer tap position	pu

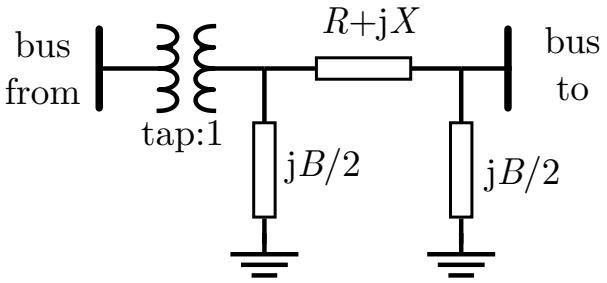

Figure A.1: Model employed for lines and transformers.

Table A.2: Bus data from the IEEE 118 bus test system.

ID	Type	V_{base}	V	θ	P_g	Q_g	Q_{max}	Q_{min}	V_{set}	P_l	Q_l	P_{gd}	B_{sh}
1	PV	138	0.955	-19	0	-0.03	0.15	-0.05	0.955	0.51	0.27	0.0147	0
2	PQ	138	0.971	-18.5	0	0	0	0	-	0.2	0.09	0.0189	0
3	PQ	138	0.968	-18.1	0	0	0	0	-	0.39	0.1	0.0435	0
4	PV	138	0.998	-14.4	-0.09	-0.15	3	-3	0.998	0.3	0.12	0.0235	0
5	PQ	138	1.002	-14	0	0	0	0	-	0	0	0	-0.4
6	PV	138	0.990	-16.7	0	0.16	0.5	-0.13	0.99	0.52	0.22	0.0591	0
7	PQ	138	0.989	-17.1	0	0	0	0	-	0.19	0.02	0.0157	0
8	PV	345	1.015	-9	-0.28	0.63	3	-3	1.015	0	0	0	0
9	PQ	345	1.043	-1.7	0	0	0	0	-	0	0	0	0
10	PV	345	1.050	5.9	4.5	-0.51	2	-1.47	1.05	0	0	0	0
11	PQ	138	0.985	-17	0	0	0	0	-	0.7	0.23	0.0853	0
12	PV	138	0.990	-17.5	0.85	0.91	1.2	-0.35	0.99	0.47	0.1	0.0457	0
13	PQ	138	0.968	-18.4	0	0	0	0	-	0.34	0.16	0.0266	0
14	PQ	138	0.984	-18.2	0	0	0	0	-	0.14	0.01	0.0147	0
15	PV	138	0.970	-18.5	0	0.03	0.3	-0.1	0.97	0.9	0.3	0.0757	0
16	PQ	138	0.984	-17.8	0	0	0	0	-	0.25	0.1	0.0219	0
17	PQ	138	0.995	-16	0	0	0	0	-	0.11	0.03	0.0141	0
18	PV	138	0.973	-18.2	0	0.26	0.5	-0.16	0.973	0.6	0.34	0.0886	0
19	PV	138	0.963	-18.7	0	-0.08	0.24	-0.08	0.962	0.45	0.25	0.0536	0
20	PQ	138	0.958	-17.8	0	0	0	0	-	0.18	0.03	0.03	0
21	PQ	138	0.959	-16.2	0	0	0	0	-	0.14	0.08	0.0065	0
22	PQ	138	0.970	-13.7	0	0	0	0	-	0.1	0.05	0.0098	0
23	PQ	138	1.000	-8.8	0	0	0	0	-	0.07	0.03	0.0069	0
24	PV	138	0.992	-8.9	-0.13	-0.15	3	-3	0.992	0	0	0	0
25	PV	138	1.050	-1.8	2.2	0.5	1.4	-0.47	1.05	0	0	0	0
26	PV	345	1.015	0	3.14	0.1	10	-10	1.015	0	0	0	0
27	PV	138	0.968	-14.4	-0.09	0.03	3	-3	0.968	0.62	0.13	0.0731	0
28	PQ	138	0.962	-16.1	0	0	0	0	-	0.17	0.07	0.0203	0
29	PQ	138	0.963	-17.1	0	0	0	0	-	0.24	0.04	0.0251	0
30	PQ	345	0.986	-11	0	0	0	0	-	0	0	0	0
31	PV	138	0.967	-17	0.07	0.32	3	-3	0.967	0.43	0.27	0.0573	0
32	PV	138	0.964	-14.9	0	-0.14	0.42	-0.14	0.963	0.59	0.23	0.01	0
33	PQ	138	0.972	-19.1	0	0	0	0	-	0.23	0.09	0.0235	0
34	PV	138	0.986	-18.5	0	-0.08	0.24	-0.08	0.984	0.59	0.26	0.0282	0.14
35	PQ	138	0.981	-18.9	0	0	0	0	-	0.33	0.09	0.0288	0
36	PV	138	0.980	-18.9	0	-0.01	0.24	-0.08	0.98	0.31	0.17	0.0451	0
37	PQ	138	0.992	-18	0	0	0	0	-	0	0	0	-0.25
38	PQ	345	0.962	-12.9	0	0	0	0	-	0	0	0	0
39	PQ	138	0.970	-21.4	0	0	0	0	-	0.27	0.11	0.0337	0
40	PV	138	0.970	-22.5	-0.46	0.27	3	-3	0.97	0.2	0.23	0.018	0
41	PQ	138	0.967	-22.9	0	0	0	0	-	0.37	0.1	0.0255	0

Table A.2: Bus data from the IEEE 118 bus test system.

ID	Type	V_{base}	V	θ	P_g	Q_g	Q_{max}	Q_{min}	V_{set}	P_l	Q_l	P_{gd}	B_{sh}
42	PV	138	0.985	-21.3	-0.59	0.41	3	-3	0.985	0.37	0.23	0.0306	0
43	PQ	138	0.978	-18.5	0	0	0	0	-	0.18	0.07	0.0199	0
44	PQ	138	0.985	-16.1	0	0	0	0	-	0.16	0.08	0.003	0.1
45	PQ	138	0.987	-14.2	0	0	0	0	-	0.53	0.22	0.0635	0.1
46	PV	138	1.005	-11.4	0.19	-0.05	1	-1	1.005	0.28	0.1	0.0303	0.1
47	PQ	138	1.017	-9.2	0	0	0	0	-	0.34	0	0.043	0
48	PQ	138	1.021	-10	0	0	0	0	-	0.2	0.11	0.0333	0.15
49	PV	138	1.025	-9	2.04	1.16	2.1	-0.85	1.025	0.87	0.3	0.0773	0
50	PQ	138	1.001	-11	0	0	0	0	-	0.17	0.04	0.0111	0
51	PQ	138	0.967	-13.6	0	0	0	0	-	0.17	0.08	0.0234	0
52	PQ	138	0.957	-14.6	0	0	0	0	-	0.18	0.05	0.023	0
53	PQ	138	0.946	-15.6	0	0	0	0	-	0.23	0.11	0.0216	0
54	PV	138	0.955	-14.6	0.48	0.04	3	-3	0.955	1.13	0.32	0.0903	0
55	PV	138	0.952	-14.9	0	0.05	0.23	-0.08	0.952	0.63	0.22	0.0679	0
56	PV	138	0.954	-14.8	0	-0.02	0.15	-0.08	0.954	0.84	0.18	0.052	0
57	PQ	138	0.971	-13.5	0	0	0	0	-	0.12	0.03	0.0119	0
58	PQ	138	0.959	-14.4	0	0	0	0	-	0.12	0.03	0.0091	0
59	PV	138	0.985	-10.5	1.55	0.77	1.8	-0.6	0.985	2.77	1.13	0.201	0
60	PQ	138	0.993	-6.8	0	0	0	0	-	0.78	0.03	0.1028	0
61	PV	138	0.995	-5.9	1.6	-0.4	3	-1	0.995	0	0	0	0
62	PV	138	0.998	-6.5	0	0.01	0.2	-0.2	0.998	0.77	0.14	0.1114	0
63	PQ	345	0.969	-7.2	0	0	0	0	-	0	0	0	0
64	PQ	345	0.984	-5.4	0	0	0	0	-	0	0	0	0
65	PV	345	1.005	-2.3	3.91	0.81	2	-0.67	1.005	0	0	0	0
66	PV	138	1.050	-2.4	3.92	-0.02	2	-0.67	1.05	0.39	0.18	0.0467	0
67	PQ	138	1.020	-5.1	0	0	0	0	-	0.28	0.07	0.0399	0
68	PQ	345	1.003	-2.4	0	0	0	0	-	0	0	0	0
69	Vθ	138	1.035	0	5.13	-0.82	3	-3	1.035	0	0	0	0
70	PV	138	0.984	-7.4	0	0.1	0.32	-0.1	0.984	0.66	0.2	0.0807	0
71	PQ	138	0.987	-7.8	0	0	0	0	-	0	0	0	0
72	PV	138	0.980	-8.9	-0.12	-0.11	1	-1	0.98	0	0	0	0
73	PV	138	0.991	-8	-0.06	0.1	1	-1	0.991	0	0	0	0.12
74	PV	138	0.958	-8.3	0	-0.06	0.09	-0.06	0.958	0.68	0.27	0.0303	0
75	PQ	138	0.967	-7.1	0	0	0	0	-	0.47	0.11	0.0607	0
76	PV	138	0.943	-8.2	0	0.05	0.23	-0.08	0.943	0.68	0.36	0.0562	0
77	PV	138	1.006	-3.2	0	0.12	0.7	-0.2	1.006	0.61	0.28	0.054	0
78	PQ	138	1.003	-3.5	0	0	0	0	-	0.71	0.26	0.0747	0.2
79	PQ	138	1.009	-3.2	0	0	0	0	-	0.39	0.32	0.0717	0
80	PV	138	1.040	-1	4.77	1.05	2.8	-1.65	1.04	1.3	0.26	0.2091	0
81	PQ	345	0.997	-1.9	0	0	0	0	-	0	0	0	0.2
82	PQ	138	0.989	-2.7	0	0	0	0	-	0.54	0.27	0.0451	0.1
83	PQ	138	0.985	-1.5	0	0	0	0	-	0.2	0.1	0.0263	0
84	PQ	138	0.980	1	0	0	0	0	-	0.11	0.07	0.0031	0
85	PV	138	0.985	2.6	0	-0.06	0.23	-0.08	0.985	0.24	0.15	0.0336	0
86	PQ	138	0.987	1.2	0	0	0	0	-	0.21	0.1	0.0185	0
87	PV	161	1.015	1.4	0.04	0.11	10	-1	1.015	0	0	0	0
88	PQ	138	0.987	5.7	0	0	0	0	-	0.48	0.1	0.0336	0
89	PV	138	1.005	9.7	6.07	-0.12	3	-2.1	1.005	0	0	0	0
90	PV	138	0.985	3.3	-0.85	0.59	3	-3	0.985	0.78	0.42	0.1378	0
91	PV	138	0.980	3.4	-0.1	-0.15	1	-1	0.98	0	0	0	0
92	PV	138	0.992	3.9	0	-0.03	0.09	-0.03	0.99	0.65	0.1	0.058	0
93	PQ	138	0.987	0.8	0	0	0	0	-	0.12	0.07	0.0075	0
94	PQ	138	0.991	-1.3	0	0	0	0	-	0.3	0.16	0.0407	0

Table A.2: Bus data from the IEEE 118 bus test system.

ID	Type	V_{base}	V	θ	P_g	Q_g	Q_{max}	Q_{min}	V_{set}	P_l	Q_l	P_{gd}	B_{sh}
95	PQ	138	0.981	-2.3	0	0	0	0	-	0.42	0.31	0.0465	0
96	PQ	138	0.993	-2.4	0	0	0	0	-	0.38	0.15	0.009	0
97	PQ	138	1.011	-2.1	0	0	0	0	-	0.15	0.09	0.0102	0
98	PQ	138	1.024	-2.6	0	0	0	0	-	0.34	0.08	0.0673	0
99	PV	138	1.010	-2.9	-0.42	-0.18	1	-1	1.01	0	0	0	0
100	PV	138	1.017	-1.9	2.52	1.1	1.55	-0.5	1.017	0.37	0.18	0.012	0
101	PQ	138	0.992	-0.3	0	0	0	0	-	0.22	0.15	0.0152	0
102	PQ	138	0.991	2.4	0	0	0	0	-	0.05	0.03	0.004	0
103	PV	138	1.001	-5.5	0.4	0.4	0.4	-0.15	1.01	0.23	0.16	0.028	0
104	PV	138	0.971	-8.3	0	0.06	0.23	-0.08	0.971	0.38	0.25	0.0356	0.2
105	PV	138	0.966	-9.4	0	-0.08	0.23	-0.08	0.965	0.31	0.26	0.0317	0
106	PQ	138	0.962	-9.6	0	0	0	0	-	0.43	0.16	0.0424	0.06
107	PV	138	0.952	-12.4	-0.22	0.06	2	-2	0.952	0.28	0.12	0.0187	0
108	PQ	138	0.967	-10.6	0	0	0	0	-	0.02	0.01	0.0025	0
109	PQ	138	0.967	-11	0	0	0	0	-	0.08	0.03	0.0067	0.06
110	PV	138	0.973	-11.9	0	0.05	0.23	-0.08	0.973	0.39	0.3	0.0327	0
111	PV	138	0.980	-10.2	0.36	-0.02	10	-1	0.98	0	0	0	0
112	PV	138	0.975	-15	-0.43	0.42	10	-1	0.975	0.25	0.13	0.0241	0
113	PV	138	0.993	-16	-0.06	0.06	2	-1	0.993	0	0	0	0
114	PQ	138	0.960	-15.3	0	0	0	0	-	0.08	0.03	0.008	0
115	PQ	138	0.960	-15.3	0	0	0	0	-	0.22	0.07	0.0372	0
116	PV	138	1.005	-2.8	-1.84	0.51	10	-10	1.005	0	0	0	0
117	PQ	138	0.974	-19	0	0	0	0	-	0.2	0.08	0.0153	0
118	PQ	138	0.949	-8.1	0	0	0	0	-	0.33	0.15	0.0231	0

Table A.3: Line data from the IEEE 118 bus test system.

From	To	R	X	B	Tap	From	To	R	X	B	Tap
1	2	0.0303	0.0999	0.0254	-	63	64	0.0017	0.02	0.216	-
1	3	0.0129	0.0424	0.0108	-	64	61	0	0.0268	0	1
4	5	0.0018	0.008	0.0021	-	38	65	0.009	0.0986	1.046	-
3	5	0.0241	0.108	0.0284	-	64	65	0.0027	0.0302	0.38	-
5	6	0.0119	0.054	0.0143	-	49	66	0.018	0.0919	0.025	-
6	7	0.0046	0.0208	0.0055	-	49	66	0.018	0.0919	0.025	-
8	9	0.0024	0.0305	1.162	-	62	66	0.0482	0.218	0.058	-
8	5	0	0.0267	0	0.985	62	67	0.0258	0.117	0.031	-
9	10	0.0026	0.0322	1.23	-	65	66	0	0.037	0	0.9
4	11	0.0209	0.0688	0.0175	-	66	67	0.0224	0.1015	0.027	-
5	11	0.0203	0.0682	0.0174	-	65	68	0.0014	0.016	0.638	-
11	12	0.006	0.0196	0.005	-	47	69	0.0844	0.2778	0.071	-
2	12	0.0187	0.0616	0.0157	-	49	69	0.0985	0.324	0.083	-
3	12	0.0484	0.16	0.0406	-	68	69	0	0.037	0	0.9
7	12	0.0086	0.034	0.0087	-	69	70	0.03	0.127	0.122	-
11	13	0.0223	0.0731	0.0188	-	24	70	0.0022	0.4115	0.102	-
12	14	0.0215	0.0707	0.0182	-	70	71	0.0088	0.0355	0.009	-
13	15	0.0744	0.2444	0.0627	-	24	72	0.0488	0.196	0.049	-
14	15	0.0595	0.195	0.0502	-	71	72	0.0446	0.18	0.044	-
12	16	0.0212	0.0834	0.0214	-	71	73	0.0087	0.0454	0.012	-
15	17	0.0132	0.0437	0.0444	-	70	74	0.0401	0.1323	0.034	-
16	17	0.0454	0.1801	0.0466	-	70	75	0.0428	0.141	0.036	-
17	18	0.0123	0.0505	0.013	-	69	75	0.0405	0.122	0.124	-
18	19	0.0112	0.0493	0.0114	-	74	75	0.0123	0.0406	0.01	-
19	20	0.0252	0.117	0.0298	-	76	77	0.0444	0.148	0.037	-

Table A.3: Line data from the IEEE 118 bus test system.

From	To	R	X	B	Tap	From	To	R	X	B	Tap
15	19	0.012	0.0394	0.0101	-	69	77	0.0309	0.101	0.104	-
20	21	0.0183	0.0849	0.0216	-	75	77	0.0601	0.1999	0.05	-
21	22	0.0209	0.097	0.0246	-	77	78	0.0038	0.0124	0.013	-
22	23	0.0342	0.159	0.0404	-	78	79	0.0055	0.0244	0.007	-
23	24	0.0135	0.0492	0.0498	-	77	80	0.017	0.0485	0.047	-
23	25	0.0156	0.08	0.0864	-	77	80	0.0294	0.105	0.023	-
26	25	0	0.0382	0	0.96	79	80	0.0156	0.0704	0.019	-
25	27	0.0318	0.163	0.1764	-	68	81	0.0018	0.0202	0.808	-
27	28	0.0191	0.0855	0.0216	-	81	80	0	0.037	0	0.9
28	29	0.0237	0.0943	0.0238	-	77	82	0.0298	0.0853	0.082	-
30	17	0	0.0388	0	0.96	82	83	0.0112	0.0367	0.038	-
8	30	0.0043	0.0504	0.514	-	83	84	0.0625	0.132	0.026	-
26	30	0.008	0.086	0.908	-	83	85	0.043	0.148	0.035	-
17	31	0.0474	0.1563	0.0399	-	84	85	0.0302	0.0641	0.012	-
29	31	0.0108	0.0331	0.0083	-	85	86	0.035	0.123	0.028	-
23	32	0.0317	0.1153	0.1173	-	86	87	0.0283	0.2074	0.045	-
31	32	0.0298	0.0985	0.0251	-	85	88	0.02	0.102	0.028	-
27	32	0.0229	0.0755	0.0193	-	85	89	0.0239	0.173	0.047	-
15	33	0.038	0.1244	0.0319	-	88	89	0.0139	0.0712	0.019	-
19	34	0.0752	0.247	0.0632	-	89	90	0.0518	0.188	0.053	-
35	36	0.0022	0.0102	0.0027	-	89	90	0.0238	0.0997	0.106	-
35	37	0.011	0.0497	0.0132	-	90	91	0.0254	0.0836	0.021	-
33	37	0.0415	0.142	0.0366	-	89	92	0.0099	0.0505	0.055	-
34	36	0.0087	0.0268	0.0057	-	89	92	0.0393	0.1581	0.041	-
34	37	0.0026	0.0094	0.0098	-	91	92	0.0387	0.1272	0.033	-
38	37	0	0.0375	0	0.935	92	93	0.0258	0.0848	0.022	-
37	39	0.0321	0.106	0.027	-	92	94	0.0481	0.158	0.041	-
37	40	0.0593	0.168	0.042	-	93	94	0.0223	0.0732	0.019	-
30	38	0.0046	0.054	0.422	-	94	95	0.0132	0.0434	0.011	-
39	40	0.0184	0.0605	0.0155	-	80	96	0.0356	0.182	0.049	-
40	41	0.0145	0.0487	0.0122	-	82	96	0.0162	0.053	0.054	-
40	42	0.0555	0.183	0.0466	-	94	96	0.0269	0.0869	0.023	-
41	42	0.041	0.135	0.0344	-	80	97	0.0183	0.0934	0.025	-
43	44	0.0608	0.2454	0.0607	-	80	98	0.0238	0.108	0.029	-
34	43	0.0413	0.1681	0.0423	-	80	99	0.0454	0.206	0.055	-
44	45	0.0224	0.0901	0.0224	-	92	100	0.0648	0.295	0.047	-
45	46	0.04	0.1356	0.0332	-	94	100	0.0178	0.058	0.06	-
46	47	0.038	0.127	0.0316	-	95	96	0.0171	0.0547	0.015	-
46	48	0.0601	0.189	0.0472	-	96	97	0.0173	0.0885	0.024	-
47	49	0.0191	0.0625	0.016	-	98	100	0.0397	0.179	0.048	-
42	49	0.0715	0.323	0.086	-	99	100	0.018	0.0813	0.022	-
42	49	0.0715	0.323	0.086	-	100	101	0.0277	0.1262	0.033	-
45	49	0.0684	0.186	0.0444	-	92	102	0.0123	0.0559	0.015	-
48	49	0.0179	0.0505	0.0126	-	101	102	0.0246	0.112	0.029	-
49	50	0.0267	0.0752	0.0187	-	100	103	0.016	0.0525	0.054	-
49	51	0.0486	0.137	0.0342	-	100	104	0.0451	0.204	0.054	-
51	52	0.0203	0.0588	0.014	-	103	104	0.0466	0.1584	0.041	-
52	53	0.0405	0.1635	0.0406	-	103	105	0.0535	0.1625	0.041	-
53	54	0.0263	0.122	0.031	-	100	106	0.0605	0.229	0.062	-
49	54	0.073	0.289	0.0738	-	104	105	0.0099	0.0378	0.01	-
49	54	0.0869	0.291	0.073	-	105	106	0.014	0.0547	0.014	-
54	55	0.0169	0.0707	0.0202	-	105	107	0.053	0.183	0.047	-
54	56	0.0028	0.0096	0.0073	-	105	108	0.0261	0.0703	0.018	-

Table A.3: Line data from the IEEE 118 bus test system.

From	To	R	X	B	Tap	From	To	R	X	B	Tap
55	56	0.0049	0.0151	0.0037	-	106	107	0.053	0.183	0.047	-
56	57	0.0343	0.0966	0.0242	-	108	109	0.0105	0.0288	0.008	-
50	57	0.0474	0.134	0.0332	-	103	110	0.0391	0.1813	0.046	-
56	58	0.0343	0.0966	0.0242	-	109	110	0.0278	0.0762	0.02	-
51	58	0.0255	0.0719	0.0179	-	110	111	0.022	0.0755	0.02	-
54	59	0.0503	0.2293	0.0598	-	110	112	0.0247	0.064	0.062	-
56	59	0.0825	0.251	0.0569	-	17	113	0.0091	0.0301	0.008	-
56	59	0.0803	0.239	0.0536	-	32	113	0.0615	0.203	0.052	-
55	59	0.0474	0.2158	0.0565	-	32	114	0.0135	0.0612	0.016	-
59	60	0.0317	0.145	0.0376	-	27	115	0.0164	0.0741	0.02	-
59	61	0.0328	0.15	0.0388	-	114	115	0.0023	0.0104	0.003	-
60	61	0.0026	0.0135	0.0146	-	68	116	0.0003	0.0041	0.164	-
60	62	0.0123	0.0561	0.0147	-	12	117	0.0329	0.14	0.036	-
61	62	0.0082	0.0376	0.0098	-	75	118	0.0145	0.0481	0.012	-
63	59	0	0.0386	0	0.96	76	118	0.0164	0.0544	0.014	-

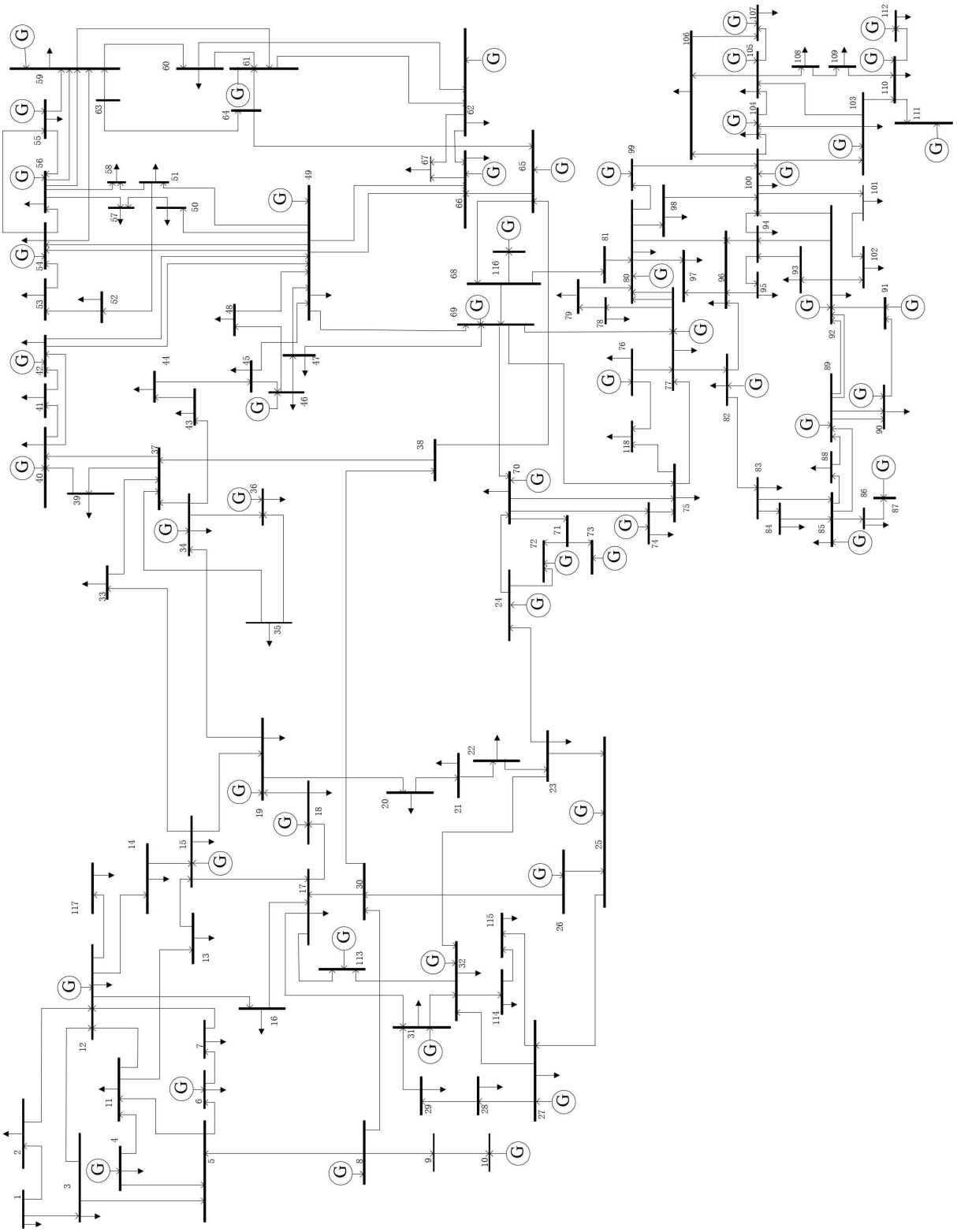

Figure A.2: One-line diagram of the IEEE 118 bus test system.
Source: IITPG (2003)

APPENDIX B

107 Bus Reduced Interconnected Brazilian Test System

The data regarding the 107 bus reduced interconnected Brazilian test system was obtained in Alves (2007). The per-unit base power is equal to 100 MW and the voltage base value is indicated in Table B.1 alongside with other bus data. The base value for generator buses were omitted because they are only connected to a step up transformer. The bus voltage magnitudes and angles presented in this table correspond to the power flow solution of the base case scenario, for which the power system load can be seen in the same table. The DG power injection in each bus is presented when the penetration level is equal to 10%. For the two other DG penetration analysed (20% and 30%), the active injection is proportional to the value mentioned. The transmission network parameters are available in Table B.2 according to the model of Figure A.1. The symbols utilized in these tables are defined in Table A.1.

Table B.1: Bus data from the 107 bus Brazilian reduced test system.

ID	Type	V_{base}	V	θ	P_g	Q_g	Q_{max}	Q_{min}	V_{set}	P_l	Q_l	P_{gd}	B_{sh}
12	PV	-	1	-0.2	3	-2.09	4.2	-5.4	1	0	0	0	0
16	PV	-	1	-2.2	8	-1.5	4.8	-7.2	1	0	0	0	0
18	Vθ	-	1.02	0	9.95	-4.05	6	-5.46	1.02	0	0	0	0
20	PV	-	1.01	1.6	9	-3.41	6.4	-6.4	1.01	0	0	0	0
21	PV	-	1	-38.7	1.4	-0.25	0.84	-0.8	1	0	0	0	0
22	PV	-	1	4.1	1.5	-0.22	1.26	-1.2	1	0	0	0	0
35	PV	-	1	-2.9	2	-0.51	1.8	-1.8	1	0	0	0	0
48	PV	-	1	-19.1	0	-4.17	12	-10.8	1	0	0	0	0
86	PQ	345	1.03	-19.1	0	0	0	0	-	0.66	0.01	0.01	0
100	PQ	500	1.058	-4.5	0	0	0	0	-	0	0	0	0
101	PQ	500	1.076	-12.2	0	0	0	0	-	0	0	0	-2
102	PQ	500	1.067	-18.8	0	0	0	0	-	0	0	0	-1
103	PQ	500	1.085	-19	0	0	0	0	-	0	0	0	0
104	PQ	500	1.072	-27.4	0	0	0	0	-	9.1	2.35	2.35	0
106	PQ	500	1.06	-28.2	0	0	0	0	-	0	0	0	-1
120	PQ	345	1.046	-17.2	0	0	0	0	-	1.8	0.9	0.9	0
122	PQ	500	1.086	-17.3	0	0	0	0	-	2	0.38	0.38	0
123	PQ	345	1.045	-21.8	0	0	0	0	-	4.5	1.75	1.75	0

Table B.1: Bus data from the 107 bus Brazilian reduced test system.

ID	Type	V_{base}	V	θ	P_g	Q_g	Q_{max}	Q_{min}	V_{set}	P_l	Q_l	P_{gd}	B_{sh}
126	PQ	345	1.036	-19.8	0	0	0	0	-	2.9	0.95	0.95	0
131	PQ	345	1.028	-3.3	0	0	0	0	-	0	0	0	0
134	PQ	345	1.027	-2.4	0	0	0	0	-	0	0	0	0
136	PQ	345	1.031	-9.1	0	0	0	0	-	0.54	0.23	0.23	0
138	PQ	345	1.043	-20	0	0	0	0	-	0.72	0.34	0.34	0
140	PQ	345	1.033	-29.4	0	0	0	0	-	7	2.5	2.5	0
210	PQ	500	1.049	-3.6	0	0	0	0	-	0	0	0	0
213	PQ	345	1.052	-4.7	0	0	0	0	-	0.93	0.39	0.39	0
216	PQ	345	1.05	-3.8	0	0	0	0	-	0.53	0.25	0.25	0
217	PQ	345	1.051	-8.3	0	0	0	0	-	3.64	0.58	0.58	0
218	PQ	345	1.025	-16	0	0	0	0	-	6	2	2	0
219	PQ	345	1.029	-14.9	0	0	0	0	-	0	0	0	0
220	PQ	345	1.052	-7.9	0	0	0	0	-	0	0	0	0
225	PQ	230	1.004	-10.6	0	0	0	0	-	0	0	0	0
228	PQ	230	1.016	-16.6	0	0	0	0	-	0.86	0.34	0.34	0
231	PQ	30	1.007	-25.5	0	0	0	0	-	0.9	0.32	0.32	0
233	PQ	500	1.04	-12.2	0	0	0	0	-	0	0	0	0
234	PQ	345	1.028	-15	0	0	0	0	-	10	3.5	3.5	0
300	PV	-	1.02	5	7	-1.85	3.92	-4.4	1.02	0	0	0	0
301	PV	-	1.01	4.6	3	-1.3	1.4	-1.4	1.01	0	0	0	0
302	PV	-	1.02	5.7	4	-1.26	1.5	-1.5	1.02	0	0	0	0
303	PV	-	1.02	-0.3	2	-2.82	6	-6	1.02	0	0	0	0
305	PV	-	1	1.9	3	-0.63	1.2	-1.2	1	0	0	0	0
320	PQ	500	1.049	-0.1	0	0	0	0	-	0	0	0	0
325	PQ	500	1.047	0.3	0	0	0	0	-	0	0	0	0
326	PQ	345	1.034	-1.9	0	0	0	0	-	2.74	1.04	1.04	0
360	PQ	500	1.047	1.6	0	0	0	0	-	0	0	0	0
370	PQ	500	1.049	-1.4	0	0	0	0	-	0	0	0	0
396	PQ	345	1.041	-1.9	0	0	0	0	-	0	0	0	0
500	PV	-	1.02	2.4	8	-1.24	5.4	-5.4	1.02	0	0	0	0
535	PQ	500	1.036	-2	0	0	0	0	-	0	0	0	0
536	PQ	440	1.024	-4.8	0	0	0	0	-	7	1.5	1.5	0
800	PV	-	1.02	16.9	11	1.1	8	-8	1.02	0	0	0	0
808	PV	-	1.02	27.4	11.5	1.05	6	-6	1.02	0	0	0	0
810	PV	-	1.02	19.9	12	-0.95	5.32	-4	1.02	0	0	0	0
814	PQ	230	1.008	-13.2	0	0	0	0	-	7.35	1.91	1.91	0
824	PQ	500	1.043	6.6	0	0	0	0	-	0	0	0	0
834	PQ	230	1	-4.6	0	0	0	0	-	0.13	0.04	0.04	0
839	PQ	230	1	17.6	0	0	0	0	-	0	0	0	0
840	PQ	138	0.987	14.6	0	0	0	0	-	1.59	0.36	0.36	0
848	PQ	138	1	18.4	0	0	0	0	-	0.94	0.18	0.18	0
856	PQ	500	1.037	13.1	0	0	0	0	-	0	0	0	0
895	PQ	500	1.057	-11	0	0	0	0	-	0	0	0	0
896	PQ	500	1.029	19.7	0	0	0	0	-	0	0	0	0
897	PQ	500	1.04	21	0	0	0	0	-	0	0	0	0
898	PQ	230	1.013	21.8	0	0	0	0	-	0	0	0	0
904	PV	-	1.02	8.9	7	-2.59	4.75	-4.75	1.02	0	0	0	0
915	PV	-	1.02	11.1	7	-1.26	4.65	-5.16	1.02	0	0	0	0
919	PV	-	1	29.7	7	0.84	2.2	-1.48	1	0	0	0	0
925	PV	-	1.02	23.8	9.5	0.62	4.2	-4.4	1.02	0	0	0	0
933	PQ	500	1.043	6.2	0	0	0	0	-	0	0	0	0
934	PQ	230	1.003	6.1	0	0	0	0	-	2.37	0.59	0.59	0
938	PQ	500	1.053	-13	0	0	0	0	-	0	0	0	0

Table B.1: Bus data from the 107 bus Brazilian reduced test system.

ID	Type	V_{base}	V	θ	P_g	Q_g	Q_{max}	Q_{min}	V_{set}	P_l	Q_l	P_{gd}	B_{sh}
939	PQ	230	1.006	-15.4	0	0	0	0	-	11.49	0.53	0.53	0
955	PQ	500	1.062	0.4	0	0	0	0	-	0	0	0	0
959	PQ	500	1.045	-10.7	0	0	0	0	-	0	0	0	1
960	PQ	230	1.007	-13.2	0	0	0	0	-	8.45	4.69	4.69	0
964	PQ	500	1.042	-6.9	0	0	0	0	-	0	0	0	0
965	PQ	230	1.007	-9.3	0	0	0	0	-	7.56	0.56	0.56	0
976	PQ	500	1.017	-9.6	0	0	0	0	-	0	0	0	0
995	PQ	500	1.052	4.6	0	0	0	0	-	0	0	0	0
1015	PQ	230	1.009	-15.4	0	0	0	0	-	0.7	0.02	0.02	0
1030	PQ	500	1.055	3.3	0	0	0	0	-	0	0	0	0
1047	PQ	230	1.018	22.8	0	0	0	0	-	0	0	0	0
1060	PQ	500	1.045	15.9	0	0	0	0	-	0	0	0	0
1210	PQ	230	1.007	-12.3	0	0	0	0	-	12.28	4.25	4.25	0
1503	PQ	500	1.071	-25.2	0	0	0	0	-	0	0	0	0
1504	PQ	138	1.038	-29.1	0	0	0	0	-	1.45	0.63	0.63	0
2458	PQ	230	1.002	17.3	0	0	0	0	-	4.03	1.26	1.26	0
4501	PQ	230	1.025	-37	0	0	0	0	-	0.31	0.07	0.07	-0.45
4521	PQ	230	1.035	-42.7	0	0	0	0	-	0	0	0	0
4522	PQ	230	1.034	-44.8	0	0	0	0	-	0	0	0	-0.2
4523	PV	-	1.01	-37	0.5	-0.1	0.3	-0.42	1.01	0	0	0	0
4530	PQ	-	1.047	-49.4	0	0	0	0	-	0	0	0	0
4532	PQ	230	1.047	-49.4	0	0	0	0	-	0	0	0	0
4533	PQ	138	1.018	-49.7	0	0	0	0	-	0.75	0.16	0.16	0
4542	PQ	230	1.029	-48.7	0	0	0	0	-	0	0	0	0
4552	PQ	230	1.012	-56.3	0	0	0	0	-	0.13	0.01	0.01	-0.2
4562	PQ	230	1.018	-64.5	0	0	0	0	-	0.24	0.07	0.07	0
4572	PQ	230	1.015	-61.6	0	0	0	0	-	0.18	0.06	0.06	0
4582	PQ	230	1.024	-67.4	0	0	0	0	-	0.66	0.17	0.17	0.3
4592	PQ	230	1.02	-43.8	0	0	0	0	-	0	0	0	0
4596	PV	-	1	-44.9	2.3	-0.37	1.6	-1.6	1	0	0	0	0
4623	PQ	138	1.02	-47.7	0	0	0	0	-	1.28	0.41	0.41	0
4703	PQ	138	1.006	-50.8	0	0	0	0	-	1.82	0.3	0.3	0
4804	PV	-	1	-51.1	0.5	-0.19	0.59	-0.86	1	0	0	0	0
4805	PQ	138	1.027	-54.9	0	0	0	0	-	0	0	0	0
4807	PQ	138	1.028	-56.1	0	0	0	0	-	1.29	0.36	0.36	0
4862	PQ	230	1.05	-54.4	0	0	0	0	-	0	0	0	-0.3

Table B.2: Line data from the 107 bus Brazilian reduced test system.

From	To	R	X	B	Tap	From	To	R	X	B	Tap
86	48	0	0.0071	0	1	824	933	0.0001	0.0012	0.152	-
86	122	0	0.0191	0	1	824	933	0.0001	0.0013	0.1543	-
100	20	0	0.0126	0	1	834	934	0.0244	0.1265	0.2171	-
100	101	0.0017	0.0272	2.314	-	839	840	0	0.0664	0	1
100	101	0.0017	0.027	2.302	-	839	840	0	0.0629	0	1
100	210	0.0021	0.0294	2.546	-	839	898	0.0113	0.0699	0.1262	-
100	213	0	0.0236	0	1	839	1047	0.0122	0.0769	0.1381	-
100	535	0.0015	0.024	2.038	-	839	2458	0.0022	0.0109	0.0186	-
101	102	0.0016	0.0246	2.085	-	839	2458	0.0017	0.0103	0.0205	-
101	103	0.0015	0.0239	2.026	-	856	810	0	0.0105	0	1
102	120	0	0.024	0	1	856	933	0.0005	0.0065	0.8049	-
102	1503	0.0011	0.0191	1.6185	-	856	1060	0.0006	0.007	0.8575	-
103	123	0	0.0242	0	1	895	122	0.0031	0.0396	4.4484	-

Table B.2: Line data from the 107 bus Brazilian reduced test system.

From	To	R	X	B	Tap	From	To	R	X	B	Tap
104	103	0.002	0.031	2.649	-	895	122	0.0031	0.0396	4.4484	-
104	1503	0.0005	0.0082	0.6936	-	896	897	0.0005	0.0073	0.7806	-
106	104	0.0015	0.0239	2.027	-	897	808	0	0.0102	0	1.024
106	104	0.0015	0.0239	2.031	-	898	848	0	0.0636	0	1
106	140	0	0.0292	0	1	898	1047	0.0015	0.0089	0.0163	-
106	140	0	0.0267	0	1	933	895	0.002	0.0255	3.1272	-
122	103	0.001	0.0162	1.3635	-	933	955	0.0016	0.0205	2.5017	-
123	120	0.0036	0.0394	0.6668	-	933	959	0.002	0.0269	3.364	-
126	86	0.0011	0.0183	0.5118	-	934	933	0.0003	0.0121	0	0.975
126	86	0.0011	0.0182	0.5118	-	934	1047	0.0304	0.1574	0.2712	-
126	120	0.006	0.0595	0.928	-	934	1047	0.0304	0.1572	0.2709	-
126	120	0.0061	0.0602	0.938	-	938	955	0.0026	0.0292	3.604	-
131	22	0	0.0883	0	1	938	959	0.0013	0.016	1.9589	-
134	12	0	0.0133	0	0.999	939	938	0.0003	0.0115	0	0.959
134	131	0.0009	0.0101	0.169	-	939	938	0.0003	0.0116	0	0.959
134	396	0.0032	0.0351	0.5924	-	939	938	0	0.0128	0	0.959
136	16	0	0.0154	0	1	939	1015	0.0127	0.0656	0.1131	-
136	120	0.0044	0.043	0.666	-	939	1015	0.0128	0.0656	0.1152	-
136	120	0.0044	0.043	0.666	-	955	964	0.0019	0.0235	2.8724	-
136	131	0.0035	0.0342	0.528	-	959	895	0.0005	0.0044	0.4758	-
136	134	0.0037	0.0413	0.699	-	960	834	0.0221	0.1147	0.1969	-
136	138	0.0065	0.0646	1.008	-	960	959	0.0003	0.0116	0	0.992
136	138	0.0056	0.0619	1.057	-	960	959	0.0003	0.0117	0	0.992
140	138	0.0065	0.065	1.014	-	960	1015	0.0189	0.0978	0.1684	-
140	138	0.0056	0.0619	1.057	-	960	1015	0.019	0.097	0.1703	-
210	18	0	0.0067	0	1	964	976	0.0007	0.0092	1.1217	-
210	217	0	0.0172	0	1	965	964	0.0002	0.0121	0	0.972
210	217	0	0.0172	0	1	965	964	0.0002	0.0123	0	0.972
210	370	0.0015	0.0232	1.966	-	976	995	0.0028	0.0385	4.937	-
213	216	0.0022	0.0242	0.407	-	995	904	0	0.0115	0	1
216	396	0.0013	0.0141	0.2377	-	995	964	0.0016	0.0303	3.5488	-
217	216	0.0056	0.0625	1.0673	-	995	1030	0.0007	0.0092	1.1226	-
217	218	0.0051	0.0561	0.956	-	995	1060	0.0017	0.0217	2.6516	-
217	218	0.0051	0.0561	0.956	-	1030	915	0	0.0207	0	1
218	234	0.0043	0.048	0.822	-	1030	955	0.0005	0.0059	0.7182	-
218	234	0.0043	0.048	0.822	-	1047	919	0	0.017	0	1.025
219	234	0.0004	0.0043	0.0734	-	1060	897	0.0008	0.0117	1.2458	-
219	234	0.0004	0.0043	0.0734	-	1060	925	0	0.0151	0	1.024
220	35	0	0.045	0	1.025	1210	976	0.0003	0.0122	0	1.011
220	217	0.0023	0.024	0.4324	-	1210	976	0.0004	0.0114	0	1.011
220	219	0.0073	0.077	1.3801	-	1210	976	0.0004	0.0122	0	1.011
225	217	0	0.0272	0	0.955	1503	1504	0	0.052	0	1
225	217	0	0.0294	0	0.955	2458	896	0	0.0127	0	0.994
225	231	0.041	0.1976	0.3608	-	4501	4522	0.0376	0.2068	0.3566	-
225	231	0.0127	0.1362	0.4947	-	4501	4522	0.0164	0.1246	0.615	-
228	219	0	0.036	0	1	4521	4523	0	0.2071	0	1
231	4501	0.0451	0.2169	0.4025	-	4522	4521	0.0153	0.076	0.1425	-
231	4501	0.0149	0.1609	0.554	-	4522	4532	0.0325	0.1792	0.3275	-
233	210	0.0028	0.0399	3.5536	-	4522	4532	0.0325	0.1792	0.3275	-
233	320	0.0027	0.0387	3.4403	-	4522	4623	0	0.0795	0	1
234	233	0	0.0111	0	1	4522	4623	0	0.0795	0	1
234	233	0	0.01	0	1	4532	4530	0	0.143	0	1
320	210	0.0013	0.0194	1.4996	-	4532	4533	0	0.086	0	1

Table B.2: Line data from the 107 bus Brazilian reduced test system.

From	To	R	X	B	Tap	From	To	R	X	B	Tap
320	300	0	0.0136	0	1	4532	4533	0	0.086	0	1
320	360	0.0008	0.0126	0.9899	-	4532	4533	0	0.086	0	1
325	301	0	0.0263	0	1	4532	4542	0.0162	0.0968	0.1915	-
325	326	0	0.0216	0	1	4533	4596	0	0.0376	0	1
325	326	0	0.0216	0	1	4542	4552	0.0183	0.1093	0.186	-
325	360	0.001	0.0152	1.1967	-	4552	4572	0.014	0.0838	0.17	-
325	370	0.0028	0.0484	4.195	-	4562	4572	0.0094	0.0559	0.1064	-
326	134	0.0007	0.0076	0.1229	-	4562	4582	0.0124	0.0738	0.1328	-
326	396	0.0024	0.0274	0.4547	-	4592	21	0	0.064	0	1
360	302	0	0.0194	0	1	4592	4542	0.01	0.0617	0.126	-
370	303	0	0.0106	0	1	4623	4533	0.1706	0.455	0.1139	-
370	535	0.0009	0.0138	1.123	-	4703	4533	0.009	0.0231	0.0058	-
396	305	0	0.022	0	1.025	4703	4533	0.009	0.0231	0.0058	-
535	500	0	0.0102	0	1	4805	4804	0	0.1333	0	1
536	535	0	0.0153	0	1	4805	4807	0.0309	0.0813	0.0209	-
536	535	0	0.0142	0	1	4805	4807	0.0309	0.0813	0.0209	-
814	895	0.0003	0.0115	0	0.965	4862	4532	0.0257	0.2368	0.9742	-
814	895	0.0003	0.0117	0	0.965	4862	4532	0.0257	0.2368	0.9742	-
824	800	0	0.0168	0	1.024	4862	4807	0	0.0405	0	1

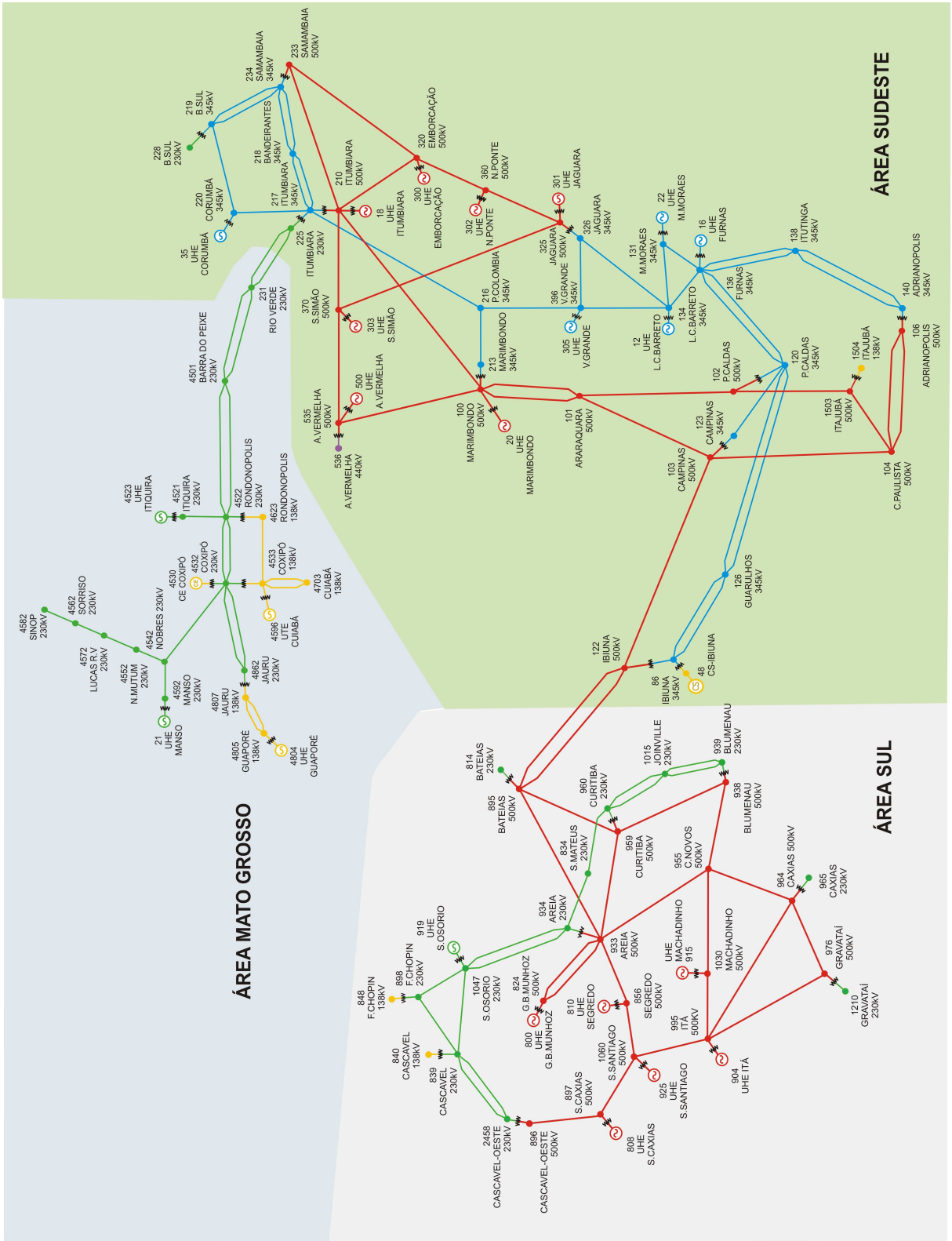

Figure B.1: One-line diagram of the 107 bus Brazilian reduced test system.
Fonte: Mansour (2013)